Temporal and genetic link between incremental pluton assembly and pulsed porphyry Cu-Mo formation in accretionary orogens

Hervé Rezeau[1,*], Robert Moritz[1], Jörn-Frederik Wotzlaw[2], Rodrik Tayan[3,†], Rafael Melkonyan[3], Alexey Ulianov[4], David Selby[5], François-Xavier d'Abzac[1] and Richard A. Stern[6]

[1]Department of Earth Sciences, University of Geneva, 1205 Geneva, Switzerland

[2]Institute of Geochemistry and Petrology, ETH Zurich, 8092 Zurich, Switzerland

[3]Institute of Geological Sciences, National Academy of Sciences, 0019 Yerevan, Armenia

[4]Institute of Earth Sciences, University of Lausanne, 1015 Lausanne, Switzerland

[5]Department of Earth Sciences, University of Durham, DH1 3LE Durham, United Kingdom

[6]Canadian Centre for Isotopic Microanalysis, University of Alberta, Edmonton, Canada

*corresponding author: herve.rezeau@unige.ch

[†]deceased March 25th 2016

ABSTRACT

Economically important porphyry Cu-Mo deposits (PCDs) are generally hosted by upper crustal plutons of variable chemical compositions related to distinct geodynamic settings. The absolute timing and duration of pluton assembly and PCD formation is critical to understand the genetic relationship between these interrelated processes. Here we present new comprehensive zircon U-Pb and molybdenite Re-Os ages that tightly constrain the timing and duration of pluton assembly and the age of mineralization in one of the largest ore-bearing plutons of the central Tethyan metallogenic belt, the Meghri-Ordubad pluton, southern Armenia and Nakhitchevan, Lesser

Caucasus. This composite pluton was incrementally assembled during three compositionally distinct magmatic episodes over about 30 m.y., comprising Middle Eocene (48.9-43.1 Ma) calc-alkaline subduction-related magmatism lasting 5.8 ± 0.8 m.y., followed by post-subduction Late Eocene - Middle Oligocene (37.8-28.1 Ma) shoshonitic magmatism over 9.7 ± 0.9 m.y, and Late Oligocene - Early Miocene (26.6-21.2 Ma) adakitic magmatism consisting of shoshonitic dikes and high-K calc-alkaline granodioritic magmas emplaced over 5.4 ± 0.4 m.y. Despite the distinct geodynamic settings and magma compositions, each intrusive suite culminated in the formation of variably sized PCDs, including the giant Oligocene Kadjaran porphyry Cu-Mo deposit associated with high Sr/Y shoshonitic magmas. Complementary *in-situ* zircon hafnium (εHf_{zircon} = +8 to +11.3) and oxygen ($\delta^{18}O_{zircon}$ = +4.6 to +6.0 ‰) isotope data support a mantle-dominated magma source with limited crustal contribution and/or cannibalization of young and juvenile lower crustal cumulates. We conclude that, independently of geodynamic setting and magma composition, long-lived (5-10 m.y.) incremental mantle-derived magmatism is a pre-requisite to form fertile magmatic-hydrothermal systems, and especially giant PCDs.

INTRODUCTION

The majority of porphyry Cu-Mo deposits (PCDs) are associated with subduction-related calc-alkaline upper-crustal plutons (Sillitoe, 2010). However, porphyry Cu-Mo systems have recently also been recognized in post-subduction settings, particularly along the Tethyan metallogenic belt (e.g., Richards, 2015; Hou et al., 2015a, b; Moritz et al., 2016). This raises a number of questions concerning the primary control on PCD formation, as most models require active oceanic subduction to generate large volumes of hydrous, oxidized, S-rich, and Cu-rich magmas derived from a subcontinental lithospheric mantle metasomatized by slab fluids, and repeated

mafic magma injections to provide sulfur, metals and volatiles into upper crustal reservoirs (e.g., Hattori and Keith, 2001; Scaillet, 2010; Audétat and Simon, 2012; Tapster et al., 2016). Ore-forming processes in PCDs occur over short timescales of $<10^3$ to 10^4 years (e.g., von Quadt et al., 2011; Chiaradia et al., 2013), which are in marked contrast to the duration of incremental assembly of the host plutons lasting 10^5 to 10^6 years (Rohrlach and Loucks, 2005; Chelle-Michou et al., 2014; Correa et al., 2016). In most magmatic-hydrothermal systems, ore formation occurs late in the magmatic evolution (e.g., Sillitoe, 2010; Audétat and Simon, 2012), but the precise temporal and genetic relationships between the entire pluton construction and PCD formation remains poorly documented.

Recently, Moritz et al. (2016) documented the regional tectonic evolution of the southernmost Lesser Caucasus from a subduction to post-collisional setting with coeval mineralization pulses, however the absolute temporal link between intrusions and PCDs remained elusive due to limited geochronological data. Here we investigate the absolute temporal relationship between incremental pluton construction and PCD formation using a large data set of new zircon U-Pb and molybdenite Re-Os data from one of the largest ore-bearing plutons of the central Tethyan metallogenic belt, the Meghri-Ordubad pluton (MOP) in southern Armenia and Nakhitchevan, Lesser Caucasus. The MOP comprises three long-lived intrusive suites, which culminated in the formation of variably sized PCDs, including the giant Oligocene Kadjaran PCD (Figs. 1 and 2). Our comprehensive U-Pb and Re-Os geochronological framework documents in detail the incremental construction of the MOP over 30 m.y. and the timing of ore formation allowing improved understanding of the conditions and processes required to form PCDs. Complementary *in-situ* zircon hafnium and oxygen isotope data are used to estimate mantle and crustal contributions to the ore-forming magmas.

GEOLOGICAL SETTING AND ANALYTICAL METHODS

The ore-bearing MOP belongs to the regional fertile Cenozoic magmatic belt extending from Turkey to Iran that formed during the final convergence and collision of the Arabian and Eurasian plates (Fig. DR1). The MOP represents the largest composite intrusion of the Lesser Caucasus (800 km^2) and intrudes a thick sequence of Cenozoic terrigenous sedimentary and subalkaline to calc-alkaline basaltic to andesitic volcanic rocks (Karamyan et al., 1974). The MOP is the result of a long-lasting Middle Eocene to Early Miocene evolution, including subduction-related calc-alkaline magmatism followed by post-subduction shoshonitic to high-K calc-alkaline magmatism (Figs. 1A and DR2; Moritz et al., 2016). The MOP is bordered by two regional NNW-oriented faults with both vertical and dextral strike-slip movements, and another parallel fault extends through its central part and controls the location of PCDs (Fig. 2; Tayan, 1998).

New zircon U-Pb ages were obtained by laser ablation inductively coupled plasma mass spectrometry (LA-ICP-MS) from thirty representative magmatic rock samples covering the entire temporal and compositional range of the MOP. Nine molybdenite Re-Os ages were obtained by isotope dilution negative thermal ionization mass spectrometry (ID-N-TIMS) from mineralization events associated with all three magmatic episodes. *In-situ* multiple collector inductively coupled plasma mass spectrometry (MC-ICP-MS) hafnium and secondary ion mass spectrometry (SIMS) oxygen isotope data were obtained on selected zircon grains. The complete analytical details and data set, together with a summary of the geochemical composition of dated samples are provided in the data repository[1].

INCREMENTAL PLUTON CONSTRUCTION

A total of 601 new LA-ICP-MS zircon U-Pb dates (Table DR2), together with previously published chemical abrasion isotope dilution thermal ionization mass spectrometry (CA-ID-TIMS) zircon U-Pb ages (Table DR1; Moritz et al., 2016), place tight spatial-temporal constraints on the MOP incremental assembly (Figs. 1A and 2).

In the southern part of the MOP (Fig. 2), the subduction-related calc-alkaline magmatism starts with two granitic and tonalitic intrusions at 48.9 ± 0.6 and 47.6 ± 0.6 Ma, followed by gabbro-diorite-tonalite-granodiorite intrusions and NNW-oriented basaltic andesite dikes emplaced between 45.9 ± 0.9 and 43.8 ± 0.6 Ma (Fig. 1A). These ages are in agreement with CA-ID-TIMS ages from similar samples (Fig. 1A; Table DR1). In the northern part of the MOP (Fig. 2), a monzodiorite is intruded by a tonalite and yield slightly younger U-Pb ages of 42.9 ± 0.5 and 43.1 ± 0.5 Ma, respectively (Fig. 1A). The Middle Eocene intrusive suite documents 5.8 ± 0.8 m.y. of incremental magmatism.

Following a magmatic lull of 5.1 ± 0.9 m.y., pluton assembly resumed with emplacement of post-subduction high Sr/Y shoshonitic intrusions (Fig. 1A). In the southeastern part of the MOP (Fig. 2), a monzogabbro and a monzodiorite yield indistinguishable ages of 37.8 ± 0.8 and 37.0 ± 0.4 Ma, respectively (Fig. 1A). Further north along the Vank-Kaler road and along the Meghri ridge (Fig. 2), five monzogabbroic-monzodioritic intrusions were emplaced between 35.7 ± 0.6 and 33.5 ± 0.6 Ma, and are crosscut by trachyandesitic and syenitic dikes that yield ages of 33.7 ± 0.5 and 33.6 ± 0.6 Ma, respectively (Fig. 1A). Along the Meghri ridge, a hornblende gabbro was dated at 33.43 ± 0.02 Ma by CA-ID-TIMS (Fig. 1A; Table DR1). Further north and west (Fig. 2), the Kadjaran ore field exposes a monzonite with an age of 31.9 ± 0.5 Ma, which is in agreement with a CA-ID-TIMS U-Pb age of 31.83 ± 0.02 Ma, and crosscut by a syenitic sill

dated at 31.1 ± 0.5 Ma (Fig. 1A; Table DR1). Younger monzonite and monzogabbro were emplaced at 28.3 ± 0.4 and 28.1 ± 0.4 Ma, respectively. The entire Late Eocene to Middle Oligocene intrusive suite comprises 9.7 ± 0.9 m.y. of episodic magmatism.

In the Kadjaran ore field (Fig. 2), the post-subduction magmatism continued with the emplacement of Late Oligocene NNW-oriented adakitic shoshonitic trachybasaltic and trachyandesitic dikes between 26.6 ± 0.3 and 24.3 ± 0.3 Ma (Fig. 1A). These dikes contain significantly older zircons reflecting recycling of Middle Eocene and Early Oligocene intrusions. A younger, voluminous Early Miocene adakitic high-K calc-alkaline porphyritic granodiorite dated at 22.8 ± 0.5 Ma is coeval with EW-oriented porphyritic granodioritic and trachyandesitic dikes dated at 22.2 ± 0.3 and 21.2 ± 0.3 Ma, respectively (Figs. 1A and 2), and overlap with CA-ID-TIMS ages for similar samples (Fig. 1A; Table DR1). The entire Late Oligocene - Early Miocene magmatism represents a third magmatic episode lasting 5.4 ± 0.4 m.y. This latest magmatic suite is characterized by an adakitic signature, and also higher Mg#, Cr and Ni contents, distinct from the Late Eocene - Middle Oligocene high Sr/Y shoshonitic intrusive suite (Fig. DR2; Table DR1).

TIMING OF MINERALIZATION

The PCDs are aligned along the central N-S-oriented Tashtun fault (Fig. 2), but they were formed at different times during the MOP construction. The small tonnage PCDs (10 to 40 Mt at 0.2-0.5 % Cu and 0.03-0.04 % Mo) yield molybdenite Re-Os ages of 44.23 ± 0.22 and 42.62 ± 0.22 Ma in the southern part of the MOP at Agarak and Aygedzor, respectively, and 43.14 ± 0.22 Ma in the northern part at Hanqasar (Figs. 1A and 2; Table DR3). These Re-Os ages are indistinguishable from the ages of the youngest Middle Eocene intrusions, which tightly

138 constrain their formation to the end of subduction-related calc-alkaline magmatism (Fig. 1A).
139 Molybdenite Re-Os dates reveal two distinct Cu-Mo mineralizing events in the giant Kadjaran
140 PCD (2244 Mt at 0.2 % Cu and 0.02 % Mo). Molybdenite from the first mineralization event
141 yields Re-Os ages between 27.28 ± 0.14 and 26.43 ± 0.13 Ma (Table DR3). This mineralization
142 is hosted by the youngest Late Eocene - Middle Oligocene shoshonitic high Sr/Y intrusions and
143 is crosscut by the oldest Late Oligocene shoshonitic adakitic mafic dike (Figs. 1A and DR3A).
144 Therefore, the first mineralizing event in Kadjaran is attributed to the very end of the Late
145 Eocene - Middle Oligocene post-subduction shoshonitic high Sr/Y magmatism. These ages are in
146 agreement with Re-Os ages reported from the Iranian side of the MOP, namely the Qaradagh
147 pluton (Simmonds and Moazzen, 2015).
148 A younger molybdenite Re-Os age of 20.48 ± 0.10 Ma reveals a second ore-forming event in
149 Kadjaran associated with a reopening of the structures hosting the 26-27 Ma-old Cu-Mo
150 mineralization. It documents a genetic link with the Early Miocene adakitic high-K calc-alkaline
151 porphyry granodiorite intrusion event (Fig. 1A; Table DR3), and supports a cogenetic link with
152 Cu-rich epithermal veins overprinting porphyritic granodioritic dikes dated at 22.2 ± 0.3 (Fig.
153 DR3B). The Early Miocene hydrothermal event was already documented by a sericite K-Ar date
154 of 22 ± 2 Ma in Kadjaran (Bagdasaryan et al., 1969), and it is consistent with a molybdenite Re-
155 Os age of 21.01 ± 0.15 Ma reported from the Sungun PCD, located 70 km further south in
156 northernmost Iran (Aghazadeh et al., 2015).
157 Placing all these Re-Os ages into our comprehensive U-Pb geochronology framework of
158 incremental pluton construction clearly links PCDs formation to the latest stage of each intrusive
159 suite (Fig. 1A).
160

ASSESSING THE SOURCES OF ORE-FORMING MAGMAS USING HAFNIUM AND OXYGEN ISOTOPES

Combined hafnium and oxygen isotopic signatures are powerful tools to trace the sources of magmas and place constraints on mantle and crustal contributions. Zircons from the MOP intrusive suites display median initial εHf values between +8.0 and +11.3, which suggest an overall predominance of mantle-derived magmas with limited crustal assimilation (Fig. 1B; Table DR3). This limited range in Hf isotopic compositions is in marked contrast with the significant differences in whole-rock geochemistry over about 30 m.y. (Fig. DR2; Table DR1). Interestingly, towards the end of the Middle Eocene calc-alkaline magmatism and throughout the Late Eocene to Early Miocene intrusive suites, Hf isotopic signatures become progressively more juvenile (Fig. 1B). Zircon oxygen isotope analyses reveal homogeneous $\delta^{18}O$ values in individual rocks and crystals (Table DR4), but display a subtle $\delta^{18}O$ increase from +5.20 ± 0.19 ‰ to +5.97 ± 0.22 ‰ over 30 m.y. (Fig. 1B). These values and pattern imply very limited assimilation of supracrustal rocks (e.g., Lackey et al., 2005), and no crustal recycling of hydrothermally altered rocks (e.g., Bindeman, 2008). A single Middle Eocene sample with a median $\delta^{18}O$ value of +4.51 ± 0.69 ‰ may be attributed to minor assimilation of altered shallow crustal material (Fig. 1B). The slight, but systematic and coeval increase of $\delta^{18}O$ and εHf values over time together with the overall limited variations support a predominance of mantle-derived magmas with decreasing crustal contribution. It is consistent with a long-lived homogeneous deep reservoir in the lower crust or lithospheric mantle. Alternatively, this isotope pattern may be attributed to progressive cannibalization of young and juvenile lower crust, formed by mantle-derived magmas. However, this process cannot be quantified due to the limited isotopic contrast.

CONTROLLING FACTORS OF PCD FORMATION

The MOP represents a unique place to investigate controlling factors leading to the formation of PCDs because all three intrusive suites share similar duration of magmatic activity, isotopic signatures and local structural setting (Figs. 1 and 2), but they were emplaced under different geodynamic settings (subduction vs. post-subduction), and they are distinct with respect to their magma composition (Fig. DR2; Table DR1).

Our results suggest that protracted magmatism is a key pre-requisite for PCD genesis, and that differences in geodynamic setting and magma chemistry may account for modulating deposit tonnage. Caricchi et al. (2014) argued that for a similar magma flux, the duration of magmatism is one of the key differences between barren and ore-bearing plutons, but their dataset only included small-volume, short-lived barren plutons (Lago della Vacca and Torres del Paine). Meanwhile, long-lived plutonic systems with variable magma chemistry and related to different geodynamic settings are either barren at the present-day erosion level (e.g., Tuolumne intrusive suite; Coleman et al., 2004) or host variably sized PCDs, including giant deposits (e.g., Bingham vs. Corrocohuayco vs. El Abra; e.g., von Quadt et al., 2011; Chelle Michou et al., 2014; Correa et al., 2016).

In the MOP, Cu-Mo deposits of variable size were all formed at the end of long-lived magmatic episodes with durations between 5.4 and 9.7 m.y. (Fig. 1A). Therefore, we propose that while long-lived magmatism is required for PCD formation, the size of the PCDs may be modulated by the frequency of repeated injections of hot, hydrous, oxidized, S-rich, and Cu-rich mafic magmas that rejuvenate the upper crustal reservoir, allowing for the accumulation of sulfur, metals and volatiles in the upper crust (e.g., Hattori and Keith, 2001; Scaillet, 2010; Audétat and Simon, 2012; Tapster et al., 2016).

SUMMARY AND CONCLUSIONS

This study documents 30 m.y. of incremental pluton construction in the central Tethyan metallogenic belt emplaced during a subduction to post-subduction geodynamic evolution. New comprehensive zircon U-Pb combined with molybdenite Re-Os geochronology in the MOP clearly links Cu-Mo mineralization to the late stages of three successive long-lived (5 to 10 m.y.) intrusive episodes. According to this study, various geodynamic settings and magmas of variable composition can produce PCDs, but the exploration challenge remains in identifying single long-lived and incrementally assembled magmatic suites associated with prospective ore zones. We conclude that protracted incremental crustal scale magmatism is a key requirement for the formation of PCDs in fertile magmatic belts, and that the frequency of upper crustal reservoir rejuvenation by mafic magmas may play a fundamental role for modulating PCD tonnage.

ACKNOWLEDGEMENTS

H.R. and R.M. acknowledge funding by the Swiss NSF projects 200020-138130 and 200020-155928, and the SCOPES Joint Research Project IZ73Z0-128324. Fieldwork of H.R. was funded by the Augustin Lombard Foundation of the Geneva SPHN Society and a SEG student grant from H.E. McKinstry Fund. J.F.W. acknowledges funding through the ETH Zurich postdoctoral fellowship program. We thank C. Chelle-Michou and S. Hovakimyan for fruitful discussions. Constructive comments by journal editor J. B. Murphy and reviews from Y. Lu, R.G. Lee and an anonymous reviewer improved the manuscript. This paper is dedicated to the memory of Rodrik Tayan, who spent his life studying the Meghri pluton and shared his knowledge with passion.

REFERENCES CITED

Aghazadeh, M., Hou, Z., Badrzadeh, Z., and Zhou, L., 2015, Temporal–spatial distribution and tectonic setting of porphyry copper deposits in Iran: Constraints from zircon U–Pb and molybdenite Re–Os geochronology: Ore Geology Reviews, v. 70, p.385-406, doi: 10.1016/j.oregeorev.2015.03.003.

Audétat, A., and Simon, A.C., 2012, Magmatic controls on porphyry Cu genesis, *in* Hedenquist, J.W., Harris, M., and Camus, F., eds, Geology and Genesis of Major Copper Deposits and Districts of the World: A Tribute to Richard Sillitoe: Society of Economic Geologists, Special Publication 16, p. 553-572.

Bagdasaryan, G.P., Gukasyan, R.Kh., and Karamyan, K.A., 1969, Absolute dating of Armenian ore formations: International Geology Review, v. 11, p. 1166–1172, doi: 10.1080/00206816909475161.

Bindeman, I., 2008, Oxygen isotopes in mantle and crustal magmas as revealed by single crystal analysis: Reviews in Mineralogy and Geochemistry, v. 69, p. 445-478, doi: 10.2138/rmg.2008.69.12.

Caricchi, L., Simpson, G., and Schaltegger, U., 2014, Zircons reveal magma fluxes in the Earth's crust: Nature, v. 511, p. 457-461, doi: 10.1038/nature13532.

Chelle-Michou, C., Chiaradia, M., Ovtcharova, M., Ulianov, A., and Wotzlaw, J.F., 2014, Zircon petrochronology reveals the temporal link between porphyry systems and the magmatic evolution of their hidden plutonic roots (the Eocene Coroccohuayco deposit, Peru): Lithos, v. 198, p. 129-140, doi: 10.1016/j.lithos.2014.03.017.

Chiaradia, M., Schaltegger, U., Spikings, R., Wotzlaw, J.F., and Ovtcharova, M., 2013, How accurately can we date the duration of magmatic-hydrothermal events in porphyry

253 systems? - An invited paper: Economic Geology, v. 108, p. 565-584, doi:
254 10.2113/econgeo.108.4.565.
255 Coleman, D.S., Gray, W., and Glazner, A.F., 2004. Rethinking the emplacement and evolution
256 of zoned plutons: Geochronologic evidence for incremental assembly of the Tuolumne
257 Intrusive Suite, California: Geology, v. 32, p. 433-436, doi: 10.1130/G20220.1.
258 Correa, K.J., Rabbia, O.M., Hernández, L.B., Selby, D., and Astengo, M., 2016, The timing of
259 magmatism and ore formation in the El Abra porphyry copper deposit, northern Chile:
260 Implications for long-lived multiple-event magmatic-hydrothermal porphyry systems:
261 Economic Geology, v. 111, p. 1-28, doi: 10.2113/econgeo.111.1.1.
262 Hattori, K.H., and Keith, J.D., 2001, Contribution of mafic melt to porphyry copper
263 mineralization: evidence from Mount Pinatubo, Philippines, and Bingham Canyon,
264 Utah, USA: Mineralium Deposita, v. 36, p.799-806, doi: 10.1007/s001260100209.
265 Hou, Z.Q., Duan, L.F., Lu, Y.J., Zheng, Y.C., Zhu, D.C., Yang, Z.M., Yang, Z.S., Wang, B.D.,
266 Pei, Y.R., Zhao, Z.D., McCuaig, T.C., 2015a, Lithospheric architecture of the Lhasa
267 Terrane and its control on ore deposits in the Himalayan-Tibetan orogeny: Economic
268 Geology, v. 110, p. 1541-1575, doi: 10.2113/econgeo.110.6.1541.
269 Hou, Z.Q., Yang, Z.M., Lu, Y.J., Kemp, A.I.S., Zheng, Y.C., Li, Q.Y., Tang, J.X., Yang, Z.S.,
270 and Duan, L.F., 2015b, A genetic linkage between subduction- and collision-related
271 porphyry Cu deposits in continental collision zones: Geology, v. 43, p. 247–250, doi: 10
272 .1130/G36362.1.
273 Karamyan, K.A., Tayan, R.N., and Guyumdjyan, O.P., 1974, The main features of intrusion
274 magmatism Zangezur region of the Armenian SSR: Izvestia of Academy of Sciences of
275 Armenian SSR, Nauki o Zemle v.1, p. 54-65, (in Russian)

Lackey, J.S., Valley, J.W., and Saleeby, J.B., 2005, Supracrustal input to magmas in the deep crust of Sierra Nevada batholith: evidence from high-$\delta^{18}O$ zircon: Earth and Planetary Science Letters, v. 235, p. 315-330, doi: 10.1016/j.epsl.2005.04.003.

Miller, J.S., Matzel, J.P., Miller, C.F., Burgess, S.D., and Miller, R.B., 2007, Zircon growth and recycling during the assembly of large, composite arc plutons: Journal of Volcanology and Geothermal Research, v. 167, p. 282–299, doi: 10.1016/j.jvolgeores.2007.04.019.

Moritz, R., Rezeau, H., Ovtcharova, M., Tayan, R., Melkonyan, R., Hovakimyan, S., Ramazanov V., Selby, D., Ulianov, A., Chiaradia, M., and Putlitz, B., 2016, Long-lived, stationary magmatism and pulsed porphyry systems during Tethyan subduction to post-collision evolution in the southernmost Lesser Caucasus, Armenia and Nakhitchevan: Gondwana Research, doi: 10.1016/j.gr.2015.10.009 (in press).

Richards, J.P., 2015, Tectonic, magmatic, and metallogenic evolution of the Tethyan orogen: from subduction to collision: Ore Geology Reviews, v. 70, p. 323-345, doi: 10.1016/j.oregeorev.2014.11.009.

Rohrlach, B.D., and Loucks, R.R., 2005, Multi-million-year cyclic ramp-up of volatiles in a lower crustal magma reservoir trapped below the Tampakan copper-gold deposit by Mio-Pliocene crustal compression in the Southern Philippines, *in* Porter, T.M. ed, Super porphyry copper and gold deposits – a global perspective: PGC Publishing, v. 2, p. 369-407.

Scaillet, B., 2010, Economic geology: Volatile destruction: Nature Geoscience, v.3, p. 456–457, doi: 10.1038/ngeo908.

Sillitoe, R.H., 2010, Porphyry copper systems: Economic Geology, v. 105, p. 3–41, doi: 10.2113/gsecongeo.105.1.3.

299 Simmonds, V. and Moazzen, M., 2015, Re–Os dating of molybdenites from Oligocene Cu–Mo–
300 Au mineralized veins in the Qarachilar area, Qaradagh batholith (northwest Iran):
301 implications for understanding Cenozoic mineralization in South Armenia,
302 Nakhichivan, and Iran. International Geology Review, v. 57, p. 290–304, doi:
303 10.1080/00206814.2014.1003339.
304 Tapster, S., Condon, D.J., Naden, J., Noble, S.R., Petterson, M.G., Roberts, N.M.W., Saunders,
305 A.D., and Smith, D.J., 2016, Rapid thermal rejuvenation of high-crystallinity magma
306 linked to porphyry copper deposit formation: evidence from the Koloula porphyry
307 prospect, Solomon Islands: Earth and Planetary Science Letters, doi:
308 http://dx.doi.org/10.1016/j.epsl.2016.02.046 (in press)
309 Tayan, R.N., 1998, On central magma-ore controlling zone of the Zangezur ore region:
310 Proceedings of the National Academy of Sciences of the Republic of Armenia, v. 51, p.
311 20-27, (in Russian with English abstract).
312 Von Quadt, A., Erni, M., Martinek, K., Moll, M., Peytcheva, I., and Heinrich, C.A., 2011, Zircon
313 crystallization and the lifetimes of ore-forming magmatic-hydrothermal systems:
314 Geology, v. 39, p. 731-734, doi: 10.1130/G31966.1.
315

316 **FIGURE CAPTIONS**

317 Figure 1. (A) Geochronology of the Meghri-Ordubad pluton and associated Cu-Mo
318 mineralizations based on 601 concordant zircon U-Pb ages from thirty samples and nine
319 molybdenite Re-Os ages. The Middle Eocene subduction-related calc-alkaline magmatism has a
320 duration of 5.8 ± 0.8 m.y. (green), the Late Eocene – Middle Oligocene shoshonitic suite lasted
321 9.7 ± 0.9 m.y. (blue), and the Late Oligocene shoshonitic to Early Miocene high-K calc-alkaline

adakitic magmas were emplaced within 5.4 ± 0.4 m.y. (red). The calculated mean age associated with each sample does not include antecryst ages (Miller et al., 2007; Appendice DR1 and Table DR2). Numbers 1 to 30 refer to the sample locations in Figure 2 and the descriptions in Tables DR1 and DR2. Asterisks indicate dike samples. (B) Zircon *in situ* hafnium (Table DR4) and oxygen isotopic data (Table DR5) as a function of age. Hf isotope data are shown as individual analyses (n=365) and as sample median values while oxygen isotopic data are only shown as median $\delta^{18}O$ values (based on 280 analyses) due to limited inter- and intragrain variability.

Figure 2. Construction of the Meghri-Ordubad pluton based on U-Pb geochronology. Stars indicate locations of porphyry Cu-Mo deposits for each intrusive stage. Numbers 1 to 30 refer to dated samples described in Figure 1 and Tables DR1 and DR2. The red dotted lines define international borders. Geological map modified after Karamyan et al. (1974).

[1]GSA Data Repository item 2016xxx, Appendice DR1, Figures DR1-DR3, and Tables DR1-DR5, is available online at www.geosociety.org/pubs/ft2016.htm, or on request from editing@geosociety.org or Documents Secretary, GSA, P.O. Box 9140, Boulder, CO 80301, USA.

Figure

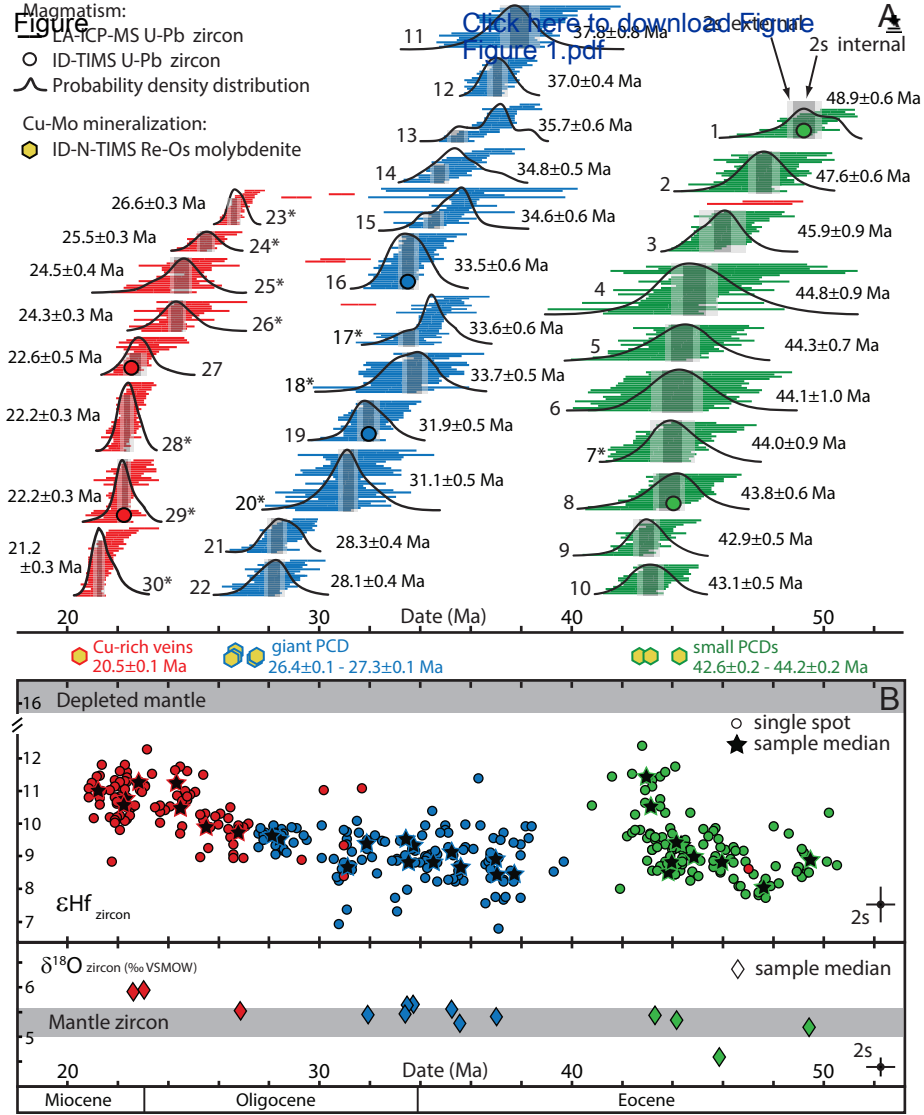
Magmatism:
LA-ICP-MS U-Pb zircon
ID-TIMS U-Pb zircon
Probability density distribution
Cu-Mo mineralization:
ID-N-TIMS Re-Os molybdenite
Click here to download Figure Figure 1.pdf
A
2σ external
2s internal
11 37.8±0.8 Ma
12 37.0±0.4 Ma
13 35.7±0.6 Ma
14 34.8±0.5 Ma
15 34.6±0.6 Ma
16 33.5±0.6 Ma
17* 33.6±0.6 Ma
18* 33.7±0.5 Ma
19 31.9±0.5 Ma
20* 31.1±0.5 Ma
21 28.3±0.4 Ma
22 28.1±0.4 Ma
23* 26.6±0.3 Ma
24* 25.5±0.3 Ma
25* 24.5±0.4 Ma
26* 24.3±0.3 Ma
27 22.6±0.5 Ma
28* 22.2±0.3 Ma
29* 22.2±0.3 Ma
30* 21.2 ±0.3 Ma
1 48.9±0.6 Ma
2 47.6±0.6 Ma
3 45.9±0.9 Ma
4 44.8±0.9 Ma
5 44.3±0.7 Ma
6 44.1±1.0 Ma
7* 44.0±0.9 Ma
8 43.8±0.6 Ma
9 42.9±0.5 Ma
10 43.1±0.5 Ma
20
30
Date (Ma)
40
50
Cu-rich veins
20.5±0.1 Ma
giant PCD
26.4±0.1 - 27.3±0.1 Ma
small PCDs
42.6±0.2 - 44.2±0.2 Ma
B
Depleted mantle
16
12
11
10
9
8
7
single spot
sample median
εHf zircon
2s
δ18O zircon (‰ VSMOW)
6
5
Mantle zircon
sample median
2s
20
30
Date (Ma)
40
50
Miocene
Oligocene
Eocene

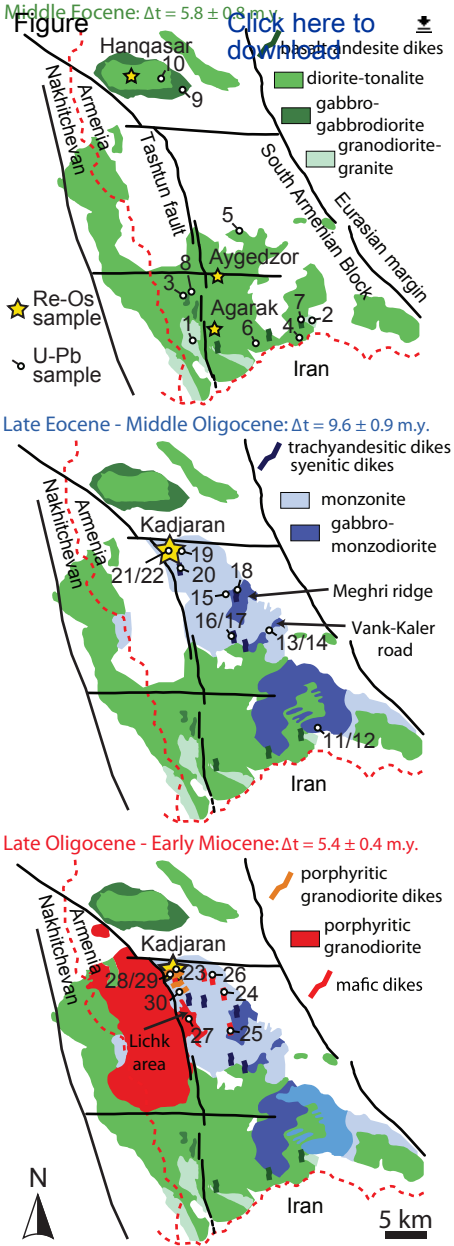
Middle Eocene: Δt = 5.8 ± 0.8 m.y.
Figure
Click here to download
Hanqasar
10
9
Armenia
Nakhitchevan
Tashtun fault
South Armenian Block
Eurasian margin
basaltandesite dikes
diorite-tonalite
gabbro-gabbrodiorite
granodiorite-granite
5
8
Aygedzor
3
Agarak
7
2
1
6
4
Re-Os sample
U-Pb sample
Iran
Late Eocene - Middle Oligocene: Δt = 9.6 ± 0.9 m.y.
trachyandesitic dikes
syenitic dikes
monzonite
gabbro-monzodiorite
Kadjaran
19
21/22
20
18
15
Meghri ridge
16/17
Vank-Kaler road
13/14
11/12
Iran
Late Oligocene - Early Miocene: Δt = 5.4 ± 0.4 m.y.
porphyritic granodiorite dikes
porphyritic granodiorite
mafic dikes
Kadjaran
23
26
28/29
24
30
Lichk area
27
25
N
Iran
5 km

Analytical methods

Major elements whole-rock geochemistry

The thirty igneous rock samples from the Meghri–Ordubad pluton selected for dating were analysed for whole rock geochemistry. The samples were crushed using a steel jaw crusher and subsequently a hydraulic press and finally powdered to <70 μm using a mortar agate mill. Major elements were analysed on fused lithium tetraborate ($Li_2B_4O_7$) glass beads by X-ray fluorescence (XRF) using a Philips PW 2400 spectrometer at the University of Lausanne, Switzerland. The 2σ uncertainties are <1%, except for MgO and K_2O <3%, based on repeated measurements of the BHVO-1, NIM-N and NIM-G standards.

In situ U-Pb zircon dating by LA-ICP-MS

The thirty igneous rock samples selected for dating were initially crushed, milled to <0.3 mm and processed using a gravity separation Wilfley table, a Frantz magnetic separator and a density separation in diiodomethane liquid at 3,32 $g.mL^{-1}$. Zircon grains were handpicked under a binocular microscope, and subsequently mounted in epoxy and polished. Zircon grains textures were revealed by cathodoluminescence images using a scanning electron microscope JEOL JSM7001F and CamScan MV2300 at the Institute of Earth Sciences of the University of Geneva and Lausanne, respectively.

In-situ U-Pb dating of zircon by laser ablation inductively coupled plasma mass spectrometry (LA-ICP-MS) was carried out using an UP-193FX excimer laser ablation system interfaced to an ELEMENT XR sector field, single-collector ICP mass spectrometer at the Institute of Earth Sciences of the University of Lausanne. The operating conditions of the ablation system included a spot size of 35 μm, a repetition rate of 5 Hz, and an on-sample energy density of ~3 J/cm^2 per pulse. The measurement protocol and details related to the mass spectrometer optimisation are outlined in Ulianov et al. (2012). A GJ-1 standard zircon with an ID-TIMS $^{206}Pb/^{238}U$ age of 600.5±0.4 Ma (Schaltegger et al., *unpublished*; in Boekhout et al., 2012) was used for the standardisation of the relative sensitivity factor. For the accuracy control, the Plešovice standard was employed (Sláma et al., 2008). Raw intensity vs. time data

were reduced in LAMTRACE (Jackson, 2008). Only homogeneous time resolved $^{206}Pb/^{238}U$ and $^{207}Pb/^{235}U$ spectra corresponding to one single isotope abundance ratio per ablation are reported in this study. Weighted mean ages and concordia diagrams were obtained using Isoplot (Ludwig, 2008).

The mean age (i.e. crystallization age) is calculated from all concordant zircon population. Based on the probability density estimate curve and the mean square weighted deviation (MSWD), some samples exhibit subpopulations (see Figure 1, samples n°1, 13, 14, 15, 17, 21, 23, 27, 28 and 30; Table DR2), and we only considered the younger subpopulation to represent the crystallization age, the older subpopulation interpreted as antecrystic or inherited zircons for adjacent rocks (Miller et al., 2007).

Reported errors (2 SD) in Figure 1 are named "internal" and "external" errors. The "internal" error corresponds to the analytical uncertainties from the sample measurement, while the "external" error includes the propagation of analytical uncertainties from the sample measurement and the reproducibility of the measurements on the primary standard GJ-1 (Fig. 1).

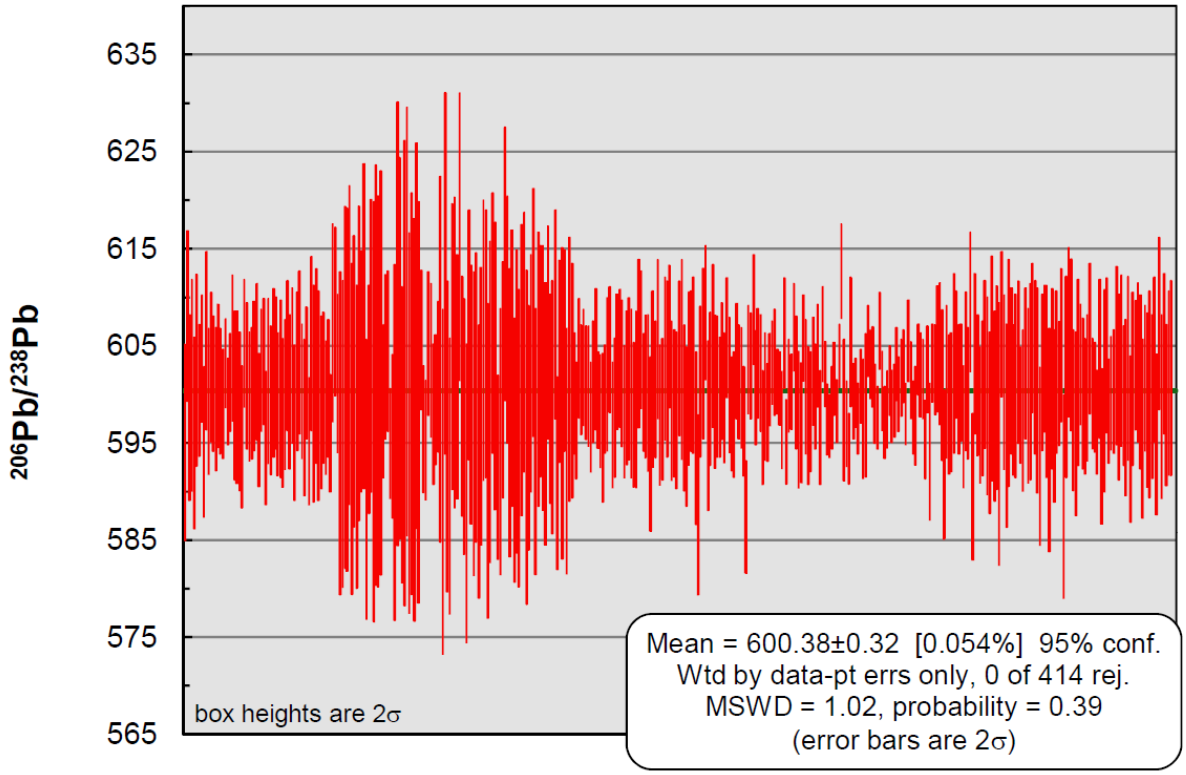

Figure 1: Reproducibility of the GJ1 standard including all analytical sessions carried out over 18 months.

Re-Os isotopes in molybdenite

Samples for Re-Os dating in molybdenite were selected from various Cu-Mo porphyry deposits throughout the Meghri-Ordubad pluton (see Figs. 1 and 2; Table DR3). Sample RO280-2_N2 corresponds to a stockwork-like veinlet mainly filled by quartz-chalcopyrite-molybdenite from Agarak deposit, whereas samples RO812-3_Ankaser_N72p and RO812-7_Aigedzor_NRM-0560 were selected from quartz-molybdenite stockwork-like veinlets from Hanqasar and Aygedzor, respectively. Six samples from quartz-molybdenite (RO280-1_NI) and quartz-chalcopyrite-molybdenite (RO758-5_KJ1509, RO596-2_KJ-13-25A, RO612-10_KJ-13-25A, RO391-2_KJ-10-13A, and RO758-6_KJ15X1) stockwork-like veinlets were collected from the giant Kadjaran Cu-Mo deposit (see Figs. 1 and 2; Table DR3). Grain size of molybdenite varies from 500μm to 2 mm.

Analyses were performed in the Laboratory for Sulfide and Source Rock Geochronology and Geochemistry in the Durham Geochemistry Center at the University of Durham (UK). The complete analytical procedure for Re-Os determinations is described in Selby and Creaser (2004) and Selby et al. (2007), and it is briefly described below. Molybdenite samples were dissolved and equilibrated with a known amount of ^{185}Re and isotopically normal Os in inverse *aqua-regia* (2:1 16 *N* HNO_3 and 12 *N* HCl, 3 mL) at 240°C for 24 h in a Carius tube. Rhenium and Os were isolated and purified by solvent extraction, microdistillation, and anion exchange chromatography, and analyzed by negative thermal ionization mass spectrometry (N-TIMS) on a Fisher Scientific TRITON mass spectrometer using Faraday collectors. Total procedural blanks for Re and Os, are 2.2 ± 0.5 pg and 0.1 ± 0.03 pg, respectively, with an ^{187}Os/^{188}Os blank composition of 0.24 ± 0.05 (n = 3). Rhenium and Os concentrations and Re-Os molybdenite date uncertainties are presented at the 2σ level, which includes the uncertainties in Re and Os mass spectrometer measurement, spike and standard Re and Os isotope compositions, and calibration uncertainties of ^{185}Re and ^{187}Os. Because a mixed ^{185}Re and Os tracer solution is used, uncertainties in weights of sample and tracer solution do not affect the calculated age, and are not considered. However, sample and

tracer solution weight uncertainties are considered in determining the uncertainty in the Re and ^{187}Os concentrations. Uncertainty with and without the ^{187}Re decay constant (Smoliar et al., 1996; Selby et al., 2007) is also considered (Table 4).

In situ zircon Hf isotope analyses

In-situ Hf isotope analyses were carried out at the University of Geneva on a Teledyne - Photon Machines "Analyte G2" laser system equipped with a two volume "HelEx-2" ablation cell (d'Abzac et al. 2014) and coupled to a Thermo « Neptune Plus » MC-ICP-MS. Ablation was performed over 35 µm spots at a fluence of ~6J.cm^{-2} and a repetition rate of 5Hz. Ablated particles were carried through a ~1.5 m PTFE tubing using a ~0.6 L.min^{-1} He gas flow (99.999% purity) and mixed with ~2.4 mL.min^{-1} N_2 and ~1 L.min^{-1} Ar before entering the plasma torch. Measurements were performed at low mass resolution (~450) over 120 × 1s cycles using the following cup configuration: ^{171}Yb (L4), ^{173}Yb (L3), ^{174}(Yb+Hf) (L2), ^{175}Lu (L1), ^{176}(Hf+Yb+Lu) (C), ^{177}Hf (H1), ^{178}(Hf+Ta) (H2), ^{179}Hf (H3), ^{181}Ta (H4). Blanks were acquired following the same method as samples, without ablation, every ca. 10 analyses. Reference zircons Plešovice (Sláma et al., 2008) and Temora-2 (Woodhead and Hergt, 2005) were measured after every 5 to 8 unknowns. Plešovice and Temora-2 zircons reach respective 0.282479±0.000027 (n=89) and 0.282670±0.000036 (n=98) over 10 months and 6 measurements sessions (see details in Table DR 3). These values show a slight offset from the reference values to which the sample data are normalized. Instrument tuning is then performed so that this offset is (i) as small as possible (<1 εHf) and (ii) similar within uncertainty for all the different reference materials used. This insures that the correction is accurately made for various trace elements concentrations potentially generating oxide species in the ICP torch and for different amounts of ^{176}Yb that need to be corrected (see below).

Data reduction was conducted after acquisition by proceeding to a blank subtraction, removing the isobaric interference of ^{176}Lu and ^{176}Yb on mass 176 (e.g. Fisher et al., 2011) and correcting the

resulting $^{176}Hf/^{177}Hf$ ratio for mass bias using an exponential law (Albarede et al., 2004). The mass bias coefficients βYb and βHf were calculated from the measured $^{173}Yb/^{171}Yb$ and $^{179}Hf/^{177}Hf$ with the reference values $^{173}Yb/^{171}Yb=1.1234$ (Thirlwall and Anczkiewicz, 2004) and $^{179}Hf/^{177}Hf=0.7325$ (Patchett and Tatsumoto, 1981) respectively. We used βYb to correct for Lu mass bias (Yuan et al., 2008) and the ^{176}Lu interference was corrected using $^{176}Lu/^{175}Lu=0.02645$ (Thirlwall and Anczkiewicz, 2004). The isobaric interference of ^{176}Yb is potentially high in zircons and was evaluated using $^{176}Yb/^{173}Yb=0.786954$ (Thirlwall and Anczkiewicz, 2004). Correction for ^{176}Hf in-growth due to ^{176}Lu β--decay has been calculated (Iizuka and Hirata, 2005) using $\lambda^{176}Lu=1.87\times10\text{-}11$ year-1 (Söderlund et al., 2004) and the age determined in this study by U-Pb dating on zircon. The data are expressed as εHf units following:

$$\varepsilon Hf = [(^{176}Hf/^{177}Hf)_{measured} / (^{176}Hf/^{177}Hf)_{CHUR} - 1] \times 10000$$

with the reference "CHUR" value of 0.282785 is taken from Bouvier et al. (2008).

In situ zircon O isotope analyses

Oxygen isotopes measurements were carried out on a different zircon sample set than those used for LA-ICPMS U-Pb zircon dating but their cathodoluminescence patterns are very consistent from one zircon sample set to another from the same crushed sample. The U-Pb weighted mean dates are considered to be representative enough to accurately trace the source evolution over 30 Ma (Table DR2).

Sample preparation and secondary ion mass spectrometry (SIMS) were carried out at the Canadian Centre for Isotopic Microanalysis (CCIM) at the University of Alberta. Polished zircon mid-sections of unknowns and zircon reference materials were exposed within a 25 mm diameter epoxy mount (M1323) using diamond grits. The mount was cleaned with a lab soap solution, and de-ionized H_2O. Prior to scanning electron microscopy (SEM), the mount was coated with 5 nm of high-purity Au. SEM characterization was carried out with a Zeiss EVO MA15 instrument equipped with a high-sensitivity,

broadband cathodoluminescence (CL) detector. Beam conditions were 15kV and 2 nA sample current. A further 25 nm of Au was subsequently deposited on the mount prior to SIMS analysis.

Oxygen isotopes (^{18}O, ^{16}O) in zircon were analyzed using a Cameca IMS 1280 multicollector ion microprobe. A $^{133}Cs+$ primary beam was operated with impact energy of 20 keV and beam current of ~ 2.5 nA. The ~12 µm diameter probe was rastered (18 x 18 µm) for 75 s prior to acquisition, and then 5 x 5 µm during acquisition, forming rectangular analyzed areas ~15 x 18 µm across and ~2 µm deep. The normal incidence electron gun was utilized for charge compensation. Negative secondary ions were extracted through 10 kV into the secondary (Transfer) column. Transfer conditions included a 122 µm entrance slit, a 5 x 5 mm pre-ESA (field) aperture, and 100x sample magnification at the field aperture, transmitting all regions of the sputtered area. No energy filtering was employed. The mass/charge separated oxygen ions were detected simultaneously in Faraday cups L'2 (^{16}O-) and H'2 (^{18}O-) at mass resolutions (m/Δm at 10%) of 1950 and 2250, respectively. Secondary ion count rates for ^{16}O- and ^{18}O- were typically ~2.5 x 10^9 and 5 x 10^6 counts/s utilizing 10^{10} Ω and 10^{11} Ω amplifier circuits, respectively. Faraday cup baselines were measured at the start of the analytical session. A single analysis took 250 s, including pre-analysis rastering, automated secondary ion tuning, and 75 s of continuous peak counting.

Instrumental mass fractionation (IMF) was monitored by repeated analysis of a zircon primary reference material (RM), S0081 (UAMT1) with $\delta^{18}O$ VSMOW = +4.87 (R. Stern, unpublished laser fluorination data from Ilya Bindeman, University of Oregon) and a secondary zircon RM, S0022 (TEM2) zircon with $\delta^{18}O$ VSMOW = +8.2 ‰ (Black et al., 2004). One analysis of the primary and secondary RM was taken after every 4 and 12 unknowns, respectively. Spot analyses of unknowns totalled 280. The data set of $^{18}O^-/^{16}O^-$ for S0081 zircon for each of two analytical sessions (N = 45, 51) was processed collectively for each session, yielding standard deviations of 0.10‰ and 0.07‰, following correction for systematic within-session drift (≤0.4 ‰). Overall IMF was +1.1 ‰ for both sessions. The individual spot uncertainties at 95% confidence for $\delta^{18}O_{VSMOW}$ reported include errors relating to within-spot counting statistics, between-spot (geometric) effects, and correction for instrumental mass

fractionation, and average ± 0.19 ‰. Results for multiple spots on multiple grains of the secondary RM, S0022, gave session mean values for $\delta^{18}O_{VSMOW}$ = +8.20 ±0.04 (MSWD = 0.79; N = 18, standard deviation = 0.08‰) and +8.19 ±0.05 (MSWD = 0.56; N = 15, standard deviation = 0.07‰).

References :

Albarede, F., Telouk, P., Blichert-Toft, J., Boyet, M., Agranier, A., and Nelson, B., 2004, Precise and accurate isotopic measurements using multiple-collector ICPMS: Geochimica and Cosmochimica Acta v. 68, p. 2725-2744, doi:10.1016/j.gca.2003.11.024.

Black, L. P., Kamo, S. L., Allen, C. M., Davis, D., Aleinikoff, J. N., Valley, J. W., Mundil, R., Campbell, I. H., Korsch, R. J., Williams, I. S., and Foudoulis, C., 2004, Improved $^{206}Pb/^{238}U$ microprobe geochronology by the monitoring of a trace-element-related matrix effect; SHRIMP, ID-TIMS, ELA-ICP-MS and oxygen isotope documentation for a series of zircon standards: Chemical Geology, v. 205, p. 115-140, doi:10.1016/j.chemgeo.2004.01.003.

Boekhout F., Spikings R., Sempere T., Chiaradia M., Ulianov A. and Schaltegger U., 2012, Mesozoic arc magmatism along the southern Peruvian margin during Gondwana breakup and dispersal: Lithos, v. 146, p. 48-64, doi:10.1016/j.lithos.2012.04.015.

Bouvier, A., Vervoort, J. D., and Patchett, P. J., 2008, The Lu–Hf and Sm–Nd isotopic composition of CHUR: Constraints from unequilibrated chondrites and implications for the bulk composition of terrestrial planets: Earth and Planetary Science Letters, v. 273, p. 48-57, doi:10.1016/j.epsl.2008.06.010.

d'Abzac, F.-X., Czaja, A. D., Beard, B. L., Schauer, J. J., and Johnson, C. M., 2014, Iron Distribution in Size-Resolved Aerosols Generated by UV-Femtosecond Laser Ablation: Influence of Cell Geometry and Implications for In Situ Isotopic Determination by LA-MC-ICP-MS: Geostandards and Geoanalytical Research, v.38, p. 293-309, doi:10.1111/j.1751-908X.2014.00281.x.

167 Fisher, C. M., Hanchar, J. M., Samson, S. D., Dhuime, B., Blichert-Toft, J., Vervoort, J. D., and Lam,
168 R., 2011, Synthetic zircon doped with hafnium and rare earth elements: A reference material for in situ
169 hafnium isotope analysis: Chemical Geology, v.286, p. 32-47, doi:10.1016/j.chemgeo.2011.04.013.

170 Iizuka, T. and Hirata, T., 2005, Improvements of precision and accuracy in in situ Hf isotope
171 microanalysis of zircon using the laser ablation-MC-ICPMS technique: Chemical Geology, v.220, p.
172 121-137, doi:10.1016/j.chemgeo.2005.03.010.

173 Jackson, S., 2008, LAMTRACE data reduction software for LA-ICP-MS. Laser ablation ICP-MS in the
174 Earth sciences: Current practices and outstanding issues: Mineralogical Association of Canada, *Short*
175 *Course Series 40*, p. 305-307.

176 Ludwig, K.R., 2008, User's Manual for Isoplot 3.70: A geochronological toolkit for Microsoft Excel:
177 Berkeley Geochronology Center, Special Publication 4, 77 p.

178 Miller, J.S., Matzel, J.P., Miller, C.F., Burgess, S.D., and Miller, R.B., 2007, Zircon growth and
179 recycling during the assembly of large, composite arc plutons. Journal of Volcanology and Geothermal
180 Research, v. 167, p. 282–299, doi: 10.1016/j.jvolgeores.2007.04.019.

181 Patchett, P. J. and Tatsumoto, M., 1981, A routine high-precision method for Lu-Hf isotope
182 geochemistry and chronology: Contributions to Mineralogy and Petrology, v.75, p. 263-267,
183 doi:10.1007/BF01166766.

184 Pearce, N.J., Perkins, W.T., Westgate, J.A., Gorton, M.P., Jackson, S.E., Neal, C.R., and Chenery, S.P.,
185 1997, A compilation of new and published major and trace element data for NIST SRM610 and NIST
186 SRM612 glass reference materials: Geostandards, Newsletter 21, p. 115–144, doi:10.1111/j.1751-
187 908X.1997.tb00538.x.

188 Selby, D., and Creaser, R.A., 2004, Macroscale NTIMS and microscale LA-MC-ICP-MS Re-Os isotopic
189 analysis of molybdenite: Testing spatial restrictions for reliable Re-Os age determinations, and
190 implications for the decoupling of Re and Os within molybdenite: Geochimica et Cosmochimica

Acta, v. 68, p. 3897–3908, doi:10.1016/j.gca.2004.03.022.

Selby, D., Creaser, R.A., Stein, H. J., Markey, R. J., and Hannah, J. L., 2007, Assessment of the 187Re decay constant accuracy and precision: Cross calibration of the ^{187}Re-^{187}Os molybdenite and U-Pb zircon chronometers: Geochimica et Cosmochimica Acta, v. 71, p.1999–2013, doi:10.1016/j.gca.2007.01.008.

Sláma, J., Košler, J., Condon, D. J., Crowley, J. L., Gerdes, A., Hanchar, J. M., Horstwood, M. S. A., Morris, G. A., Nasdala, L., Norberg, N., Schaltegger, U., Schoene, B., Tubrett, M. N., and Whitehouse, M. J., 2008, Plešovice zircon - A new natural reference material for U–Pb and Hf isotopic microanalysis: Chemical Geology, v.249, p. 1-35, doi:10.1016/j.chemgeo.2007.11.005.

Smoliar, M.I., Walker, R.J., and Morgan, J.W., 1996, Re-Os isotope constraints on the age of Group IIA, IIIA, IVA, and IVB iron meteorites: Science, v. 271, p. 1099–1102, doi: 10.1126/science.271.5252.1099.

Söderlund, U., Patchett, P. J., Vervoort, J. D., and Isachsen, C. E., 2004, The ^{176}Lu decay constant determined by Lu–Hf and U–Pb isotope systematics of Precambrian mafic intrusions: Earth and Planetary Science Letters, v. 219, p. 311-324, doi:10.1016/S0012-821X(04)00012-3.

Thirlwall, M. F. and Anczkiewicz, R., 2004, Multidynamic isotope ratio analysis using MC–ICP–MS and the causes of secular drift in Hf, Nd and Pb isotope ratios: International Journal of Mass Spectrometry, v.235, p.59-81, doi:10.1016/j.ijms.2004.04.002.

Ulianov A., Muntener O., Schaltegger U. and Bussy F., 2012, The data treatment dependent variability of U-Pb zircon ages obtained using mono-collector, sector field, laser ablation ICP-MS: Journal of Analytical Atomic Spectrometry, v.27, p. 663-676, doi:10.1039/C2JA10358C.

Woodhead, J. D. and Hergt, J. M., 2005, A Preliminary Appraisal of Seven Natural Zircon Reference Materials for In Situ Hf Isotope Determination: Geostandards and Geoanalytical Research, v.29, p. 183-195, doi:10.1111/j.1751-908X.2005.tb00891.x.

Yuan, H. L., Gao, S., Dai, M. N., Zong, C. L., Günther, D., Fontaine, G. H., Liu, X. M., and Diwu, C., 2008, Simultaneous determinations of U–Pb age, Hf isotopes and trace element compositions of zircon by excimer laser-ablation quadrupole and multiple-collector ICP-MS: Chemical Geology, v.247, p. 100-118, doi:10.1016/j.chemgeo.2007.10.003.

Table DR1: Summary of location, classification, major (XRF) and selected trace elements (LA-ICP-MS) geochemistry, weighted mean U-Pb zircon ages, median εHf and δ18O for 30 representative samples from this study and 6 additional samples from Moritz et al. (2016)

							Whole-rock analysis														zircons			
Samples	N° Figs. 1 & 2	Location	Longitude	Latitude	Altitude	Rock type (TAS classification in Fig. DR2)	SiO_2	TiO_2	Al_2O_3	Fe_2O_3	MnO	MgO	CaO	Na_2O	K_2O	P_2O_5	LOI	Mg#	Cr	Ni	Sr	Y	Mean Age ± 2SD (Ma)	Mean εHf ± 2SD	Mean $\delta^{18}O$ (SMOW) ± 2SD	References
					(m)		(wt. %)												(ppm)				(Ma)		(‰)	
AG1304A	1	Agarak area	E46 11.734	N38 53.804	923	Granodiorite/Granite	70.26	0.34	15.28	2.52	0.01	0.48	2.38	5.81	0.55	0.09	0.86	0.27	26.69	2.00	332.44	14.70	48.0 ± 0.6	8.7 ± 1.1	5.20 ± 0.19	this study
AG1006A	-	Agarak area	E46 11.780	N38 53.735	-	Granite	71.20	0.35	15.51	2.77	0.01	0.91	2.58	5.30	0.72	0.11	0.67	0.39	13.00	b.d.	380.00	17.00	**48.99 ± 0.07**	-	-	Moritz et al. 2016
MR1501	2	Alvank area	E46 19.892	N38 56.303	772	Tonalite	64.92	0.51	15.75	5.22	0.13	1.92	4.99	3.47	2.08	0.15	0.33	0.42	16.00	3.00	269.00	16.00	47.6 ± 0.6	8.0 ± 0.6	-	this study
AG1401	3	Vahravar area	E46 10.329	N38 57.179	1345	Hornblende Gabbro	45.77	0.90	20.17	10.61	0.17	5.41	11.54	2.27	1.10	0.44	0.65	0.50	10.29	14.19	467.73	20.36	45.9 ± 0.9	8.8 ± 1.0	4.51 ± 0.19	this study
AG1404	4	Araksashen area	E46 17.324	N38 55.012	749	Diorite/Tonalite	60.61	0.64	16.36	6.63	0.14	2.82	5.85	3.38	2.31	0.16	0.48	0.46	21.72	5.56	407.44	22.81	44.8 ± 0.9	9.0 ± 0.9	-	this study
VK1403	5	Vank-Kaler road	E46 13.036	N39 02.034	1787	Quartz monzonite	65.87	0.65	14.99	4.65	0.09	1.11	3.35	3.22	4.45	0.16	0.57	0.32	15.70	2.97	179.93	37.88	44.3 ± 0.7	9.3 ± 0.9	-	this study
AG1403	6	Araksashen area	E46 17.324	N38 55.012	749	Diorite	58.34	0.90	13.86	9.96	0.21	4.16	5.63	2.63	2.43	0.21	0.73	0.45	20.41	8.22	297.85	37.18	44.1 ± 1	9.4 ± 0.9	-	this study
AG1007	-	Agarak area	E46 13.274	N38 53.862	-	Granodiorite	69.40	0.28	16.51	2.39	0.09	0.46	3.22	5.12	2.01	0.08	0.38	0.28	10.00	b.d.	635.00	7.70	**44.03 ± 0.02**	-	-	Moritz et al. 2016
AG1406	7	Alvank area	E46 19.892	N38 56.303	772	Basaltic-andesite dike	55.05	0.70	17.07	8.29	0.15	4.68	8.02	3.71	1.24	0.14	0.46	0.53	100.37	22.85	433.90	19.27	44 ± 0.9	8.8 ± 0.9	-	this study
AG1402	8	Vahravar area	E46 10.329	N38 57.179	1345	Diorite	59.65	0.68	16.25	7.03	0.16	2.96	6.70	3.24	1.89	0.18	0.37	0.45	21.62	6.09	405.26	24.60	43.8 ± 0.6	8.5 ± 0.9	5.32 ± 0.19	this study
HQ1402	9	Hanqasar area	E46 08.393	N39 13.702	1626	Monzodiorite	52.16	0.57	21.78	6.76	0.17	2.36	9.24	4.31	1.03	0.27	0.57	0.41	12.11	5.10	1511.22	16.38	42.9 ± 0.5	11.3 ± 1.0	-	this study
HQ1403	10	Hanqasar area	E46 07.348	N39 13.805	1699	Tonalite	63.93	0.38	16.37	4.37	0.11	1.74	4.70	3.88	2.93	0.19	0.50	0.44	52.70	11.23	382.26	15.92	43.1 ± 0.5	10.4 ± 1.0	5.42 ± 0.20	this study
AG1308A1	11	Schwanidzor area	E46 22.594	N38 56.873	849	Monzogabbro (Tephrite?)	47.37	1.06	19.73	8.77	0.23	3.81	8.63	4.09	3.25	0.67	1.61	0.46	47.40	17.22	1907.06	26.94	37.8 ± 0.8	8.4 ± 1.3	-	this study
AG1308A	12	Schwanidzor area	E46 22.594	N38 56.873	849	Monzodiorite	53.52	0.51	22.51	4.25	0.12	1.29	7.17	5.05	3.44	0.32	1.05	0.38	13.14	1.97	2891.82	18.76	37 ± 0.4	8.4 ± 1.3	5.37 ± 0.19	this study
VK1404	13	Near Kaler	E46 16.975	N39 03.411	2267	Monzogabbro	48.95	0.92	17.85	9.44	0.16	5.20	10.24	3.55	1.45	0.49	0.36	0.52	18.84	15.56	1371.15	21.51	35.7 ± 0.6	8.9 ± 1.0	-	this study
VK1405	14	Near Kaler	E46 16.975	N39 03.411	2267	Monzodiorite	53.03	0.54	21.27	6.08	0.09	2.14	8.27	4.08	2.55	0.67	0.40	0.41	21.33	14.23	1534.87	20.80	34.8 ± 0.5	8.6 ± 1.2	5.26 ± 0.20	this study
MR1403	15	Meghri ridge	E46 14.495	N39 05.877	2762	Monzodiorite	52.66	0.74	20.00	6.33	0.14	2.64	7.19	4.58	3.80	0.55	0.57	0.45	16.17	6.32	1460.97	25.11	34.6 ± 0.6	9.1 ± 1.3	5.58 ± 0.18	this study
LI1303A1	16	Vank-Kaler road	E46 15.578	N39 03.458	2000	Monzogabbro	47.86	0.93	21.53	8.77	0.13	3.43	10.85	3.26	1.62	0.51	0.91	0.44	2.80	3.59	1332.91	22.62	33.5 ± 0.6	8.8 ± 1.0	5.64 ± 0.19	this study
LI1303	17	Vank-Kaler road	E46 15.578	N39 03.458	2000	Syenitic dike	59.80	0.59	18.54	4.73	0.13	1.29	3.38	5.29	5.35	0.31	0.49	0.35	6.20	b.d.	665.43	27.37	33.6 ± 0.6	8.8 ± 1.5	-	this study
MR1402/KJ1207	-	Meghri ridge	E46 13.287	N39 06.159	2685	Hornblende Gabbro	41.69	1.46	19.04	11.89	0.21	6.84	12.89	2.30	0.69	1.23	0.53	0.53	14.06	b.d.	1816.68	34.15	**33.49 ± 0.02**	9.5 ± 0.6	5.51 ± 0.18	this study / Moritz et al. 2016
KJ1316	18	Meghri ridge	E46 13.287	N39 06.159	2685	Trachyandesite dike	60.26	0.50	17.54	5.35	0.13	1.77	5.09	4.37	3.57	0.40	0.34	0.40	13.99	2.76	1103.98	24.42	33.7 ± 0.5	9.4 ± 0.5	5.62 ± 0.19	this study
KJ1006A	19	Atkis	E46 12.745	N39 09.076	1682	Monzonite	57.09	0.82	18.62	5.29	0.12	2.02	4.00	4.28	6.05	0.41	0.71	0.43	8.00	5.28	692.00	21.93	31.9 ± 0.5	9.4 ± 0.8	-	this study
KJ1002	-	Atkis	E46 09.528	N39 09.584	-	Monzonite	56.86	0.85	17.66	6.50	0.13	2.69	4.97	3.85	4.63	0.39	0.55	0.45	11.00	8.31	722.00	25.80	**31.83 ± 0.02**	-	5.47 ± 0.19	Moritz et al. 2016
KJ1308	20	Road to Meghri	E46 11.134	N39 08.656	1929	Syenitic dike	60.88	0.90	18.67	4.24	0.09	0.99	2.00	3.57	7.98	0.17	0.50	0.32	2.50	b.d.	512.01	19.69	31.1 ± 0.5	8.7 ± 1.0	-	this study
KJ1508	21	Kadjaran Open pit	E46 08.026	N39 08.972	1866	Gabbro (weakly altered)	47.48	0.97	18.27	10.28	0.15	5.97	10.45	2.90	1.02	0.56	1.09	0.53	54.60	37.00	1368.70	18.30	28.3 ± 0.4	9.5 ± 0.6	-	this study
KJ1509	22	Kadjaran open pit	E46 08.026	N39 08.972	1866	Monzonite (heavily altered)	-	-	-	-	-	-	-	-	-	-	-	-	-	-	-	-	28.1 ± 0.4	9.6 ± 0.5	-	this study
KJ1302A	23	Kadjaran Open pit	E46 08.414	N39 08.757	1887	Trachyandesite dike	58.41	0.64	14.20	4.70	0.12	1.72	4.39	0.23	6.73	0.44	6.48	0.42	74.30	39.96	225.79	10.48	26.6 ± 0.3	9.7 ± 0.9	5.54 ± 0.19	this study
KJ1303A1	24	Near Karnarut	E46 12.629	N39 07.513	2142	Trachybasalt dike	46.93	1.06	13.68	7.52	0.14	7.13	8.56	2.84	2.44	0.56	8.76	0.65	397.90	143.68	2370.03	16.19	25.5 ± 0.3	9.9 ± 1.1	-	this study
MR1401	25	Meghri Ridge	E46 12.808	N39 06.430	2547	Trachyandesite dike	61.43	0.60	15.49	4.47	0.08	2.29	4.11	3.66	3.85	0.27	2.97	0.50	44.51	19.92	801.97	13.21	24.5 ± 0.4	11.2 ± 0.9	-	this study
KJ1307	26	Road to Pukhut	E46 12.907	N39 08.182	1865	Trachybasalt dike	50.95	0.78	14.13	6.72	0.11	7.82	7.18	3.17	2.01	0.37	6.59	0.70	279.10	200.54	759.34	14.66	24.3 ± 0.3	10.4 ± 0.8	-	this study
LI1301	27	Lichk area	E46 10.368	N39 01.780	1797	Porphyritic Granodiorite	66.66	0.47	14.95	3.27	0.05	2.02	3.21	4.01	3.72	0.22	0.61	0.55	68.98	33.39	618.28	9.51	22.6 ± 0.5	11.2 ± 1.2	5.97 ± 0.19	this study
LI1003	-	Lichk area	E46 10.375	N39 02.777	-	Porphyritic Granodiorite	66.97	0.48	15.26	3.35	0.05	2.06	3.19	3.88	3.50	0.21	0.6	0.55	58.00	39.00	670.00	10.00	**22.46 ± 0.02**	-	-	Moritz et al. 2016
KJ1325A	28	Kadjaran Open pit	E46 08.416	N39 08.840	1901	porphyritic granodioritic dike	61.25	0.42	14.35	3.24	0.06	2.09	4.23	1.46	4.02	0.20	8.6	0.56	35.10	26.29	404.38	9.44	22.2 ± 0.3	10.7 ± 0.8	-	this study
KJ1324A	29	Kadjaran Open pit	E46 08.026	N39 08.972	1866	porphyritic granodioritic dike	62.85	0.44	15.19	3.62	0.06	1.69	2.85	1.36	3.56	0.23	8.15	0.48	31.60	23.97	433.59	10.16	22.2 ± 0.3	10.5 ± 1.0	5.92 ± 0.19	this study
KJ1211A	-	Kadjaran Open pit	E46 08.316	N39 08.610	-	Basalt-Andesite dike	54.26	0.54	15.06	3.92	0.11	2.82	5.98	0.17	4.59	0.28	11.95	0.59	60.00	28.00	274.00	11.00	**22.22 ± 0.01**	-	-	Moritz et al. 2016
KJ1313	30	Road to Meghri	E46 11.054	N39 08.547	1952	Trachyandesite dike	58.42	0.64	14.94	4.54	0.10	1.47	6.24	3.57	3.49	0.37	5.56	0.39	91.70	44.02	719.68	12.75	21.2 ± 0.3	10.9 ± 0.8	-	this study

Red numbers corresponds to trace elements measured by XRF

Bold ages refer to CA-ID-TIMS ages from Moritz et al. (2016)

Table DR2: Results of in situ LA-ICP-MS U-Pb dating. Shaded area indicates the zircons used to calculate the weighted mean age.

Analysis (n=601)	Dates (Ma)				Isotopic ratios							
AG1304A (n°1 in Fig. 1)	$^{206}Pb/^{238}Pb$	± 2 SD	$^{207}Pb/^{235}U$	± 2 SD	$^{206}Pb/^{238}U$	± SD %	$^{207}Pb/^{235}U$	± SD %	$^{207}Pb/^{206}Pb$	± SD %	Corr. Coef.	Comment
de11f06	47.6	1.4	55.3	5.3	0.0074	1.46	0.0544	5.54	0.05335	5.34	0.2637	
de11f08	48	1.5	54.4	5.6	0.0075	1.53	0.0537	5.86	0.05193	5.66	0.2610	
de11e09	48.6	1.1	52.9	5.2	0.0076	1.17	0.0538	5.23	0.05141	5.1	0.2236	
de11f07	49	1.6	52	5.4	0.0076	1.59	0.0512	5.73	0.04884	5.5	0.2777	
de11f09	49.1	0.9	51.6	3.1	0.0077	0.88	0.0531	3.31	0.05002	3.19	0.2659	
de11f10	49.1	0.8	52.8	3.5	0.0077	0.78	0.0558	3.70	0.0526	3.62	0.2106	
de11e11	49.2	0.9	47.7	3.8	0.0077	0.94	0.0487	4.36	0.04591	4.26	0.2155	
de11f14	49.3	1.2	51.5	5.2	0.0077	1.2	0.0530	4.91	0.04994	4.76	0.2445	
de11e14	49.4	1.2	56.5	5.3	0.0077	1.19	0.0569	5.01	0.05363	4.87	0.2374	
de11e10	50.1	1.2	55.9	4.7	0.0078	1.17	0.0570	4.81	0.05304	4.67	0.2430	antecryst
de11e13	50.1	1.1	47.3	5	0.0078	1.06	0.0474	5.28	0.04406	5.17	0.2009	antecryst
de11f11	50.2	0.6	48.9	1.6	0.0078	0.61	0.0509	1.62	0.04734	1.5	0.3767	antecryst
de11f13	50.5	0.7	48.6	2.3	0.0079	0.7	0.0515	2.35	0.04727	2.24	0.2983	antecryst
Mean (n=9)	**48.94**	**0.36**										
2 SD propagated		**0.60**										

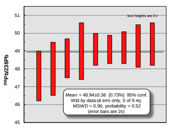

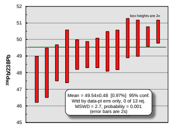

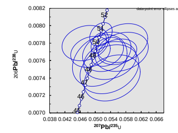

MA1501 (n°2 in Fig. 1)	$^{206}Pb/^{238}Pb$	± 2 SD	$^{207}Pb/^{235}U$	± 2 SD	$^{206}Pb/^{238}U$	± SD %	$^{207}Pb/^{235}U$	± SD %	$^{207}Pb/^{206}Pb$	± SD %	Corr. Coef.	Comment
jl10h11	46.4	2.1	47.9	4.4	0.0072	2.32	0.0481	6.13	0.04848	5.67	0.3787	
jl09k09	46.7	1.3	47.4	3.3	0.0073	1.39	0.0472	3.82	0.04687	3.56	0.3637	
jl09l12	46.7	1.2	48.7	4.7	0.0073	1.3	0.0493	5.05	0.049	4.88	0.2574	
jl09l11	46.9	2.3	45.8	3.9	0.0073	2.42	0.0460	5.25	0.04577	4.66	0.4609	
jl09l13	47.2	1.1	46.7	4.6	0.0074	1.17	0.0481	4.98	0.04714	4.84	0.2350	
jl10h10	47.2	1.6	49.1	5.2	0.0074	1.69	0.0513	5.19	0.05035	4.91	0.3255	
jl09k07	47.4	1.4	49.1	4.1	0.0074	1.47	0.0503	4.60	0.04932	4.36	0.3195	
jl09l09	47.4	1.1	49	3.8	0.0074	1.13	0.0498	4.40	0.04884	4.25	0.2570	
jl09k10	47.6	1.4	48.1	4.2	0.0074	1.51	0.0483	4.84	0.0474	4.6	0.3119	
jl09k12	47.6	1.7	48.8	4.4	0.0074	1.79	0.0489	5.34	0.04795	5.03	0.3353	
jl09l05	47.6	1.9	47.6	6	0.0074	1.99	0.0485	6.38	0.04759	6.06	0.3120	
jl09k08	47.7	1.7	47.1	3.5	0.0074	1.77	0.0481	4.44	0.04719	4.07	0.3988	
jl09l07	47.7	1.2	45.8	3.2	0.0074	1.29	0.0459	3.98	0.04499	3.76	0.3245	
jl09l08	47.7	1.3	50.6	3.8	0.0074	1.39	0.0508	4.01	0.04981	3.76	0.3467	
jl09l06	47.8	1.2	48.2	3.2	0.0074	1.28	0.0482	4.15	0.04723	3.95	0.3083	
jl09k11	47.9	1.1	50.1	3.6	0.0075	1.19	0.0515	3.91	0.04984	3.72	0.3047	
jl09k06	48	1.9	48.7	3.4	0.0075	1.99	0.0501	3.71	0.04851	3.13	0.5365	
jl10h12	48	2.4	53.1	6.8	0.0075	2.52	0.0544	6.62	0.05263	6.12	0.3807	
jl10h14	48	1.4	49.1	5.2	0.0075	1.46	0.0502	5.59	0.04859	5.4	0.2610	
jl10h13	48.1	1.2	45.5	3.5	0.0075	1.29	0.0466	4.09	0.04508	3.88	0.3155	
jl09l10	48.2	1.9	48	3.1	0.0075	2.02	0.0488	3.84	0.04721	3.27	0.5255	
jl09k13	48.9	1.4	43.7	3.2	0.0076	1.46	0.0450	4.28	0.04292	4.02	0.3414	
Mean (n=22)	**47.58**	**0.3**										
2 SD propagated		**0.61**										

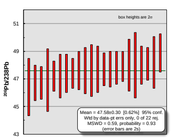

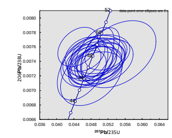

AG1401 (n°3 in Fig. 1)	$^{206}Pb/^{238}Pb$	± 2 SD	$^{207}Pb/^{235}U$	± 2 SD	$^{206}Pb/^{238}U$	± SD %	$^{207}Pb/^{235}U$	± SD %	$^{207}Pb/^{206}Pb$	± SD %	Corr. Coef.	Comment
de10a08	44.7	0.9	48.7	9.5	0.007	1.04	0.0499	10.87	0.05176	10.82	0.0957	
de10b05	44.9	1	46	3.4	0.007	1.13	0.0469	4.16	0.04865	4	0.2719	
de10a09	45.1	1	45.3	3.4	0.007	1.11	0.0458	4.25	0.04749	4.1	0.2613	
de10a12	45.6	1.3	45.3	6.2	0.0071	1.39	0.0460	6.52	0.04701	6.37	0.2132	
de10b07	45.7	1.4	43.5	5.9	0.0071	1.56	0.0435	6.36	0.04448	6.17	0.2451	
de10a10	45.9	1.2	48.3	6.9	0.0072	1.36	0.0502	7.20	0.05062	7.07	0.1889	
de10a13	45.9	1.2	42.1	5.4	0.0072	1.34	0.0433	6.74	0.04364	6.61	0.1987	
de10b06	45.9	1.1	49.8	11	0.0071	1.18	0.0505	8.38	0.05156	8.3	0.1408	
de10a07	46	1.1	42.5	4.4	0.0072	1.18	0.0443	5.34	0.0446	5.21	0.2209	
de10a06	46.1	1.3	37.3	7.1	0.0072	1.39	0.0380	9.62	0.03826	9.52	0.1445	
de10b09	46.1	1.2	45.7	2.9	0.0072	1.35	0.0465	3.56	0.04687	3.29	0.3796	
de10b12	46.1	1.4	46.9	4.7	0.0072	1.58	0.0481	4.95	0.04845	4.69	0.3193	
de10a11	46.3	0.8	45.3	3.5	0.0072	0.86	0.0473	4.69	0.04765	4.61	0.1834	
de10a14	46.3	0.9	43.6	2.9	0.0072	0.93	0.0449	3.69	0.04525	3.57	0.2521	
de10b08	46.6	1.2	44.3	3.9	0.0073	1.31	0.0455	4.68	0.04527	4.49	0.2801	
de10b10	46.6	1.2	44.6	3.6	0.0072	1.25	0.0467	4.06	0.04708	3.86	0.3081	
de10b14	46.8	2	48	3.6	0.0073	2.11	0.0489	4.31	0.04864	3.76	0.4894	
de10b13	46.9	1.4	47.5	4	0.0073	1.52	0.0478	4.54	0.04754	4.28	0.3347	
de10b11	47.2	1.2	45.8	3.8	0.0073	1.27	0.0468	4.56	0.04656	4.38	0.2785	
Mean (n=19)	**45.94**	**0.33**										
2 SD propagated		**0.91**										

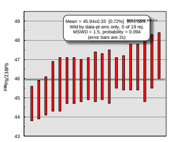

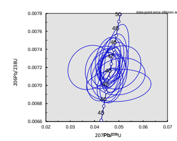

AG1404 (n°4 in Fig. 1)	$^{206}Pb/^{238}Pb$	± 2 SD	$^{207}Pb/^{235}U$	± 2 SD	$^{206}Pb/^{238}U$	± SD %	$^{207}Pb/^{235}U$	± SD %	$^{207}Pb/^{206}Pb$	± SD %	Corr. Coef.	Comment
de10d05	43.2	2	47.8	7.5	0.0067	2.37	0.0470	7.40	0.05086	7.01	0.3203	
de10d09	43.2	1.8	62.6	29.1	0.0067	2.12	0.0633	15.60	0.06857	15.46	0.1359	
de10c11	43.7	4.7	42.3	11.3	0.0068	5.38	0.0416	14.32	0.04441	13.27	0.3757	
de10d11	43.8	1.9	49.8	7.1	0.0068	2.21	0.0499	7.91	0.05321	7.59	0.2796	
de11n05	43.8	1.2	44.1	5.4	0.0068	1.4	0.0437	6.33	0.04662	6.17	0.2213	
de10c14	43.9	3.7	45	8	0.0068	4.22	0.0442	10.05	0.04718	9.12	0.4199	
de11n08	44.2	1.5	53.9	10	0.0069	1.68	0.0543	10.44	0.05708	10.3	0.1610	
de11n07	44.3	1.4	45	5.9	0.0069	1.58	0.0453	7.37	0.04765	7.2	0.2143	
de10d14	44.4	1.4	42.9	6.2	0.0069	1.53	0.0428	7.38	0.04502	7.22	0.2073	
de10d08	44.5	2.7	46.6	8.7	0.0069	3	0.0461	9.81	0.0485	9.34	0.3058	
de10d13	44.7	1.5	47.4	6.8	0.007	1.73	0.0470	7.67	0.04873	7.47	0.2256	
de10c09	44.8	3.2	44	10.1	0.007	3.56	0.0448	11.50	0.04646	10.94	0.3094	
de11n11	45.3	1.8	40.8	6.4	0.0071	1.98	0.0423	8.49	0.0432	8.26	0.2331	
de11n12	45.4	1.3	43.9	5.7	0.0071	1.42	0.0441	6.92	0.04511	6.77	0.2053	
de10d12	45.5	2	39.2	6.1	0.0071	2.17	0.0392	8.43	0.04008	8.15	0.2573	
de10c10	45.6	3	56.4	22.2	0.0071	3.29	0.0547	31.96	0.05587	31.79	0.1029	
de10d06	45.6	1.8	41.5	7.5	0.0071	1.95	0.0415	10.43	0.04238	10.25	0.1869	
de11n10	45.7	1.8	45.1	6	0.0071	1.93	0.0451	7.59	0.04614	7.34	0.2543	
de11n06	46.3	1.9	46.9	7.9	0.0072	2.11	0.0465	9.35	0.04686	9.11	0.2256	
de10c05	46.4	4.4	44.4	19.4	0.0072	4.78	0.0431	31.18	0.04347	30.81	0.1533	
de10c08	46.4	4.9	41.1	9.6	0.0072	5.26	0.0379	12.71	0.03823	11.57	0.4139	
de11n14	46.4	3	43.5	7.5	0.0072	3.24	0.0423	10.87	0.04266	10.38	0.2980	
de10c07	46.5	3.6	33.7	13.8	0.0072	3.89	0.0335	30.26	0.03377	30.01	0.1285	
de11n13	47.4	1.9	48.2	6.6	0.0074	2	0.0491	6.65	0.04819	6.34	0.3008	
Mean (n=24)	**44.82**	**0.45**										
2 SD propagated		**0.94**										

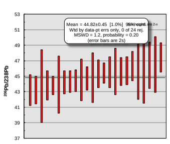

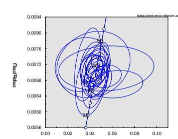

VK1403 (n°5 in Fig. 1)	$^{206}Pb/^{238}Pb$	± 2 SD	$^{207}Pb/^{235}U$	± 2 SD	$^{206}Pb/^{238}U$	± SD %	$^{207}Pb/^{235}U$	± SD %	$^{207}Pb/^{206}Pb$	± SD %	Corr. Coef.	Comment
de12n07	42.2	2.3	50.4	9.2	0.0066	2.7	0.0486	9.95	0.05343	9.58	0.2713	
de12o11	43.1	2.3	49.8	11	0.0067	2.63	0.0486	12.71	0.05263	12.44	0.2068	
de12o08	43.3	1.8	44.2	5.8	0.0067	2.05	0.0427	7.19	0.04626	6.89	0.2852	
de12n13	43.4	2	45.3	7.2	0.0068	2.26	0.0445	9.11	0.04752	8.83	0.2480	
de12o12	43.7	2.3	44.9	9.4	0.0068	2.62	0.0440	10.75	0.04698	10.43	0.2436	
de12o14	44	1.8	42.7	8.6	0.0069	2.01	0.0420	10.17	0.04413	9.97	0.1976	
de12o07	44.3	1.3	45.5	5.6	0.0069	1.52	0.0448	6.21	0.04706	6.02	0.2448	
de12n06	44.3	2.4	54.7	18	0.0069	2.75	0.0554	11.12	0.05827	10.77	0.2474	
de12o05	44.4	1.6	44.2	6.1	0.0069	1.82	0.0446	7.05	0.04689	6.81	0.2582	
de12n09	44.5	2.7	46.1	6.4	0.0069	2.99	0.0452	7.66	0.0475	7.05	0.3904	
de12o09	44.8	1.8	53.7	11.6	0.007	1.96	0.0530	15.26	0.05489	15.13	0.1285	
de12n10	44.8	1.5	41.5	5.8	0.007	1.72	0.0410	6.67	0.04255	6.44	0.2580	
de12o06	44.9	2	39.6	9.2	0.007	2.25	0.0395	13.09	0.04098	12.9	0.1718	
de12n12	44.9	1.6	42.5	6.8	0.007	1.76	0.0418	8.14	0.04336	7.95	0.2162	
de12o10	45	1.8	38.8	5.7	0.007	2.05	0.0384	7.46	0.03977	7.17	0.2749	
de12n05	45	2.6	49.2	8.1	0.007	2.91	0.0483	8.58	0.05004	8.07	0.3392	
de12n14	45.4	1.6	45.5	7.7	0.0071	1.79	0.0447	8.25	0.04565	8.05	0.2171	
Mean (n=17)	**44.34**	**0.44**										
2 SD propagated		**0.70**										

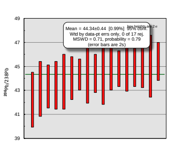

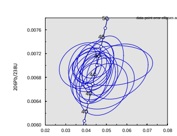

AG1403 (n°6 in Fig. 1)	$^{206}Pb/^{238}Pb$	± 2 SD	$^{207}Pb/^{235}U$	± 2 SD	$^{206}Pb/^{238}U$	± SD %	$^{207}Pb/^{235}U$	± SD %	$^{207}Pb/^{206}Pb$	± SD %	Corr. Coef.	Comment
de10i05	43.5	2.8	38.2	4.9	0.0068	3.22	0.0387	7.42	0.04134	6.69	0.4337	
de10i06	44.4	2.6	32	11.9	0.0069	2.91	0.0324	19.80	0.03404	19.59	0.1469	
de10i07	43	2.4	48.9	8.2	0.0067	2.83	0.0491	9.12	0.05313	8.67	0.3103	
de10i08	44.2	2.7	53	14.1	0.0069	3.06	0.0515	14.95	0.05418	14.63	0.2047	
de10i09	43.3	2.3	55.2	15.5	0.0067	2.64	0.0554	20.24	0.05999	20.07	0.1304	
de10i10	44	2.1	46.3	6.9	0.0068	2.36	0.0462	7.83	0.04934	7.47	0.3013	
de10i11	44.2	2.5	42	8.4	0.0069	2.83	0.0425	9.49	0.04467	9.06	0.2982	
de10i12	44.4	2.4	44.9	8.1	0.0069	2.69	0.0452	12.32	0.04752	12.02	0.2184	
de10i13	44.1	3.4	54.3	58.9	0.0069	3.89	0.0538	25.10	0.05657	24.8	0.1550	
de10i14	45.2	3.1	47.2	9.8	0.007	3.46	0.0473	10.23	0.04904	9.63	0.3381	
de10j05	44	3.4	46.6	10.2	0.0068	3.94	0.0470	11.99	0.05015	11.32	0.3287	
de10j06	43.6	3.5	39.2	9.3	0.0068	4	0.0387	11.37	0.04133	10.64	0.3519	
de10j07	45.5	2.5	53	24.6	0.0071	2.79	0.0533	14.92	0.05442	14.66	0.1870	
de10j08	43.9	2.6	56.4	14.9	0.0068	2.95	0.0568	10.52	0.06066	10.1	0.2804	
de10j09	43.9	2.7	40.7	9.2	0.0068	3.12	0.0406	10.61	0.04337	10.14	0.2941	
de10j10	44.9	2.9	45.3	10.9	0.007	3.23	0.0457	11.68	0.04737	11.22	0.2766	
de10j12	43.1	3.1	37	10.5	0.0067	3.58	0.0364	16.79	0.03941	16.4	0.2133	
de10j13	45.8	2.9	40.6	10.3	0.0071	3.18	0.0397	14.36	0.04054	14	0.2215	
Mean (n=18)	**44.14**	**0.62**										
2 SD propagated		**1.02**										

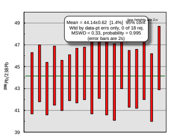

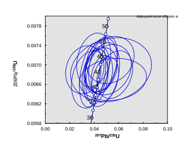

AG1406 (n°7 in Fig. 1)	$^{206}Pb/^{238}Pb$	± 2 SD	$^{207}Pb/^{235}U$	± 2 SD	$^{206}Pb/^{238}U$	± SD %	$^{207}Pb/^{235}U$	± SD %	$^{207}Pb/^{206}Pb$	± SD %	Corr. Coef.	Comment
de10e14	43	1.7	51.2	13.6	0.0067	2.04	0.0515	20.06	0.05574	19.96	0.1017	
de10f10	43.1	1.5	40.3	8.1	0.0067	1.73	0.0399	10.22	0.04326	10.07	0.1693	
de10f14	43.1	1.7	55.7	30	0.0067	2	0.0547	26.28	0.05928	26.2	0.0761	
de10e06	43.2	1.7	53.7	26.8	0.0067	1.96	0.0549	21.25	0.05942	21.16	0.0922	
de10f11	43.2	1.5	40.4	8	0.0067	1.72	0.0401	9.86	0.04347	9.71	0.1744	
de10f09	43.4	2	48.8	8.8	0.0068	2.35	0.0488	9.23	0.05207	8.93	0.2545	
de10f12	43.4	1.9	48.7	10.2	0.0068	2.17	0.0493	12.65	0.05258	12.46	0.1716	
de10e12	43.5	1.5	46	7	0.0068	1.75	0.0462	8.94	0.0493	8.77	0.1957	
de10f05	43.8	1.4	61.6	14.2	0.0068	1.55	0.0623	13.27	0.06643	13.18	0.1168	
de10e07	44	1.6	43.8	12.8	0.0068	1.88	0.0430	15.60	0.04593	15.49	0.1205	
de10e09	44	1.5	42.6	6	0.0069	1.74	0.0433	7.25	0.0455	7.04	0.2399	
de10e11	44.1	1.6	35.9	12.2	0.0069	1.8	0.0356	15.08	0.03748	14.97	0.1194	
de10e05	44.2	1.3	59.7	15.4	0.0069	1.49	0.0608	16.07	0.06393	16	0.0927	
de10f13	44.5	2	54.7	8.3	0.0069	2.27	0.0540	8.34	0.05674	8.03	0.2720	
de10e10	45.1	1.7	53.5	17	0.007	1.84	0.0543	21.30	0.0563	21.22	0.0864	
de10f07	45.2	1.6	54	15.4	0.007	1.79	0.0537	14.10	0.05569	13.99	0.1269	
de10e08	45.3	2	44.2	19.1	0.007	2.22	0.0444	19.47	0.04602	19.34	0.1140	
de10f08	45.7	1.8	52	14.6	0.0071	1.94	0.0518	13.36	0.05296	13.22	0.1452	
Mean (n=18)	**43.95**	**0.38**										
2 SD propagated		**0.89**										

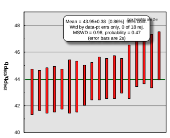

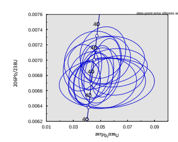

AG1402 (n°8 in Fig. 1)	$^{206}Pb/^{238}Pb$	± 2 SD	$^{207}Pb/^{235}U$	± 2 SD	$^{206}Pb/^{238}U$	± SD %	$^{207}Pb/^{235}U$	± SD %	$^{207}Pb/^{206}Pb$	± SD %	Corr. Coef.	Comment
de11d09	41.9	1.4	45.9	7	0.0065	1.67	0.0453	8.22	0.05062	8.05	0.2031	
de11c09	42.2	1.6	42	8.7	0.0066	1.87	0.0407	10.95	0.04471	10.79	0.1708	
de11c11	43.2	1.1	58.5	13.2	0.0067	1.27	0.0575	11.85	0.06222	11.78	0.1072	
de11d10	43.4	1.3	49.3	8.8	0.0068	1.46	0.0498	9.38	0.05313	9.27	0.1556	
de11d12	43.4	1.6	45	7.6	0.0068	1.89	0.0452	9.04	0.04826	8.84	0.2091	
de11c06	43.7	1.4	44.6	7.2	0.0068	1.56	0.0448	8.65	0.0478	8.51	0.1803	
de11d11	43.7	1.5	42	6.1	0.0068	1.69	0.0420	7.59	0.04477	7.4	0.2226	
de11c13	44.1	1.6	47.9	8.4	0.0069	1.82	0.0489	9.41	0.05144	9.23	0.1935	
de11d06	44.1	1.5	46.6	5.5	0.0069	1.75	0.0473	6.61	0.04975	6.37	0.2649	
de11d08	44.1	1.4	40.3	8.3	0.0069	1.61	0.0401	10.09	0.04212	9.96	0.1596	
de11c07	44.3	1.2	51.8	7.1	0.0069	1.4	0.0515	6.81	0.05415	6.66	0.2057	
de11c08	44.3	1.3	53.2	10.7	0.0069	1.5	0.0536	11.05	0.05638	10.95	0.1357	
de11c12	44.4	1.2	53.8	16.9	0.0069	1.37	0.0521	21.64	0.05479	21.6	0.0633	
de11c10	44.5	1.5	50.7	7.3	0.0069	1.74	0.0505	8.41	0.05314	8.23	0.2068	
de11d07	44.6	1.4	38.5	6.6	0.0069	1.56	0.0381	9.23	0.04008	9.1	0.1690	
de11d05	44.7	1.8	40	7.3	0.007	1.97	0.0408	10.40	0.0423	10.21	0.1895	
de11d13	45	1.7	42.7	6.4	0.007	1.84	0.0420	8.30	0.0435	8.09	0.2218	
Mean (n=17)	**43.83**	**0.42**										
2 SD propagated		**0.62**										

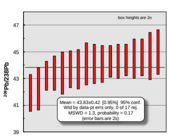

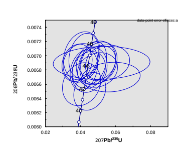

HQ1402 (n°9 in Fig. 1)	$^{206}Pb/^{238}Pb$	± 2 SD	$^{207}Pb/^{235}U$	± 2 SD	$^{206}Pb/^{238}U$	± SD %	$^{207}Pb/^{235}U$	± SD %	$^{207}Pb/^{206}Pb$	± SD %	Corr. Coef.	Comment
de11g05	41.6	1.2	42.8	5.4	0.0065	1.46	0.0432	6.21	0.04819	6.04	0.2350	
de11h08	42.3	1	43.6	3.2	0.0066	1.22	0.0439	3.88	0.04824	3.68	0.3147	
de11h06	42.4	0.6	44.4	3.9	0.0066	0.77	0.0453	4.51	0.04978	4.44	0.1709	
de11g08	42.5	0.9	47.2	5.5	0.0066	1.03	0.0469	6.11	0.0516	6.02	0.1686	
de11h12	42.7	1.2	43.4	4.3	0.0066	1.38	0.0434	5.63	0.04769	5.46	0.2450	
de11g12	42.8	0.7	46	4.2	0.0067	0.85	0.0475	5.55	0.05143	5.48	0.1533	
de11g09	42.9	0.5	43.6	1.1	0.0067	0.58	0.0450	1.33	0.0487	1.2	0.4352	
de11g06	43	0.9	43.1	2.5	0.0067	1.04	0.0437	3.12	0.0473	2.94	0.3335	
de11g13	43	1.1	47.3	5.6	0.0067	1.34	0.0479	5.80	0.05185	5.64	0.2312	
de11h07	43	0.9	45	4.6	0.0067	1.08	0.0454	5.79	0.0492	5.69	0.1865	
de11h13	43.1	1.4	44.5	3.7	0.0067	1.65	0.0452	4.38	0.04893	4.06	0.3765	
de11g07	43.2	0.8	43.8	2.2	0.0067	0.95	0.0444	2.74	0.04811	2.57	0.3467	
de11g10	43.3	0.7	42.8	1.9	0.0067	0.83	0.0439	2.32	0.04758	2.17	0.3572	
de11g14	43.5	0.6	43.3	1.6	0.0068	0.73	0.0454	2.03	0.04841	1.89	0.3603	
de11h11	43.5	0.9	42.6	2.2	0.0068	1.08	0.0443	2.96	0.04726	2.76	0.3644	
de11g11	44.1	0.8	42.6	2.7	0.0069	0.9	0.0446	3.35	0.0469	3.23	0.2684	antecryst
de11h09	44.1	1	42.2	1.3	0.0069	1.13	0.0445	1.81	0.04679	1.41	0.6254	antecryst
Mean (n=15)	**42.92**	**0.25**										
2 SD propagated		**0.51**										

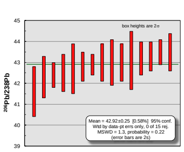

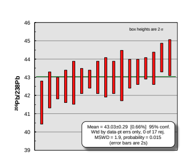

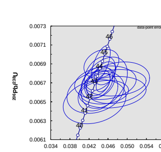

HQ1403 (n°10 in Fig. 1)	^{206}Pb/^{238}Pb	± 2 SD	^{207}Pb/^{235}U	± 2 SD	^{206}Pb/^{238}U	± SD %	^{207}Pb/^{235}U	± SD %	^{207}Pb/^{206}Pb	± SD %	Corr. Coef.	Comment
de11i08	42.4	1.2	38.5	5.2	0.0066	1.37	0.0382	7.28	0.04197	7.15	0.1882	
de11j08	42.4	0.9	45.7	3.8	0.0066	1.08	0.0456	4.52	0.05013	4.39	0.2389	
de11i06	42.5	1.2	46.7	5.2	0.0066	1.39	0.0475	5.72	0.05222	5.55	0.2429	
de11i12	42.7	1.1	40.1	7	0.0067	1.32	0.0399	9.97	0.04325	9.88	0.1324	
de11i09	42.9	0.9	44.5	4.2	0.0067	1.08	0.0452	5.31	0.04897	5.2	0.2034	
de11j07	42.9	1	41.9	5	0.0067	1.19	0.0415	6.53	0.04498	6.42	0.1823	
de11i11	43.2	1.4	42.7	6.1	0.0067	1.68	0.0433	8.01	0.04694	7.83	0.2098	
de11j06	43.2	1.4	43.8	5.3	0.0067	1.6	0.0440	6.55	0.04765	6.35	0.2443	
de11j09	43.2	1.2	45.1	5.1	0.0067	1.42	0.0439	5.75	0.04757	5.57	0.2470	
de11i13	43.5	1.2	44.5	6.2	0.0068	1.41	0.0441	6.94	0.04703	6.8	0.2030	
de11i07	43.6	1	50.1	4.3	0.0068	1.19	0.0507	4.58	0.05406	4.42	0.2600	
de11i10	43.7	0.9	45.6	3.8	0.0068	0.99	0.0466	4.62	0.04972	4.51	0.2144	
de11j13	43.7	1.3	43.7	4.5	0.0068	1.46	0.0427	5.60	0.04551	5.41	0.2605	
de11j10	43.8	1.2	44.7	5.4	0.0068	1.33	0.0447	6.14	0.04767	5.99	0.2168	
Mean (n=14)	43.1	0.29										
2 SD propagated		0.53										

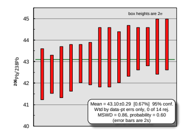

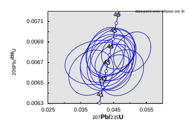

AG1308A1 (n°11 in Fig. 1)	^{206}Pb/^{238}Pb	± 2 SD	^{207}Pb/^{235}U	± 2 SD	^{206}Pb/^{238}U	± SD %	^{207}Pb/^{235}U	± SD %	^{207}Pb/^{206}Pb	± SD %	Corr. Coef.	Comment
de10g08	36.8	2.1	34.9	4.3	0.0057	2.85	0.0371	6.23	0.04721	5.54	0.4575	
de10h06	36.8	1.9	37.6	4.7	0.0057	2.62	0.0386	6.67	0.04917	6.13	0.3930	
de10h08	36.9	2.3	33.9	2.8	0.0057	3.13	0.0345	4.81	0.04392	3.65	0.6510	
de10g09	37	1.6	36	4.2	0.0058	2.11	0.0374	5.38	0.04675	4.95	0.3921	
de10g12	37	1.5	36.7	2	0.0058	2.04	0.0391	3.15	0.04889	2.4	0.6476	
de10g05	37.1	2.4	36.7	3.6	0.0058	3.23	0.0388	5.11	0.04855	3.96	0.6321	
de10g06	37.2	2	33.4	3.2	0.0058	2.68	0.0348	5.19	0.04351	4.45	0.5159	
de10h10	37.3	1.6	37.1	3.1	0.0058	2.11	0.0391	4.22	0.04892	3.66	0.4994	
de10h14	37.7	1.1	38.4	4.2	0.0059	1.51	0.0404	5.91	0.04963	5.71	0.2557	
de10h12	37.8	1.2	38	4.1	0.0059	1.6	0.0399	6.03	0.04905	5.81	0.2655	
de10h13	37.9	1.1	36	3.2	0.0059	1.51	0.0381	4.79	0.04691	4.55	0.3150	
de10g07	38	1.7	39.4	3.1	0.0059	2.23	0.0422	4.59	0.05187	4.01	0.4860	
de10g11	38	1.7	36.1	3.8	0.0059	2.23	0.0372	5.23	0.04574	4.73	0.4264	
de10g13	38	1.8	35.4	3.5	0.0059	2.4	0.0378	5.41	0.04651	4.85	0.4435	
de10h09	38.2	2	38.4	5.3	0.0059	2.64	0.0404	6.00	0.04973	5.39	0.4399	
de10h11	38.4	1.2	38.6	6.3	0.006	1.56	0.0420	8.36	0.05075	8.21	0.1867	
de10g10	38.5	1.7	38.4	2.4	0.006	2.25	0.0413	4.19	0.04994	3.53	0.5375	
de10h07	39.3	2.2	36.1	2.8	0.0061	2.81	0.0386	3.95	0.04588	2.78	0.7109	
de10g14	39.7	2.2	35.9	3.3	0.0062	2.81	0.0379	5.25	0.04437	4.43	0.5356	
Mean (n=19)	37.78	0.36										
2 SD propagated		0.78										

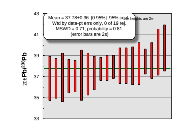

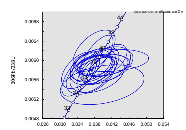

AG1308A (n°12 in Fig. 1)	^{206}Pb/^{238}Pb	± 2 SD	^{207}Pb/^{235}U	± 2 SD	^{206}Pb/^{238}U	± SD %	^{207}Pb/^{235}U	± SD %	^{207}Pb/^{206}Pb	± SD %	Corr. Coef.	Comment
de11b05	36.4	0.8	36.9	2.6	0.0057	1.04	0.0383	3.75	0.04871	3.6	0.2775	
de11a08	36.5	0.8	35.1	2.4	0.0057	1.06	0.0367	3.55	0.04666	3.39	0.2984	
de11a06	36.6	0.6	34.5	1.7	0.0057	0.83	0.0366	2.68	0.04661	2.55	0.3095	
de11b08	36.6	0.8	36.7	1.5	0.0057	1.16	0.0377	2.33	0.04802	2.02	0.4980	
de11b09	36.7	1	34.7	3	0.0057	1.43	0.0368	4.84	0.04686	4.62	0.2957	
de11a05	36.8	0.5	36.9	1.9	0.0057	0.68	0.0379	2.52	0.04827	2.43	0.2695	
de11a11	36.8	1	36.1	3	0.0057	1.31	0.0371	4.58	0.04723	4.39	0.2859	
de11b10	36.8	1.1	36.3	3.2	0.0057	1.54	0.0375	4.63	0.04772	4.37	0.3324	
de11a14	36.9	0.9	33.9	2.5	0.0057	1.25	0.0354	3.85	0.04508	3.64	0.3248	
de11a07	37	0.7	35.8	1.3	0.0058	0.94	0.0381	2.17	0.04767	1.96	0.4324	
de11b14	37	0.8	35.3	1.6	0.0057	1.08	0.0365	2.48	0.04651	2.23	0.4359	
de11a12	37.1	0.8	35.7	1.5	0.0058	1.05	0.0376	2.15	0.0471	1.88	0.4876	
de11b07	37.2	0.5	36.3	1.4	0.0058	0.73	0.0377	2.09	0.04721	1.96	0.3490	
de11b06	37.4	0.6	37.7	1.7	0.0058	0.85	0.0389	2.41	0.04872	2.25	0.3534	
de11b11	37.4	1	37.3	2.3	0.0058	1.38	0.0393	3.78	0.04912	3.52	0.3650	
de11a13	37.5	0.7	35.4	1.3	0.0058	0.94	0.0372	2.25	0.04651	2.04	0.4185	
de11a09	37.7	0.9	36.2	2.3	0.0059	1.23	0.0381	3.37	0.04689	3.14	0.3647	
de11b12	37.7	0.8	36.6	2.9	0.0059	1.11	0.0389	3.99	0.04789	3.83	0.2784	
Mean (n=18)	37.01	0.17										
2 SD propagated		0.42										

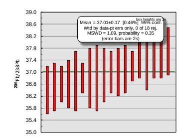

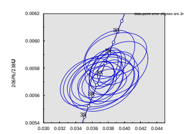

VK1404 (n°13 in Fig. 1)	^{206}Pb/^{238}Pb	± 2 SD	^{207}Pb/^{235}U	± 2 SD	^{206}Pb/^{238}U	± SD %	^{207}Pb/^{235}U	± SD %	^{207}Pb/^{206}Pb	± SD %	Corr. Coef.	Comment
de12i06	35.4	0.7	32.5	1.8	0.0055	1.04	0.0356	3.04	0.04699	2.86	0.3417	
de12j05	35.4	0.5	33	1.5	0.0055	0.67	0.0349	2.57	0.04609	2.48	0.2608	
de12i05	35.7	0.8	32.4	1.4	0.0055	1.06	0.0353	2.41	0.04651	2.16	0.4406	
de12j06	36	0.6	32.1	1.7	0.0056	0.8	0.0349	2.68	0.04517	2.56	0.2983	
de12i10	36.3	0.8	33.9	1.5	0.0056	1.11	0.0372	2.63	0.04815	2.38	0.4227	
de12j09	36.7	0.4	31.1	1.3	0.0057	0.57	0.0349	2.15	0.04438	2.07	0.2655	antecryst
de12i07	36.8	0.8	31.6	1.4	0.0057	1.09	0.0357	2.35	0.0454	2.08	0.4642	antecryst
de12i08	36.8	0.8	33.2	2.5	0.0057	1.11	0.0370	3.96	0.04708	3.8	0.2804	antecryst
de12i11	37	0.8	32.4	1.7	0.0058	1.03	0.0372	2.96	0.04654	2.78	0.3474	antecryst
de12j07	37.1	0.6	33.2	1.3	0.0058	0.81	0.0372	2.24	0.04651	2.09	0.3614	antecryst
de12j14	37.1	0.6	32.5	1.1	0.0058	0.77	0.0373	1.91	0.04666	1.75	0.4027	antecryst
de12j12	37.2	0.5	32.5	1.5	0.0058	0.67	0.0367	2.52	0.04588	2.43	0.2658	antecryst
de12j13	37.2	0.6	33.3	1.5	0.0058	0.77	0.0380	2.42	0.04755	2.29	0.3187	antecryst
de12j10	37.3	0.5	32.3	1.2	0.0058	0.68	0.0367	2.17	0.04589	2.06	0.3135	antecryst
de12i09	37.6	1.2	32.2	1.8	0.0059	1.62	0.0369	2.99	0.04538	2.51	0.5423	antecryst
de12j11	38	0.5	32.8	1.3	0.0059	0.62	0.0377	2.10	0.04638	2.01	0.2948	antecryst
de12i12	38.3	0.4	33.5	1	0.006	0.57	0.0391	1.76	0.04726	1.67	0.3230	antecryst
Mean (n=5)	35.7	0.47										
2 SD propagated		0.65										

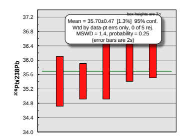

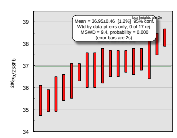

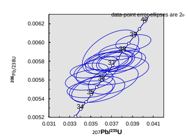

VK1405 (n°14 in Fig. 1)	^{206}Pb/^{238}Pb	± 2 SD	^{207}Pb/^{235}U	± 2 SD	^{206}Pb/^{238}U	± SD %	^{207}Pb/^{235}U	± SD %	^{207}Pb/^{206}Pb	± SD %	Corr. Coef.	Comment
de12m09	34.1	0.8	36.4	4.6	0.0053	1.17	0.0376	6.66	0.05148	6.56	0.1756	
de12l05	34.2	0.9	37.9	4.4	0.0053	1.27	0.0385	6.10	0.05272	5.97	0.2081	
de12m08	34.7	0.8	36.2	3.3	0.0054	1.22	0.0375	4.58	0.05045	4.41	0.2666	
de12l12	34.9	1.1	36.2	4.8	0.0054	1.51	0.0368	7.24	0.04941	7.08	0.2086	
de12m12	35.1	0.7	31.2	2.5	0.0055	0.94	0.0337	3.88	0.0445	3.76	0.2425	
de12l11	35.1	0.9	37.4	3.8	0.0055	1.27	0.0390	5.08	0.05143	4.92	0.2499	
de12m11	35.3	1.1	36.5	4.1	0.0055	1.51	0.0377	6.14	0.04971	5.95	0.2460	
de12l10	35.3	0.9	34.4	4	0.0055	1.3	0.0360	5.96	0.04753	5.82	0.2180	
de12m05	35.5	0.6	34.2	2.5	0.0055	0.89	0.0360	4.03	0.04754	3.93	0.2209	antecryst
de12l13	35.5	1.1	33.9	5.5	0.0055	1.62	0.0356	9.44	0.04693	9.3	0.1716	antecryst
de12m13	35.6	0.8	36.3	3.4	0.0055	1.1	0.0382	4.76	0.05043	4.63	0.2311	antecryst
de12l08	35.8	0.8	33.2	2.2	0.0056	1.18	0.0363	3.67	0.04697	3.48	0.3211	antecryst
de12m10	36.2	0.5	33.5	2.1	0.0056	0.74	0.0371	3.10	0.04804	3.01	0.2387	antecryst
de12l14	36.7	1	32.8	2	0.0057	1.42	0.0365	3.17	0.04641	2.83	0.4485	antecryst
de12m06	36.8	0.8	32.4	1.2	0.0057	1.04	0.0363	2.03	0.04625	1.74	0.5130	antecryst
de12l06	37.3	0.8	33.5	1.9	0.0058	1.01	0.0375	3.31	0.0469	3.15	0.3053	antecryst
Mean (n=8)	34.81	0.3										
2 SD propagated		0.52										

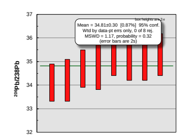

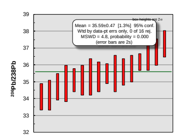

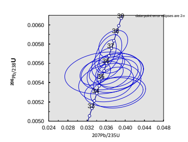

MR1403 (n°15 in Fig. 1)	^{206}Pb/^{238}Pb	± 2 SD	^{207}Pb/^{235}U	± 2 SD	^{206}Pb/^{238}U	± SD %	^{207}Pb/^{235}U	± SD %	^{207}Pb/^{206}Pb	± SD %	Corr. Coef.	Comment
de12f05	34	0.5	33.5	2.4	0.0053	0.79	0.0350	4.12	0.04798	4.04	0.1919	
de12f13	34.2	0.8	33.6	2.8	0.0053	1.24	0.0347	4.71	0.04746	4.54	0.2635	
de12e13	34.4	1.5	32.3	2.4	0.0054	2.18	0.0349	3.79	0.04687	3.1	0.5752	
de12f09	34.8	0.7	34.4	2.2	0.0054	1.06	0.0361	3.27	0.04847	3.09	0.3245	
de12e12	35	1.2	33.1	2.5	0.0054	1.79	0.0349	4.07	0.04694	3.65	0.4403	
de12f11	35	0.6	34.3	2.2	0.0054	0.88	0.0364	3.20	0.0489	3.08	0.2747	
de12f12	35	0.7	32.5	2	0.0054	1	0.0339	3.23	0.04558	3.07	0.3097	
de12e09	35.1	2.6	31.9	2	0.0055	3.7	0.0336	4.68	0.04433	2.87	0.7902	
de12f07	35.3	0.6	35.2	2.1	0.0055	0.8	0.0373	3.14	0.04927	3.04	0.2545	antecryst
de12e11	35.5	0.5	32.4	1.6	0.0055	0.76	0.0355	2.46	0.04677	2.34	0.3089	antecryst
de12e05	35.7	1.3	31.9	1.7	0.0056	1.87	0.0347	3.01	0.04492	2.36	0.6210	antecryst
de12f06	35.7	0.5	32.6	1.2	0.0056	0.64	0.0365	2.02	0.04727	1.92	0.3162	antecryst
de12f10	35.7	0.5	34.2	1.8	0.0055	0.68	0.0363	2.76	0.04792	2.68	0.2459	antecryst
de12f14	35.7	0.6	32.5	1.2	0.0056	0.79	0.0359	1.99	0.04654	1.83	0.3963	antecryst
de12e06	35.8	3.9	33.1	3	0.0056	5.42	0.0340	6.75	0.04401	4.02	0.8032	antecryst
de12e10	35.8	1.5	33.5	1.5	0.0056	2.13	0.0364	2.72	0.04711	1.69	0.7834	antecryst
de12e14	36	0.5	33.9	1.6	0.0056	0.68	0.0375	2.51	0.04864	2.42	0.2705	antecryst
de12e08	36.1	3.5	32	3.1	0.0056	4.86	0.0344	6.46	0.0446	4.26	0.7520	antecryst
de12e07	36.3	3.9	34.1	3	0.0056	5.44	0.0371	6.28	0.04802	3.13	0.8668	antecryst
Mean (n=8)	34.57	0.4										
2 SD propagated		0.58										

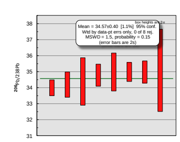

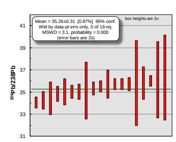

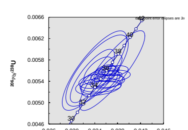

LI1303A1 (n°16 in Fig. 1)	^{206}Pb/^{238}Pb	± 2 SD	^{207}Pb/^{235}U	± 2 SD	^{206}Pb/^{238}U	± SD %	^{207}Pb/^{235}U	± SD %	^{207}Pb/^{206}Pb	± SD %	Corr. Coef.	Comment
jn22d06	32.6	0.9	34.6	2.8	0.0051	1.31	0.0356	4.50	0.05066	4.31	0.2908	
jn22d07	32.8	0.8	32	3.2	0.0051	1.15	0.0322	5.18	0.04588	5.05	0.2220	
jn22d12	32.8	0.9	33.2	3.6	0.0051	1.41	0.0330	6.11	0.04695	5.95	0.2306	
jn22e11	32.9	0.9	36.9	3.6	0.0051	1.44	0.0367	4.95	0.05216	4.74	0.2907	
jn22d10	33	0.9	33.2	3.3	0.0051	1.44	0.0323	6.01	0.04602	5.84	0.2394	
jn22d13	33	0.9	31	2.7	0.0051	1.3	0.0310	4.76	0.04414	4.58	0.2731	
jn22e10	33	1.1	35.3	4.5	0.0051	1.69	0.0356	6.83	0.05058	6.62	0.2474	
jn22d08	33.1	0.7	34.6	3	0.0051	1.07	0.0342	4.45	0.04864	4.32	0.2404	
jn22d11	33.1	0.8	35.9	3.8	0.0051	1.25	0.0355	5.81	0.05044	5.67	0.2153	
jn22e12	33.1	1	35.2	3.2	0.0051	1.47	0.0351	4.89	0.04998	4.66	0.3008	
jn22f10	33.2	0.9	33.7	3.5	0.0052	1.41	0.0342	5.99	0.04779	5.82	0.2355	
jn22d09	33.4	0.6	34.3	2.4	0.0052	0.95	0.0346	3.94	0.04828	3.82	0.2413	
jn22f08	33.4	1.1	34.8	4.9	0.0052	1.61	0.0357	7.43	0.04984	7.25	0.2168	
jn22e13	33.7	1.2	29.6	4.3	0.0052	1.78	0.0296	7.74	0.04124	7.53	0.2300	
jn22f06	33.7	0.8	34.7	3.6	0.0052	1.26	0.0350	5.29	0.0488	5.14	0.2381	
jn22e06	33.8	0.9	35	3.6	0.0053	1.29	0.0353	5.57	0.04838	5.42	0.2315	
jn22f11	33.8	0.7	33.3	2.4	0.0053	1.08	0.0342	3.83	0.04681	3.67	0.2823	
jn22f05	33.9	0.7	34.4	2.1	0.0053	1.1	0.0349	3.15	0.04776	2.95	0.3494	
jn22f09	33.9	1.1	36.2	4.9	0.0053	1.65	0.0371	7.00	0.05084	6.8	0.2358	
jn22e07	34	0.9	33.1	3.4	0.0053	1.36	0.0331	5.17	0.04525	4.99	0.2630	
jn22e08	34.1	0.8	33.2	3.2	0.0053	1.13	0.0334	4.87	0.04574	4.74	0.2319	
jn22e09	34.2	1.1	32.8	4.4	0.0053	1.54	0.0324	6.86	0.04439	6.68	0.2246	
jn22f12	34.2	0.8	33.9	2.2	0.0053	1.15	0.0343	3.49	0.04696	3.29	0.3300	
jn22f07	34.3	1.1	32.3	4.5	0.0053	1.57	0.0317	7.15	0.04336	6.98	0.2194	
jn22f13	34.6	1.2	35.8	4.1	0.0054	1.81	0.0365	7.09	0.04898	6.86	0.2551	
Mean (n=25)	33.48	0.22										
2 SD propagated		0.55										

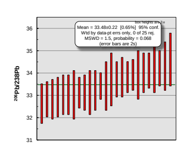

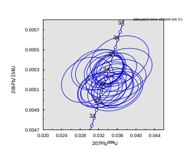

LI1303 (n°17 in Fig. 1)	^{206}Pb/^{238}Pb	± 2 SD	^{207}Pb/^{235}U	± 2 SD	^{206}Pb/^{238}U	± SD %	^{207}Pb/^{235}U	± SD %	^{207}Pb/^{206}Pb	± SD %	Corr. Coef.	Comment
jn22b05	33.1	1.4	34.6	1.9	0.0052	2.18	0.0349	3.48	0.04872	2.71	0.6268	
jn22b07	33.1	1.7	33	2.1	0.0051	2.64	0.0329	3.57	0.04684	2.41	0.7385	
jn22c07	33.3	0.9	33.3	1.6	0.0052	1.29	0.0327	2.53	0.04566	2.18	0.5093	
jn22a05	33.5	0.6	33.2	1.8	0.0052	0.84	0.0329	3.10	0.04594	2.98	0.2713	
jn22a12	33.5	1.3	34.3	1.9	0.0052	1.92	0.0344	3.03	0.04807	2.34	0.6343	
jn22b08	33.5	1.1	34.5	2	0.0052	1.64	0.0349	3.01	0.04866	2.52	0.5455	
jn22b06	33.6	1.5	33.6	2.3	0.0052	2.19	0.0341	3.74	0.04759	3.03	0.5858	
de18a05	34	0.7	33.5	1.3	0.0053	1.06	0.0337	2.36	0.0462	2.11	0.4489	
jn22a11	34.2	0.5	34	1.6	0.0053	0.75	0.0338	2.49	0.04634	2.37	0.3017	antecryst
jn22a13	34.3	0.5	35	1.7	0.0053	0.74	0.0352	2.67	0.04815	2.57	0.2767	antecryst
jn22c06	34.3	0.5	33.8	1.7	0.0053	0.79	0.0340	2.77	0.0465	2.66	0.2847	antecryst
jn22c10	34.3	0.5	36.1	1.4	0.0053	0.67	0.0360	2.10	0.04924	1.99	0.3191	antecryst
de18a06	34.4	0.4	34.3	1.3	0.0053	0.52	0.0342	2.04	0.04683	1.97	0.2552	antecryst
jn22a10	34.4	0.5	33.8	1.5	0.0054	0.72	0.0338	2.34	0.04548	2.23	0.3073	antecryst
jn22b12	34.4	0.5	35.5	1.6	0.0054	0.78	0.0363	2.49	0.04872	2.36	0.3138	antecryst
jn22b13	34.4	0.5	35.2	1.4	0.0053	0.79	0.0349	2.33	0.04782	2.19	0.3393	antecryst
jn22c05	34.4	0.5	33.9	1.7	0.0054	0.78	0.0347	2.73	0.04661	2.62	0.2853	antecryst
jn22a09	34.5	0.5	34.8	1.4	0.0054	0.76	0.0351	2.22	0.04722	2.09	0.3417	antecryst
jn22c08	34.6	1.6	33.8	1.7	0.0054	2.25	0.0345	3.21	0.04636	2.29	0.7008	antecryst
jn22b11	34.7	0.5	34	1.3	0.0054	0.67	0.0341	2.27	0.04577	2.17	0.2950	antecryst
jn22c09	34.7	1.1	34.6	1.9	0.0054	1.6	0.0351	2.87	0.04717	2.38	0.5579	antecryst
jn22b10	34.8	0.4	34.8	1.5	0.0054	0.61	0.0356	2.27	0.04777	2.19	0.2683	antecryst
jn22c13	34.8	1.2	34.8	1.6	0.0054	1.75	0.0350	2.93	0.04708	2.35	0.5973	antecryst
jn22c11	35	0.7	35.3	1.6	0.0054	0.98	0.0355	2.54	0.04765	2.34	0.3863	antecryst
jn22a08	35.1	0.6	35	1.7	0.0055	0.8	0.0357	2.51	0.04712	2.38	0.3186	antecryst
jn22b09	35.1	0.5	35.8	1.4	0.0055	0.75	0.0361	2.23	0.0476	2.1	0.3363	antecryst
jn22a06	35.4	0.5	36.5	1.7	0.0055	0.71	0.0365	2.49	0.0482	2.39	0.2848	antecryst
jn22c12	35.5	1.2	34.9	2.2	0.0055	1.73	0.0354	3.76	0.04665	3.34	0.4599	antecryst
Mean (n=8)	33.55	0.33										
2 SD propagated		0.60										

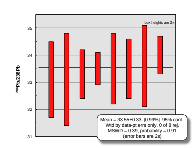

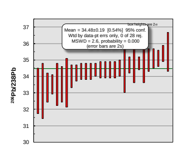

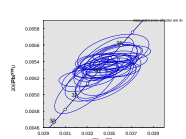

KJ1316 (n°18 in Fig. 1)	^{206}Pb/^{238}Pb	± 2 SD	^{207}Pb/^{235}U	± 2 SD	^{206}Pb/^{238}U	± SD %	^{207}Pb/^{235}U	± SD %	^{207}Pb/^{206}Pb	± SD %	Corr. Coef.	Comment
de12r13	32.6	1.2	33.2	4.8	0.0051	1.78	0.0340	7.73	0.04836	7.52	0.2303	
de12r07	32.7	1.8	35.1	4.2	0.0051	2.69	0.0357	6.04	0.05076	5.41	0.4452	
de12s10	32.8	3.1	34	4.7	0.0051	4.74	0.0351	7.77	0.04999	6.16	0.6098	
de12r14	33	1	36.4	3.8	0.0051	1.55	0.0358	5.59	0.05093	5.37	0.2773	
de12r09	33.2	1.5	35	6.1	0.0052	2.21	0.0359	9.12	0.05014	8.85	0.2423	
de12r10	33.4	1.4	30.9	3	0.0052	2.15	0.0319	4.90	0.04447	4.4	0.4390	
de12s06	33.4	1.3	29.2	5	0.0052	1.97	0.0292	8.87	0.04072	8.65	0.2221	
de12s07	33.4	1.7	37.7	7.7	0.0052	2.49	0.0377	11.04	0.05267	10.76	0.2255	
de12r05	33.6	2.1	39.1	5	0.0052	3.15	0.0398	6.97	0.05549	6.22	0.4518	
de12r06	33.6	2.1	37.1	7.3	0.0052	3.11	0.0368	13.76	0.0513	13.4	0.2261	
de12s08	33.6	1.8	28.3	4.6	0.0052	2.63	0.0287	8.52	0.03999	8.1	0.3088	
de12s14	33.6	1.6	31	3.7	0.0052	2.37	0.0313	5.81	0.04363	5.31	0.4076	
de12s09	33.8	2.1	32.5	3.9	0.0053	3.16	0.0327	6.88	0.04476	6.11	0.4594	
de12s11	33.8	2	31.5	4.5	0.0053	2.9	0.0330	7.77	0.04518	7.21	0.3732	
de12r12	33.9	0.6	32.9	2.7	0.0053	0.95	0.0347	4.31	0.04751	4.2	0.2206	
de12s05	34.4	0.7	35.7	1.9	0.0053	1	0.0378	2.94	0.05175	2.76	0.3406	
de12r11	34.5	1.1	34.4	3.5	0.0054	1.65	0.0374	6.02	0.05019	5.79	0.2741	
de12r08	34.7	1.8	32.1	1.6	0.0054	2.67	0.0352	3.38	0.04731	2.07	0.7903	
Mean (n=18)	33.73	0.29										
2 SD propagated		0.51										

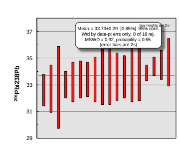

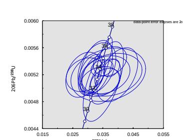

Aa1606A (4*23 in Fig. 1)	$^{208}Pb/^{232}Th$	± 2 SD	$^{207}Pb/^{235}U$	± 2 SD	$^{206}Pb/^{238}U$	± SD %	$^{207}Pb/^{206}Pb$	± SD %	$^{207}Pb/^{206}Pb$	± SD %	Corr. Coef.	Comment
det2b06	31.1	1.5	31.6	4.5	0.0048	2.49	0.0104	7.21	0.09192	6.77	0.3452	
det2b07	31.1	1.1	36.4	12.7	0.0048	1.74	0.0165	15.86	0.05153	15.76	0.1097	
det2b08	31.5	0.6	33.2	2.4	0.0049	0.93	0.0136	3.97	0.06976	3.86	0.2042	
det2d05	31.6	0.7	31.6	3.2	0.0049	1.19	0.0118	5.59	0.06704	5.46	0.2129	
det2d06	31.6	0.7	32.3	2.3	0.0049	1.04	0.0129	3.80	0.06876	3.66	0.2733	
det2b12	31.7	1.2	31.9	2.5	0.0049	1.94	0.0121	4.57	0.06751	4.14	0.4243	
det2d10	31.8	1	31.6	1.7	0.0049	1.65	0.0135	3.47	0.06816	3.05	0.4758	
det2d07	31.9	0.7	31	2.9	0.005	1.12	0.0116	5.08	0.06584	4.96	0.2203	
det2d09	31.9	0.8	33.1	2.8	0.005	1.33	0.0165	4.07	0.05294	3.85	0.3265	
det2d12	31.9	1.2	28.5	2.2	0.005	1.96	0.0298	4.43	0.04329	3.97	0.4427	
det2b05	32	1.3	30.6	2.5	0.005	1.98	0.0211	4.79	0.04509	4.36	0.4131	
det2b11	32.1	1.2	31.3	2.8	0.005	1.89	0.0119	4.34	0.06433	3.91	0.4352	
det2b09	32.2	1.1	34.8	3.6	0.005	1.72	0.0149	5.58	0.05059	5.31	0.3082	
det2d16	32.6	1.2	31.3	2	0.005	1.91	0.0122	3.93	0.06667	3.44	0.4854	
det2b08	32.5	1	31.3	2.1	0.0051	1.52	0.0129	3.64	0.0648	3.31	0.4173	
det2b10	32.6	0.9	32.3	2.1	0.0051	1.36	0.0141	3.43	0.06849	3.15	0.3964	
det2b16	32.6	1.2	30.1	2.4	0.0051	1.82	0.0312	4.27	0.04438	3.86	0.4265	
det2d13	32.8	1.2	30.9	1.7	0.0051	1.81	0.0322	3.05	0.04177	2.45	0.5942	
Mean (n=18)	**31.89**	**0.22**										
2 SD propagated		**0.45**										

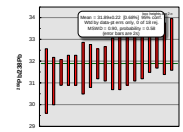

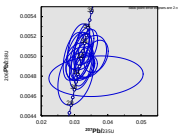

Aa1608 (4*29 in Fig. 1)	$^{208}Pb/^{232}Th$	± 2 SD	$^{207}Pb/^{235}U$	± 2 SD	$^{206}Pb/^{238}U$	± SD %	$^{207}Pb/^{206}Pb$	± SD %	$^{207}Pb/^{206}Pb$	± SD %	Corr. Coef.	Comment
jc2206	30.1	1.1	29.4	4.5	0.0047	1.84	0.0296	8.32	0.04575	8.11	0.2213	
jc2207	30.1	1.5	32.6	3.6	0.0047	2.42	0.0126	6.49	0.05039	6.02	0.3730	
jc2210	30.3	2.5	32.5	4.6	0.0047	4.17	0.0125	6.37	0.05033	4.82	0.6643	
jc2d07	30.6	1.4	34.1	5.3	0.0048	2.27	0.0240	7.80	0.05147	7.46	0.2911	
jc2d09	30.6	2	29.2	2.3	0.0048	3.29	0.0295	4.79	0.0446	3.48	0.6870	
jc2d07	30.7	0.8	29.9	3.3	0.0048	1.26	0.0265	5.54	0.04543	5.39	0.2276	
jc2209	30.8	2.2	32.1	3.3	0.0048	3.58	0.0130	7.52	0.04986	6.61	0.4762	
jc2d07	30.8	1.4	30.9	3	0.0048	2.31	0.0317	4.86	0.04795	4.28	0.4750	
jc2d10	30.9	2.7	32.9	4.7	0.0048	4.35	0.0332	8.73	0.05024	7.57	0.4962	
jc2d06	30.9	2	31	5.9	0.0048	3.19	0.0312	8.58	0.04712	7.96	0.3720	
jc2d09	30.9	0.9	29.4	3.1	0.0048	1.48	0.0295	5.73	0.04661	5.54	0.2581	
jc2d12	30.9	0.8	28.7	2.3	0.0048	1.26	0.0295	4.24	0.04583	4.05	0.2671	
jc2213	31	1.6	31.1	4.5	0.0048	2.61	0.0316	7.38	0.04771	6.9	0.3538	
jc2d11	31	0.6	34.4	3.7	0.0048	1.44	0.0245	5.63	0.05208	5.48	0.2559	
jc2d12	31.1	0.5	31.1	2.2	0.0048	0.8	0.0313	3.40	0.04737	3.3	0.2356	
jc2d13	31.1	0.6	33	2.5	0.0048	0.97	0.0334	3.99	0.05042	3.87	0.2431	
jc2211	31.1	2.1	30.1	6	0.0048	3.39	0.0296	11.48	0.04479	10.97	0.2952	
jc2d05	31.1	1.8	33.7	4.7	0.0048	2.96	0.0327	7.00	0.0495	6.47	0.4056	
jc2d08	31.2	2	33.7	5.2	0.0049	3.26	0.0349	7.86	0.05165	7.15	0.4149	
jc2d11	31.3	1.5	32.8	3.7	0.0049	2.34	0.0323	5.97	0.04776	5.49	0.3921	
jc22m11	31.3	1.2	34.4	6	0.0049	1.95	0.0372	8.92	0.05103	8.7	0.2187	
jc22m13	31.3	0.9	31	3.5	0.0049	1.37	0.0311	6.34	0.04608	6.19	0.2161	
jc22m10	31.5	1.1	33.9	2.9	0.0049	1.69	0.0345	4.70	0.0511	4.38	0.3593	
jc2208	31.7	1.5	32.4	2.6	0.0049	2.43	0.0331	4.49	0.04895	3.77	0.5418	
jc22m08	31.7	1.6	32	2.9	0.0049	2.55	0.0315	5.23	0.04661	4.57	0.4873	
jc22d05	31.8	2.7	30	2.5	0.0049	4.26	0.0302	5.64	0.04469	5.69	0.7559	
jc22m10	32.2	0.9	31	3.4	0.005	1.4	0.0314	5.76	0.04558	5.59	0.2429	
jc22m12	32.5	1.3	30.5	5	0.0051	1.98	0.0312	8.70	0.04434	8.47	0.2276	
Mean (n=28)	**31.11**	**0.21**										
2 SD propagated		**0.51**										

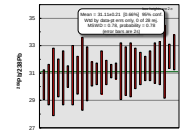

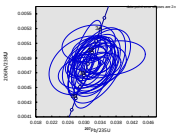

Aa1608 (4*21 in Fig. 1)	$^{208}Pb/^{232}Th$	± 2 SD	$^{207}Pb/^{235}U$	± 2 SD	$^{206}Pb/^{238}U$	± SD %	$^{207}Pb/^{206}Pb$	± SD %	$^{207}Pb/^{206}Pb$	± SD %	Corr. Coef.	Comment
jl04e01	27.7	0.6	27.8	3	0.0043	1.05	0.0277	9.72	0.04678	9.57	0.3822	
jl04e08	27.8	0.6	28.5	2	0.0043	1.02	0.0283	3.66	0.04776	3.52	0.2763	
jl04f09	27.8	0.8	28	2.9	0.0043	2.46	0.0276	5.58	0.04642	5.01	0.4608	
jl04g05	27.8	0.9	28.1	1.8	0.0043	1.65	0.0279	3.46	0.04703	3.04	0.4770	
jl04f12	27.9	0.7	28.2	2.1	0.0043	1.31	0.0282	4.20	0.04765	3.99	0.3119	
jl04g06	28.1	0.6	28.3	1.8	0.0044	1.1	0.0289	3.22	0.0476	3.03	0.3412	
jl04e06	28.3	0.8	29.6	0.7	0.0044	0.71	0.0294	1.49	0.04845	1.31	0.4765	
jl04e07	28.3	0.8	27	2.5	0.0044	1.33	0.0271	4.82	0.04475	4.63	0.2761	
jl04f13	28.5	0.8	27.5	2.2	0.0044	1.35	0.0277	4.29	0.04573	4.07	0.3148	
jl04e12	28.6	0.8	29.5	2	0.0044	1.42	0.0297	3.59	0.04906	3.3	0.3953	
jl04f05	28.6	0.8	27.3	1.7	0.0044	1.34	0.0277	3.20	0.04564	2.91	0.4183	
jl04f13	28.6	0.9	29	1.7	0.0044	1.56	0.0293	3.35	0.04784	2.97	0.4650	
jl04e09	28.7	0.6	29.6	2	0.0045	1.09	0.0304	3.73	0.04901	3.57	0.2620	
jl04f07	28.7	1.1	29.2	2	0.0045	1.88	0.0303	3.83	0.04883	3.34	0.4905	
jl04f12	28.9	0.8	30.4	1.7	0.0045	1.4	0.0302	3.16	0.04874	2.81	0.4659	
jl04e13	29	0.9	29.5	1.3	0.0045	1.6	0.0293	2.60	0.04729	2.05	0.6153	antecryst
jl04f08	29	0.7	28.8	1.5	0.0045	1.27	0.0293	3.09	0.04719	2.82	0.4106	antecryst
jl04f06	29.1	0.7	29	1.9	0.0045	1.25	0.0289	3.67	0.04667	3.45	0.3406	antecryst
jl04f10	29.2	0.7	30.1	2	0.0045	1.18	0.0301	3.81	0.04858	3.62	0.3099	antecryst
jl04f11	29.4	0.5	28.5	1.7	0.0046	0.94	0.0291	3.36	0.04595	3.23	0.2794	antecryst
Mean (n=51)	**28.26**	**0.21**										
2 SD propagated		**0.38**										

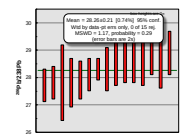

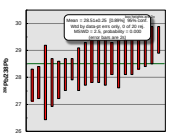

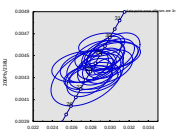

Aa1609 (4*22 in Fig. 1)	$^{208}Pb/^{232}Th$	± 2 SD	$^{207}Pb/^{235}U$	± 2 SD	$^{206}Pb/^{238}U$	± SD %	$^{207}Pb/^{206}Pb$	± SD %	$^{207}Pb/^{206}Pb$	± SD %	Corr. Coef.	Comment
jl06e05	27.1	1.1	27.5	4.1	0.0042	2.1	0.027151178	7.202020318	0.06691	6.89	0.291568205	
jl06e10	27.6	0.9	28.1	2.7	0.0043	1.63	0.028410078	5.284676168	0.06794	4.99	0.310501772	
jl06e02	27.5	1	30.6	3.6	0.0043	1.79	0.030729917	6.0412747	0.05189	5.77	0.296295085	
jl06e08	27.6	0.8	26.7	2.6	0.0043	1.53	0.026881135	5.890210373	0.06536	5.69	0.259609138	
jl06e09	27.6	1.1	29.7	3.8	0.0043	1.94	0.029673353	6.559336666	0.05097	6.3	0.294290602	
jl06f05	27.6	1.5	29.2	5.1	0.0043	2.8	0.029095749	7.734609562	0.04941	7.21	0.362009481	
jl06e07	27.7	1.2	27.6	3.6	0.0043	2.17	0.027631749	6.399164008	0.06663	6.02	0.319336795	
jl06f05	27.9	0.9	27.4	2.3	0.0043	1.53	0.026869273	4.698199564	0.06534	4.23	0.340136082	
jl06b12	28.2	0.8	28.1	2.9	0.0044	1.45	0.02875545	5.755840712	0.06742	5.57	0.251926775	
jl06e01	28.2	1	30.5	2.6	0.0044	1.8	0.030580712	5.257718136	0.05043	4.94	0.342353861	
jl06e13	28.2	1	27.9	3	0.0044	1.85	0.027712443	5.717549416	0.0457	5.41	0.323564065	
jl06e11	28.3	1.1	30.1	3.8	0.0044	1.95	0.030132088	6.709612507	0.05002	6.42	0.299427812	
jl06e10	28.3	1.2	28.1	3.7	0.0044	2.05	0.028015643	8.006878293	0.0462	7.74	0.256029869	
jl06b11	28.3	0.7	29.4	2.1	0.0044	1.27	0.029598233	3.713892836	0.04948	3.49	0.341950248	
jl06e12	28.3	0.9	29.4	3.5	0.0044	1.54	0.029803962	6.777285592	0.0475	6.6	0.227229616	
jl06e06	28.5	1.5	28.2	3.3	0.0044	2.6	0.028421631	6.621799798	0.04687	6.09	0.392443089	
jl06b07	28.5	0.7	29.3	2.6	0.0044	1.26	0.029604409	6.904630076	0.04882	4.74	0.256901156	
jl06b08	28.5	0.8	27.5	2.3	0.0044	1.35	0.027609156	6.421315096	0.04553	4.21	0.305350163	
jl06b13	28.5	1	28.4	3.2	0.0044	1.73	0.028227883	6.606616892	0.06655	5.75	0.288111733	
jl06b10	28.6	0.8	28	2.7	0.0044	1.42	0.027651804	6.747346427	0.0456	4.53	0.299134455	
jl06b06	29.5	0.7	29.3	1.5	0.0046	1.22	0.029698289	3.763837911	0.06653	2.48	0.441415177	inherited core
Mean (n=28)	**28.09**	**0.21**										
2 SD propagated		**0.38**										

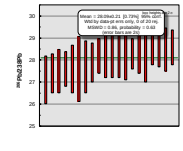

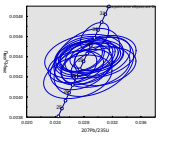

Aa1606A (4*24 in Fig. 1)	$^{208}Pb/^{232}Th$	± 2 SD	$^{207}Pb/^{235}U$	± 2 SD	$^{206}Pb/^{238}U$	± SD %	$^{207}Pb/^{206}Pb$	± SD %	$^{207}Pb/^{206}Pb$	± SD %	Corr. Coef.	Comment
det2d02	26.2	0.6	27.1	1.9	0.0041	0.89	0.0265	2.96	0.04626	2.82	0.3016	
det2d07	26.4	0.4	27.2	1.1	0.0041	0.69	0.0273	2.27	0.04824	2.16	0.3043	
det2d03	26.4	0.3	24.9	1.4	0.0041	0.64	0.0249	2.87	0.04408	2.8	0.2238	
det2d11	26.4	0.4	27.2	1.6	0.0041	0.8	0.0273	3.03	0.04833	2.92	0.2642	
det2d12	26.5	0.5	27.1	1.7	0.0041	0.94	0.0272	3.28	0.04817	3.14	0.2868	
det2d07	26.5	0.4	25.7	1.1	0.0041	0.79	0.0259	2.34	0.04576	2.2	0.3380	
det2e02	26.5	0.3	27.2	1.3	0.0041	0.61	0.0274	2.53	0.04852	2.46	0.2407	
det2d09	26.6	0.4	27.2	1.1	0.0041	0.71	0.0270	2.31	0.04787	2.2	0.3071	
det2d13	26.6	0.4	27	1.2	0.0041	0.83	0.0273	2.63	0.04791	2.38	0.3421	
det2e08	26.6	0.3	26.2	1.3	0.0041	0.64	0.0262	2.58	0.04632	2.5	0.2480	
det2d08	26.8	0.4	28	1.5	0.0042	0.68	0.0286	2.71	0.04946	2.52	0.2512	
det2e11	26.8	0.3	26.1	1.2	0.0042	0.65	0.0266	2.54	0.04595	2.46	0.2555	
det2d01	26.9	0.4	26.4	1.3	0.0042	0.68	0.0270	2.58	0.04617	2.44	0.2555	
det2d05	26.9	0.4	26.5	1.4	0.0042	0.68	0.0271	2.76	0.04682	2.67	0.2468	
det2d04	26.9	0.4	27.1	1.4	0.0042	0.69	0.0274	2.75	0.04728	2.66	0.2511	
det2e13	27	0.4	28.6	1.5	0.0042	0.72	0.0298	2.78	0.04967	2.69	0.2586	antecryst
det2e06	27	0.4	27.1	1.1	0.0042	0.81	0.0273	2.19	0.0472	2.04	0.3690	antecryst
det2d06	27.2	0.4	27	1.2	0.0042	0.6	0.0271	2.49	0.04679	2.25	0.3020	antecryst
det2e09	27.3	0.3	28	1	0.0042	0.62	0.0284	1.86	0.04898	1.75	0.3339	antecryst
det2d08	27.4	0.3	27.8	1.4	0.0043	0.72	0.0283	2.55	0.04754	2.45	0.2820	antecryst
det2d17	47.9	1.2	55.4	5.5	0.0075	1.28	0.0540	5.09	0.05303	5.35	0.2227	antecryst
det2e10	66.9	1.7	51.6	8.7	0.0073	1.82	0.0519	8.73	0.0501	9.14	0.1913	antecryst
det2c11	29.2	0.7	30	3.5	0.0045	1.22	0.0300	5.89	0.04875	5.34	0.2227	antecryst
det2e05	31	0.6	29.8	2.3	0.0048	0.91	0.0298	3.94	0.04924	3.86	0.2295	antecryst
Mean (n=51)	**26.61**	**0.09**										
2 SD propagated		**0.26**										

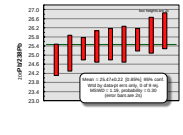

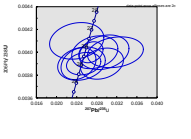

Aa1608A1 (4*25 in Fig. 1)	$^{208}Pb/^{232}Th$	± 2 SD	$^{207}Pb/^{235}U$	± 2 SD	$^{206}Pb/^{238}U$	± SD %	$^{207}Pb/^{206}Pb$	± SD %	$^{207}Pb/^{206}Pb$	± SD %	Corr. Coef.	Comment
det1b10	24.8	0.7	23.9	2.6	0.0039	1.46	0.0244	5.84	0.04532	5.65	0.2502	
det1b11	25.1	0.8	25.1	2.9	0.0039	1.53	0.0250	7.76	0.04643	7.61	0.1971	
det1b11	25.3	0.5	25.6	2.6	0.0039	1.03	0.0254	5.50	0.04723	5.4	0.1874	
det1b12	25.4	0.7	29.5	3.4	0.0039	1.43	0.0298	6.02	0.05401	5.85	0.2375	
det1b10	25.5	0.7	31.6	4.3	0.004	1.38	0.0317	7.16	0.05714	7.03	0.1926	
det1b13	25.5	0.8	29	3.8	0.004	1.55	0.0295	6.87	0.05143	6.69	0.2257	
det1b08	25.7	0.6	26.3	1.8	0.004	0.94	0.0268	3.67	0.04867	3.55	0.2560	
det1b09	25.9	0.8	27.7	3.6	0.004	1.47	0.0276	6.80	0.05007	6.64	0.2162	
det1b07	26.1	0.8	24	6.2	0.0041	1.6	0.0248	9.19	0.04348	9.05	0.1741	
Mean (n=9)	**25.47**	**0.22**										
2 SD propagated		**0.52**										

Aa1606 (4*31 in Fig. 1)	$^{208}Pb/^{232}Th$	± 2 SD	$^{207}Pb/^{235}U$	± 2 SD	$^{206}Pb/^{238}U$	± SD %	$^{207}Pb/^{206}Pb$	± SD %	$^{207}Pb/^{206}Pb$	± SD %	Corr. Coef.	Comment
det2g06	23.4	1.7	22.1	1.8	0.0036	3.56	0.0219	5.04	0.04608	3.57	0.7061	
det2h13	23.4	0.7	21.2	3.2	0.0036	1.49	0.0210	8.73	0.04236	8.6	0.1707	
det2g10	24	1.8	27	3.9	0.0037	3.8	0.0265	8.47	0.05188	7.57	0.4486	
det2g07	24.2	1.9	21.7	3.7	0.0038	3.95	0.0215	9.33	0.041	8.45	0.4235	
det2h14	24.2	1	28.1	4.4	0.0038	2.12	0.0284	9.05	0.05418	8.8	0.2342	
det2g11	24.3	1.5	28.1	4.6	0.0038	3.02	0.0288	8.52	0.05347	7.97	0.3543	
det2h09	24.3	0.8	19.5	2.7	0.0038	1.65	0.0197	7.51	0.03756	7.33	0.2196	
det2h06	24.5	1	23	2.3	0.0038	1.98	0.0229	6.01	0.0438	5.67	0.3297	
det2h01	24.6	0.7	26.2	2.7	0.0038	1.38	0.0261	5.51	0.04983	5.33	0.2506	
det2h11	24.6	0.8	24.6	2.9	0.0038	1.55	0.0247	6.55	0.04707	6.36	0.2368	
det2h07	24.7	1	24	2.6	0.0038	1.94	0.0241	5.93	0.046	5.4	0.3273	
det2h10	24.7	1	23.4	3.6	0.0038	2.01	0.0233	7.85	0.04648	7.59	0.2560	
det2g08	24.8	2	25.5	3.9	0.0039	3.94	0.0255	8.79	0.04735	7.86	0.4481	
det2g14	24.8	0.9	26.8	3.9	0.0039	1.74	0.0275	8.07	0.05113	7.88	0.2156	
det2h12	25.2	1	26.4	4	0.0039	1.92	0.0261	8.30	0.04851	8.07	0.2315	
det2g12	25.4	0.9	25.7	4.7	0.0039	1.73	0.0255	9.39	0.04743	9.23	0.1842	
det2g13	50.2	0.8	30.5	2.6	0.0047	1.4	0.0313	4.63	0.04834	4.41	0.3016	antecryst
det2h04	31	1	27.9	3	0.0048	1.59	0.0280	5.40	0.04239	5.16	0.2945	antecryst
Mean (n=14)	**24.47**	**0.3**										
2 SD propagated		**0.42**										

5/13/07 (n°25 in File 1)	$^{206}Pb/^{238}U$	± 2 SD	$^{207}Pb/^{235}U$	± 2 SD	$^{206}Pb/^{238}U$	± SD %	$^{207}Pb/^{235}U$	± SD %	$^{207}Pb/^{206}Pb$	± SD %	Conc. Conf	Comment
det18f2	23.7	0.8	28.6	3.3	0.0037	3.6	0.0281	6.16	0.05508	5.46	0.2597	
det1g07	23.7	1	24.4	3.8	0.0037	2.12	0.0245	7.73	0.04816	7.43	0.2744	
det4g11	23.7	1.3	24.6	4.9	0.0037	2.68	0.0247	11.87	0.04835	11.56	0.2258	
det1f06	23.9	0.8	24.5	3.7	0.0037	1.67	0.0246	8.25	0.04819	8.08	0.2024	
det4g13	24.1	0.5	26.8	2.4	0.0037	1.11	0.0267	4.70	0.05228	4.57	0.2460	
det4g08	24.2	1.6	23.2	4.4	0.0038	3.33	0.0236	9.76	0.04501	9.17	0.3413	
det4f07	24.4	0.5	23.6	2.5	0.0038	1.1	0.0235	5.47	0.04593	5.36	0.2010	
det4f09	24.4	0.8	25	3	0.0038	1.57	0.0249	6.58	0.04761	6.39	0.2186	
det4f10	24.5	0.9	24.2	3.7	0.0038	1.76	0.0239	7.67	0.04742	7.47	0.2293	
det4g10	24.5	1.9	25.7	4.3	0.0038	3.81	0.0257	8.85	0.04912	7.99	0.4304	
det4f13	24.6	1.4	24.9	3.7	0.0038	2.26	0.0250	8.30	0.04771	7.99	0.2722	
det4f12	24.8	0.9	27.2	4.4	0.0039	1.8	0.0275	8.51	0.0512	8.32	0.2115	
det4e12	24.9	0.7	23.1	3.8	0.0039	1.38	0.0232	8.46	0.04321	8.35	0.1631	
det4g09	25.3	1.8	25.5	3.8	0.0039	3.48	0.0250	8.65	0.04646	7.92	0.4023	
det4g06	31.7	0.9	32.4	3.5	0.0049	1.5	0.0324	5.49	0.0487	5.31	0.2718	anterycet
Mean (n=14)	**24.3**	**0.22**										
2 SD propagated		**0.31**										

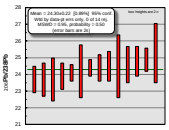

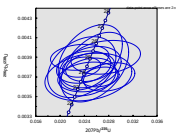

11/30/1 (n°27 in File 1)	$^{206}Pb/^{238}U$	± 2 SD	$^{207}Pb/^{235}U$	± 2 SD	$^{206}Pb/^{238}U$	± SD %	$^{207}Pb/^{235}U$	± SD %	$^{207}Pb/^{206}Pb$	± SD %	Conc. Conf	Comment
det1m05	22	0.6	23.1	1.7	0.0034	1.33	0.0230	3.78	0.04906	3.54	0.3517	
det1h07	22.3	0.5	23.3	2.2	0.0035	1.21	0.0241	4.93	0.04998	4.78	0.2454	
det1h06	22.4	0.6	21.9	2.2	0.0035	1.35	0.0224	5.17	0.04653	4.99	0.2612	
det1h08	22.4	0.5	20.5	2.3	0.0035	1.04	0.0208	5.91	0.04309	5.82	0.1759	
det1h11	22.6	0.7	23.4	5.6	0.0035	1.51	0.0237	14.36	0.04904	14.26	0.1052	
det1h09	22.7	0.5	21	1.9	0.0035	1.1	0.0209	5.05	0.04343	4.91	0.2178	
det1h14	22.7	0.5	22.3	1.6	0.0035	1.15	0.0232	3.71	0.04819	3.53	0.3098	
det1m14	22.8	0.6	22.7	2	0.0035	1.11	0.0228	4.65	0.04736	4.72	0.2269	
det1h10	22.9	0.5	24.3	2.1	0.0036	1.16	0.0255	4.83	0.05132	4.69	0.2401	
det1h13	22.9	0.6	24.6	4.6	0.0036	1.35	0.0252	9.13	0.05201	9.03	0.1479	
det1m06	23.1	0.5	23.4	1.6	0.0036	1.14	0.0239	3.71	0.04826	3.53	0.3073	anterycet
det1m08	23.1	0.6	22.7	1.6	0.0036	1.86	0.0233	4.34	0.0465	3.92	0.4287	anterycet
det1m11	23.1	1.2	22.7	2.3	0.0036	2.53	0.0233	6.55	0.04704	6.04	0.3863	anterycet
det1m07	23.2	0.4	22	1.1	0.0036	0.88	0.0223	3.02	0.04685	2.89	0.2913	anterycet
det1m12	23.4	0.6	23.1	1.6	0.0036	2.91	0.0234	4.26	0.04714	3.31	0.6832	anterycet
det1m09	23.5	1.2	24	1.6	0.0037	2.46	0.0249	4.39	0.04883	3.64	0.5199	anterycet
det1m10	23.6	1	23.2	1.8	0.0037	2.21	0.0236	4.28	0.04625	3.67	0.5159	anterycet
Mean (n=18)	**22.58**	**0.17**										
2 SD propagated		**0.46**										

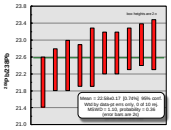

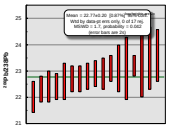

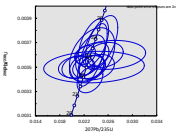

11/3/1A (n°28 in File 1)	$^{206}Pb/^{238}U$	± 2 SD	$^{207}Pb/^{235}U$	± 2 SD	$^{206}Pb/^{238}U$	± SD %	$^{207}Pb/^{235}U$	± SD %	$^{207}Pb/^{206}Pb$	± SD %	Conc. Conf	Comment
det1f01	21.7	0.6	23	1.3	0.0034	1.31	0.0234	3.57	0.04988	3.32	0.3670	
det1f07	21.9	0.3	22.3	1.2	0.0034	0.72	0.0226	2.91	0.04818	2.82	0.2474	
det1f06	22	0.5	23.6	1.4	0.0034	1.15	0.0237	3.69	0.05029	3.39	0.3300	
det1h12	22	0.3	24.6	1.4	0.0036	0.97	0.0223	3.96	0.0533	2.95	0.2449	
det1f05	22.1	0.3	21.5	1.3	0.0034	0.71	0.0217	3.01	0.0464	2.99	0.2015	
det1f06	22.1	0.3	21.8	0.7	0.0034	0.67	0.0222	1.94	0.04736	1.82	0.3455	
det1f11	22.1	0.8	22.2	1.7	0.0034	1.73	0.0220	4.36	0.04701	4	0.3670	
det1f09	22.1	0.4	21.6	1.6	0.0034	1.14	0.0218	3.75	0.04585	3.65	0.3062	
det1g09	22.1	0.6	22.6	1.3	0.0034	1.27	0.0225	3.33	0.04793	3.04	0.4109	
det1g11	22.1	0.6	21.6	1.4	0.0034	1.44	0.0217	3.67	0.04637	3.38	0.3919	
det1f08	22.2	0.6	22.5	1.4	0.0036	0.97	0.0223	3.96	0.04784	3.17	0.3449	
det1f07	22.3	0.6	20.8	2	0.0035	1.24	0.0213	5.31	0.04606	5.16	0.2237	
det1f10	22.3	0.5	21.9	1.3	0.0035	1.09	0.0225	3.33	0.04659	3.31	0.3308	
det1g12	22.3	0.6	23.9	1.5	0.0035	1.43	0.0243	3.45	0.05034	3.14	0.4145	
det1h11	22.3	0.4	22.8	1.2	0.0036	0.97	0.0223	3.96	0.04848	2.4	0.2449	
det1f08	22.4	0.4	22.5	1.5	0.0035	1	0.0229	3.52	0.04747	3.37	0.2845	
det1f08	22.4	0.4	22.5	1.2	0.0035	0.72	0.0232	2.79	0.04834	2.6	0.2669	
det1f10	22.4	0.4	23.2	1.3	0.0035	0.93	0.0235	3.26	0.0487	3.12	0.2857	
det1f06	22.4	0.4	21.4	1.3	0.0035	0.99	0.0218	3.88	0.04729	3.75	0.2553	
det1f07	22.4	0.5	23.4	1.3	0.0036	0.97	0.0223	3.96	0.04954	2.83	0.2449	
det1h10	22.4	0.4	22.3	1.3	0.0036	0.97	0.0223	3.96	0.04704	2.99	0.2449	
det1e12	22.5	0.6	22	1.4	0.0035	1.43	0.0222	3.51	0.04612	3.21	0.4069	
det1g05	22.5	0.5	22.6	1.7	0.0035	1.1	0.0226	4.10	0.04687	3.95	0.2683	
det1g06	22.5	0.5	21.9	1.1	0.0035	1.03	0.0224	2.50	0.04635	2.38	0.4117	
det1g08	22.5	0.6	22.4	1.4	0.0035	1.3	0.0225	3.44	0.04663	3.19	0.3774	
det1h09	22.6	0.5	22.2	1.2	0.0035	1.19	0.0225	3.13	0.04662	2.89	0.3807	
det1g07	22.7	0.5	27.4	1.3	0.0035	2.06	0.0243	3.86	0.05758	2.45	0.5130	anterycet
det1g10	22.7	0.4	22.9	1.2	0.0035	0.98	0.0231	2.89	0.04781	2.72	0.3390	anterycet
det1f11	22.8	0.4	21.6	1.3	0.0035	1.03	0.0220	3.13	0.04554	2.96	0.3286	anterycet
det1e13	22.9	0.4	22.7	1	0.0036	0.92	0.0235	2.31	0.0474	2.12	0.3981	anterycet
det1g13	22.9	0.6	21.9	1.4	0.0035	1.61	0.0224	2.87	0.04577	3.12	0.5603	anterycet
det1h04	22.9	0.5	23.4	1.5	0.0036	0.97	0.0223	3.96	0.04805	3.31	0.2449	anterycet
Mean (n=25)	**22.23**	**0.08**										
2 SD propagated		**0.25**										

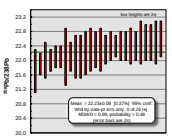

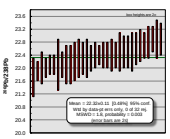

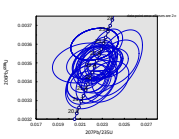

11/3/2A (n°29 in File 1)	$^{206}Pb/^{238}U$	± 2 SD	$^{207}Pb/^{235}U$	± 2 SD	$^{206}Pb/^{238}U$	± SD %	$^{207}Pb/^{235}U$	± SD %	$^{207}Pb/^{206}Pb$	± SD %	Conc. Conf	Comment
det1e07	21.6	1	21.7	1.3	0.0034	2.42	0.0222	3.53	0.0474	2.57	0.6855	
det1e07	21.7	0.7	21.6	1.3	0.0034	1.53	0.0221	3.61	0.04712	3.27	0.4238	
det1e06	21.9	0.5	21.6	1.7	0.0034	1.08	0.0217	4.14	0.04624	4	0.2607	
det1e09	21.9	1.2	22.3	1.4	0.0034	2.64	0.0221	4.50	0.04724	3.64	0.5871	
det1e10	21.9	1	22.3	1.5	0.0034	2.35	0.0226	3.94	0.04824	3.16	0.5967	
det1e08	21.9	0.9	22.4	1.4	0.0034	2.17	0.0229	3.63	0.04889	2.91	0.5978	
det1e05	22	0.3	21.6	1.2	0.0034	0.73	0.0216	3.24	0.04601	3.16	0.2251	
det1h13	22	0.5	21.9	1.5	0.0034	1.15	0.0221	3.55	0.04716	3.36	0.3198	
det1c13	22	0.4	21.6	1.7	0.0034	1	0.0218	3.87	0.0465	3.74	0.2583	
det1h10	22.1	0.4	22.2	1.4	0.0034	0.91	0.0222	3.60	0.04734	3.27	0.2756	
det1c05	22.1	0.4	21.6	1.2	0.0034	1.02	0.0218	3.00	0.04653	2.82	0.3401	
det1d06	22.1	0.5	21.3	1.4	0.0034	1.21	0.0214	3.43	0.04566	3.21	0.3527	
det1c12	22.1	0.6	21.2	1.2	0.0034	1.3	0.0216	3.27	0.04616	3	0.3976	
det1d07	22.1	0.5	21.8	1.7	0.0034	1.14	0.0218	3.75	0.04653	3.57	0.3042	
det1h11	22.2	0.4	21.5	1.2	0.0034	0.93	0.0215	3.04	0.0458	2.89	0.3063	
det1h12	22.2	0.4	23.6	1.4	0.0034	0.9	0.0234	3.22	0.05002	3.09	0.2796	
det1h09	22.2	0.4	21.2	1.1	0.0035	0.87	0.0218	2.76	0.04512	2.62	0.3151	
det1e11	22.3	0.9	22	1.5	0.0035	2.1	0.0224	3.52	0.04645	2.83	0.5959	
det1h08	22.3	0.5	21.2	1.1	0.0035	1.11	0.0218	3.11	0.04524	2.91	0.3564	
det1h09	22.3	1.3	22.5	1.6	0.0035	2.9	0.0229	4.34	0.04739	3.23	0.6681	
det1h04	22.4	0.9	23.7	1.6	0.0035	2.06	0.0243	3.86	0.05046	3.27	0.5330	
det1d05	22.4	0.5	23.4	1.7	0.0035	1.02	0.0238	3.79	0.04939	3.65	0.2691	
det1d12	22.4	0.6	21	1.2	0.0035	1.26	0.0217	3.06	0.04509	2.79	0.4116	
det1e12	22.5	1	22.4	1.2	0.0035	2.13	0.0226	3.38	0.04727	2.63	0.6294	
det1e08	22.6	0.9	23.1	1.4	0.0035	1.96	0.0237	3.26	0.04916	2.6	0.6020	
det1f06	22.6	0.5	22.3	1.8	0.0035	1.03	0.0223	4.29	0.04623	4.16	0.2403	
det1e13	22.7	0.7	22.1	1.1	0.0035	1.61	0.0224	2.87	0.04637	2.38	0.5603	
det1d11	22.8	0.5	23.3	1.3	0.0035	1.18	0.0236	2.98	0.04891	2.74	0.3955	
det1h08	23	0.4	22	1.7	0.0036	0.97	0.0223	3.96	0.04697	3.84	0.2449	
Mean (n=29)	**22.23**	**0.12**										
2 SD propagated		**0.27**										

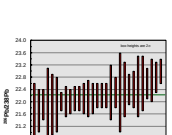

5/13/13 (n°30 in File 1)	$^{206}Pb/^{238}U$	± 2 SD	$^{207}Pb/^{235}U$	± 2 SD	$^{206}Pb/^{238}U$	± SD %	$^{207}Pb/^{235}U$	± SD %	$^{207}Pb/^{206}Pb$	± SD %	Conc. Conf	Comment
p22g06	20.9	0.6	21.4	2.5	0.0032	1.35	0.0208	6.41	0.04725	6.27	0.2105	
p22g10	20.9	0.5	20.7	1.5	0.0032	1.09	0.0206	3.77	0.04664	3.61	0.2891	
p22h09	20.9	0.4	21.7	1.1	0.0033	0.94	0.0220	2.82	0.04829	2.66	0.3332	
p22i07	20.9	0.5	21.9	3	0.0032	1.29	0.0218	6.54	0.0493	6.41	0.1973	
p22i05	21	0.4	21.6	1.3	0.0033	0.95	0.0218	3.32	0.04795	3.18	0.2862	
p22j07	21	0.5	21.6	2	0.0033	1.29	0.0218	5.04	0.04803	4.87	0.2561	
p22g07	21.1	0.3	20.3	1.4	0.0033	0.81	0.0208	3.63	0.04566	3.54	0.2230	
p22h11	21.1	0.4	21.4	1.9	0.0033	1.04	0.0214	4.78	0.04707	4.67	0.2174	
p22h13	21.1	0.4	21.6	1.7	0.0033	1.02	0.0218	3.93	0.04803	3.8	0.2592	
p22i10	21.2	0.4	22.3	1.9	0.0033	0.98	0.0223	4.56	0.049	4.45	0.2151	
p22j06	21.2	0.5	21.2	1.7	0.0033	1.15	0.0215	4.17	0.04725	4.01	0.2757	
p22j08	21.2	0.4	21.9	2	0.0033	1.01	0.0219	4.65	0.05213	4.33	0.2272	
p22g05	21.3	0.5	20.3	2.1	0.0033	1.11	0.0199	5.36	0.04366	5.24	0.2072	
p22g08	21.3	0.5	22.4	1.9	0.0033	1.12	0.0220	4.60	0.04908	4.26	0.2543	
p22g09	21.3	0.5	21.7	1.9	0.0033	1.12	0.0216	4.53	0.04743	4.39	0.2472	
p22h10	21.3	0.5	21	1.9	0.0033	1.01	0.0212	4.64	0.04668	4.48	0.2407	
p22j09	21.3	0.5	20.9	2	0.0033	1.18	0.0205	4.97	0.04518	4.83	0.2373	
p22j13	21.3	0.5	22.2	2.5	0.0033	1.29	0.0218	5.69	0.04787	5.54	0.2268	
p22g13	21.4	0.5	22.3	1.9	0.0033	1.09	0.0221	4.54	0.0486	4.41	0.2399	
p22h07	21.4	0.4	22.8	1.4	0.0033	1	0.0227	3.45	0.04989	3.3	0.2600	
p22i11	21.5	0.5	22.6	1.6	0.0033	1.21	0.0225	3.66	0.04944	3.45	0.3310	
p22j10	21.5	0.7	22.2	2.3	0.0033	1.58	0.0220	5.59	0.04839	5.36	0.3827	
p22h12	21.6	0.4	21.8	1.8	0.0034	0.86	0.0221	4.00	0.04707	3.91	0.2148	
p22i09	21.7	0.6	23	2.1	0.0034	1.41	0.0230	5.07	0.04686	4.87	0.2781	
p22i12	21.7	0.5	21.5	2	0.0034	1.19	0.0219	5.00	0.04664	4.86	0.2378	
p22h06	21.8	0.4	22.1	1.5	0.0034	1.02	0.0220	3.75	0.04697	3.61	0.2719	anterycet
p22g12	21.9	0.5	22.7	1.7	0.0034	1.12	0.0228	4.25	0.04872	4.1	0.2635	anterycet
p22g11	22	0.5	22.6	1.9	0.0034	1.24	0.0224	4.25	0.04779	4.06	0.2621	anterycet
p22i06	22.1	0.6	23.4	2	0.0034	1.32	0.0231	4.24	0.04935	4.03	0.3113	anterycet
p22i08	22.2	0.6	22.9	1.9	0.0034	1.29	0.0226	4.52	0.04821	4.33	0.2855	anterycet
p22j13	23	0.6	24.1	1.7	0.0036	1.23	0.0244	3.91	0.04922	3.71	0.3147	anterycet
Mean (n=31)	**21.22**	**0.09**										
2 SD propagated		**0.31**										

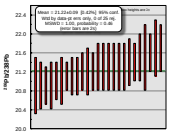

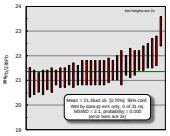

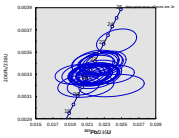

Table DR3: Re-Os data for molybdenite from various PCDs hosted by the Meghri-Ordubad pluton

Sample	Location	wt (g)	Re (ppm)	±	^{187}Re (ppm)	±	^{187}Os (ppb)	±	Age (Ma)	±[a]	±[b]	Description
RO280-2_N2[d]	Agarak	0.024	538.8	1.9	338.7	1.2	249.6	0.7	44.23	0.18	0.22	stockwork-like veins (quartz-molybdenite-chalcopyrite)
RO812-3_Ankaser_N72p[d]	Hanqasar	0.022	76.3	0.3	47.9	0.2	34.5	0.1	43.14	0.17	0.22	stockwork-like veins (quartz-molybdenite)
RO812-7_Aigedzor_NRM-0560[d]	Aygedzor	0.011	1141.0	5.5	717.2	3.5	509.5	2.3	42.62	0.17	0.22	stockwork-like veins (quartz-molybdenite)
RO758-5_KJ1509	Kadjaran	0.020	238.6	0.9	150.0	0.6	68.2	0.2	27.28	0.11	0.14	stockwork-like veins (quartz-molybdenite-chalcopyrite)
RO280-1_NI[d]	Kadjaran	0.042	368.3	1.2	231.5	0.8	104.9	0.3	27.19	0.11	0.14	stockwork-like veins (quartz-molybdenite)
RO596-2_KJ-13-25A	Kadjaran	0.015	350.8	1.4	220.5	0.9	97.9	0.4	26.65	0.11	0.14	sheared stockwork-like veins (quartz-molybdenite-chalcopyrite)
RO612-10_KJ-13-25A[c]	Kadjaran	0.027	365.4	1.3	229.6	0.8	101.9	0.3	26.64	0.11	0.14	sheared stockwork-like veins (quartz-molybdenite-chalcopyrite)
RO391-2_KJ-10-13A[d]	Kadjaran	0.050	160.4	0.5	100.8	0.3	44.4	0.1	26.43	0.11	0.13	stockwork-like veins (quartz-molybdenite-chalcopyrite)
RO758-6_KJ15X1	Kadjaran	0.020	360.6	1.3	226.6	0.8	77.4	0.2	20.48	0.08	0.10	reopening of moly stockwork-like veins (quartz-molybdenite-chalcopyrite)

[a] age uncertainty includes all analytical sources of uncertainty

[b] age uncertainty includes all analytical sources of uncertainty and the uncertainty in the ^{187}Re decay constant

[c] repeat analysis. Aliquot analyzed comes from one mineral separate.

[d] Re-Os ages cited in Moritz et al. (2016)

Table DR4: Results of in situ MC-ICP-MS εHf isotope analyses.

SAMPLES

Analysis (n=365)	# cycles integrated	176Hf/177Hf	176Hf/177Hf std corrected	2se	176Lu/177Hf	2se	173Yb/177Hf	1se	174Hf/177Hf	2se	178Hf/177Hf	2se	U-Pb Age (Ma)[a]	176Hf/177Hf (t) CHUR[b]	176Hf/177Hf (t)	εHf (t)	2se
AG1304A (s080515) n=11																	
AG1304A_1.dat	80	0.283003	0.283000	1.88E-05	0.003034	3.03E-04	0.149593	9.62E-03	0.008679	2.36E-05	1.467268	0.000126601	50.5	0.282753	0.282997	8.6	1.3
AG1304A_2.dat	60	0.282996	0.282993	1.47E-05	0.001209	4.18E-05	0.056566	1.93E-03	0.008655	1.36E-05	1.467249	0.000156556	49.3	0.282754	0.282991	8.4	1.0
AG1304A_3.dat	100	0.283055	0.283052	2.80E-05	0.009890	7.42E-05	0.417537	5.05E-03	0.008741	3.57E-05	1.467267	0.000111033	50.2	0.282753	0.283043	10.2	2.0
AG1304A_4.dat	70	0.282994	0.282991	1.61E-05	0.003402	1.27E-04	0.159420	4.16E-03	0.008686	2.06E-05	1.467285	0.000143296	49.1	0.282754	0.282988	8.3	1.1
AG1304A_5.dat	60	0.283001	0.282997	1.75E-05	0.000922	1.12E-05	0.041956	9.24E-04	0.008665	1.26E-05	1.467278	0.000147851	49	0.282754	0.282997	8.6	1.2
AG1304A_6.dat	50	0.283037	0.283034	2.41E-05	0.001793	3.04E-05	0.072572	1.92E-03	0.008675	2.40E-05	1.467385	0.000219672	48	0.282755	0.283032	9.8	1.7
AG1304A_7.dat	90	0.282996	0.282992	1.46E-05	0.001019	2.58E-05	0.043738	2.83E-04	0.008667	1.13E-05	1.467227	0.000122337	49.4	0.282754	0.282991	8.4	1.0
AG1304A_8.dat	120	0.283014	0.283010	1.15E-05	0.001317	3.55E-05	0.053413	4.81E-04	0.008668	1.09E-05	1.467277	9.41902E-05	49.2	0.282754	0.283009	9.0	0.8
AG1304A_9.dat	100	0.283030	0.283026	1.60E-05	0.000971	7.38E-06	0.042508	7.74E-04	0.008672	1.10E-05	1.467245	0.000119325	48.6	0.282754	0.283025	9.6	1.1
AG1304A_11.dat	70	0.283016	0.283013	1.39E-05	0.001040	1.42E-05	0.043985	9.39E-04	0.008658	1.23E-05	1.467229	0.000127835	49.1	0.282754	0.283012	9.1	1.0
AG1304A_12.dat	70	0.283005	0.283002	1.46E-05	0.001327	4.72E-05	0.056823	9.52E-04	0.008655	1.23E-05	1.467268	0.000129036	50.1	0.282754	0.283000	8.7	1.0
Median ± 2SD																**8.7**	**1.3**
MA1501 (s07-081015) n=13																	
MA1501_01	110	0.282958	0.282974	9.84E-06	0.001256	5.18E-05	0.049253	1.04E-03	0.008658	7.28E-06	1.467266	0.000106828	47.4	0.282755	0.282973	7.7	0.7
MA1501_02	120	0.282967	0.282983	8.60E-06	0.001364	7.51E-05	0.056342	1.86E-03	0.008675	7.13E-06	1.467258	7.82789E-05	47.6	0.282755	0.282982	8.0	0.6
MA1501_03	120	0.282967	0.282983	7.40E-06	0.001352	2.34E-05	0.053815	7.77E-04	0.008659	7.07E-06	1.467255	9.08356E-05	46.7	0.282756	0.282981	8.0	0.5
MA1501_04	90	0.282973	0.282988	1.10E-05	0.001508	2.46E-05	0.060278	6.83E-04	0.008666	8.44E-06	1.467236	9.20218E-05	47.7	0.282755	0.282987	8.2	0.8
MA1501_05	100	0.282974	0.282989	9.60E-06	0.001596	1.89E-05	0.065849	6.63E-04	0.008665	7.79E-06	1.467253	0.000101266	46.4	0.282756	0.282988	8.2	0.7
MA1501_06	120	0.282983	0.282999	8.93E-06	0.001151	1.16E-05	0.045856	3.81E-04	0.008657	6.67E-06	1.467247	8.13576E-05	48.1	0.282755	0.282998	8.6	0.6
MA1501_07	120	0.282966	0.282982	8.11E-06	0.001537	6.91E-05	0.058773	1.29E-03	0.008661	7.86E-06	1.467282	6.80146E-05	47.9	0.282755	0.282981	8.0	0.6
MA1501_08	120	0.282978	0.282994	7.48E-06	0.001591	4.80E-05	0.062274	6.66E-04	0.008657	7.07E-06	1.467246	7.60765E-05	48.9	0.282754	0.282992	8.4	0.5
MA1501_09	120	0.282968	0.282984	8.26E-06	0.001367	1.65E-05	0.052438	5.92E-04	0.008660	6.31E-06	1.467247	9.8991E-05	48.2	0.282755	0.282983	8.1	0.6
MA1501_10	120	0.282961	0.282977	8.27E-06	0.001603	6.01E-05	0.060294	1.15E-03	0.008668	7.59E-06	1.467280	7.29194E-05	47.4	0.282755	0.282975	7.8	0.6
MA1501_11	120	0.282977	0.282992	7.72E-06	0.001417	2.11E-05	0.053355	3.79E-04	0.008674	6.72E-06	1.467242	7.79709E-05	47.2	0.282755	0.282991	8.3	0.5
MA1501_12	120	0.282959	0.282975	7.77E-06	0.001455	4.59E-05	0.056207	8.00E-04	0.008667	6.62E-06	1.467251	8.18464E-05	46.9	0.282756	0.282974	7.7	0.5
MA1501_13	120	0.282956	0.282971	8.14E-06	0.001530	8.49E-05	0.058721	1.78E-03	0.008652	7.00E-06	1.467258	7.78984E-05	47.7	0.282755	0.282970	7.6	0.6
Median ± 2SD																**8.0**	**0.6**
AG1401 (s080515) n=10																	
AG1401_1.dat	90	0.283018	0.283015	1.50E-05	0.003241	1.04E-04	0.138299	2.55E-03	0.008677	2.21E-05	1.467263	0.000102319	46.8	0.282756	0.283012	9.1	1.1
AG1401_2.dat	110	0.283007	0.283004	1.41E-05	0.001694	2.48E-05	0.063874	5.54E-04	0.008665	1.31E-05	1.467314	9.79871E-05	46.9	0.282756	0.283002	8.7	1.0
AG1401_3.dat	110	0.283019	0.283016	1.43E-05	0.002534	8.09E-05	0.097771	1.29E-03	0.008675	1.54E-05	1.467284	0.000102142	46.1	0.282756	0.283013	9.1	1.0
AG1401_4.dat	110	0.282987	0.282984	1.44E-05	0.002684	1.17E-04	0.106953	3.11E-03	0.008670	1.48E-05	1.467292	0.000104865	46.6	0.282756	0.282981	8.0	1.0
AG1401_5.dat	110	0.283038	0.283034	1.33E-05	0.002511	2.12E-04	0.097452	4.17E-03	0.008688	1.73E-05	1.467278	0.000107767	45.7	0.282756	0.283032	9.8	0.9
AG1401_6.dat	110	0.282998	0.282995	1.41E-05	0.001853	5.46E-05	0.076193	1.95E-03	0.008664	1.42E-05	1.467297	0.000112907	45.9	0.282756	0.282993	8.4	1.0
AG1401_7.dat	90	0.283000	0.282996	1.46E-05	0.001565	4.65E-05	0.064399	1.95E-03	0.008658	1.30E-05	1.467264	0.000118399	45.9	0.282756	0.282995	8.4	1.0
AG1401_8.dat	110	0.283011	0.283007	1.38E-05	0.002660	1.98E-04	0.112226	4.79E-03	0.008669	1.61E-05	1.467307	0.00010478	46.3	0.282756	0.283005	8.8	1.0
AG1401_9.dat	110	0.283021	0.283018	1.41E-05	0.002409	1.17E-04	0.098998	2.11E-03	0.008688	1.51E-05	1.467266	0.000113874	45.9	0.282756	0.283016	9.2	1.0
AG1401_10.dat	110	0.283004	0.283001	1.49E-05	0.002540	1.85E-04	0.104073	3.67E-03	0.008674	1.39E-05	1.467274	0.00010908	45.6	0.282756	0.282999	8.6	1.1
Median ± 2SD																**8.8**	**1.0**
AG1404 (s080515) n=12																	
AG1404_1.dat	120	0.283019	0.283015	1.23E-05	0.001403	4.59E-05	0.066975	1.17E-03	0.008671	1.21E-05	1.467264	9.12944E-05	44.7	0.282757	0.283014	9.1	0.9
AG1404_2.dat	110	0.283012	0.283009	1.29E-05	0.001814	6.08E-05	0.084014	1.67E-03	0.008662	1.50E-05	1.467310	0.000150863	44.4	0.282757	0.283007	8.9	0.9
AG1404_3.dat	120	0.283008	0.283004	1.71E-05	0.001814	4.66E-05	0.081269	1.52E-03	0.008677	1.50E-05	1.467347	0.00012073	43.8	0.282757	0.283003	8.7	1.2
AG1404_4.dat	35	0.283034	0.283031	1.87E-05	0.000916	3.95E-05	0.048791	1.96E-03	0.008693	1.89E-05	1.467425	0.000287254	45.6	0.282756	0.283030	9.7	1.3
AG1404_5.dat	110	0.283019	0.283016	1.29E-05	0.001448	1.99E-05	0.068346	1.32E-03	0.008679	1.18E-05	1.467236	0.000108509	43.2	0.282758	0.283015	9.1	0.9
AG1404_5bis.da	80	0.282991	0.282988	1.28E-05	0.001163	4.05E-05	0.052753	5.13E-04	0.008649	1.06E-05	1.467248	0.000152603	44.7	0.282757	0.282987	8.1	0.9
AG1404_6.dat	120	0.283013	0.283010	1.28E-05	0.001282	4.14E-05	0.057093	1.52E-03	0.008666	1.18E-05	1.467194	0.000108189	43.9	0.282757	0.283009	8.9	0.9
AG1404_7.dat	120	0.283024	0.283021	1.11E-05	0.001303	3.38E-05	0.055913	9.42E-04	0.008678	1.21E-05	1.467240	0.000107691	43.7	0.282758	0.283020	9.3	0.8
AG1404_8.dat	100	0.283008	0.283005	1.23E-05	0.001455	7.56E-05	0.066207	2.67E-03	0.008660	1.13E-05	1.467244	0.000117788	45.6	0.282756	0.283004	8.8	0.9
AG1404_9.dat	60	0.283020	0.283016	1.46E-05	0.001292	3.38E-05	0.062955	1.89E-03	0.008665	1.30E-05	1.467225	0.000153355	46.4	0.282756	0.283015	9.2	1.0
AG1404_10.dat	100	0.283016	0.283013	1.20E-05	0.001160	3.74E-05	0.053469	1.67E-03	0.008656	1.03E-05	1.467218	0.000123368	46.5	0.282756	0.283012	9.1	0.8
AG1404_11.dat	110	0.283006	0.283003	1.28E-05	0.001180	3.13E-05	0.054368	1.68E-03	0.008651	1.01E-05	1.467239	0.000112072	46.4	0.282756	0.283002	8.7	0.9
Median ± 2SD																**9.0**	**0.8**
VK1403 (s050215) n=10																	
VK1403_01.dat	120	0.283026	0.283030	1.09E-05	0.001158	4.68E-05	0.049072	1.18E-03	0.008681	8.84E-06	1.467323	0.000108324	44	0.282757	0.283029	9.6	0.8
VK1403_02.dat	120	0.283023	0.283027	1.18E-05	0.001397	7.98E-05	0.060613	1.74E-03	0.008673	1.42E-05	1.467308	0.000134138	43.3	0.282758	0.283026	9.5	0.8
VK1403_03.dat	100	0.283022	0.283026	1.23E-05	0.000838	1.18E-05	0.035341	3.02E-04	0.008668	8.73E-06	1.467306	0.000130929	45.4	0.282756	0.283025	9.5	0.9
VK1403_04.dat	120	0.283001	0.283005	1.40E-05	0.001270	1.95E-05	0.056495	4.73E-04	0.008660	1.40E-05	1.467310	0.000116722	44.4	0.282757	0.283004	8.7	1.0
VK1403_05.dat	120	0.283014	0.283018	1.28E-05	0.001264	1.94E-05	0.054698	6.41E-04	0.008667	1.11E-05	1.467337	0.000143412	43.4	0.282758	0.283017	9.2	0.9
VK1403_06.dat	55	0.282992	0.282996	1.68E-05	0.001561	3.06E-05	0.072153	2.50E-04	0.008655	1.58E-05	1.467301	0.000148304	44.8	0.282757	0.282995	8.4	1.2
VK1403_07.dat	120	0.283024	0.283028	1.11E-05	0.001195	2.26E-05	0.053725	5.47E-04	0.008670	1.03E-05	1.467323	0.000125565	42.2	0.282758	0.283027	9.5	0.8
VK1403_08.dat	80	0.283014	0.283017	1.91E-05	0.000856	6.15E-06	0.035171	1.61E-04	0.008650	1.21E-05	1.467333	0.000116064	44.03	0.282757	0.283016	9.2	1.3
VK1403_09.dat	120	0.282989	0.282992	1.75E-05	0.001802	1.11E-04	0.080490	2.32E-03	0.008657	1.77E-05	1.467333	0.000134448	45	0.282757	0.282991	8.3	1.2
VK1403_10.dat	120	0.283020	0.283024	1.21E-05	0.001145	1.21E-05	0.050849	3.52E-04	0.008671	9.09E-06	1.467311	0.000120973	44.5	0.282757	0.283023	9.4	0.9
Median ± 2SD																**9.3**	**1.0**
AG1403 (s080515) n=11																	
AG1403_1.dat	120	0.283018	0.283015	1.18E-05	0.000762	3.48E-06	0.035838	3.85E-04	0.008666	1.27E-05	1.467248	0.000106941	44.4	0.282757	0.283014	9.1	0.8
AG1403_2.dat	120	0.283030	0.283026	1.34E-05	0.001361	1.25E-05	0.063821	6.28E-04	0.008670	1.57E-05	1.467269	0.000105299	43	0.282758	0.283025	9.4	0.9
AG1403_3.dat	120	0.283033	0.283029	1.14E-05	0.001008	3.67E-05	0.046551	5.48E-04	0.008676	1.19E-05	1.467192	8.45698E-05	43.1	0.282758	0.283028	9.6	0.8
AG1403_4.dat	120	0.283027	0.283024	1.31E-05	0.001509	2.87E-05	0.071004	7.80E-04	0.008685	1.55E-05	1.467238	0.000105583	45.8	0.282756	0.283023	9.4	0.9
AG1403_5.dat	120	0.283038	0.283035	1.17E-05	0.001225	2.66E-05	0.058243	9.94E-04	0.008682	1.30E-05	1.467239	8.50988E-05	43.9	0.282757	0.283034	9.8	0.8
AG1403_6.dat	120	0.283028	0.283025	1.21E-05	0.001658	4.34E-05	0.075674	9.45E-04	0.008671	1.11E-05	1.467267	0.00010136	43.3	0.282758	0.283024	9.4	0.9
AG1403_7.dat	70	0.283006	0.283002	1.40E-05	0.001169	4.06E-05	0.054738	1.34E-03	0.008652	1.03E-05	1.467254	0.000134733	44.2	0.282757	0.283001	8.6	1.0
AG1403_8.dat	120	0.283023	0.283020	1.22E-05	0.001286	9.95E-05	0.057704	2.50E-03	0.008668	8.94E-06	1.467238	9.7369E-05	44.1	0.282757	0.283019	9.3	0.9
AG1403_9.dat	40	0.283030	0.283026	2.34E-05	0.001143	5.26E-05	0.050157	1.75E-03	0.008681	1.63E-05	1.467522	0.000262473	43.6	0.282758	0.283025	9.5	1.7
AG1403_10.dat	100	0.283023	0.283019	1.09E-05	0.001056	1.35E-05	0.046736	4.10E-04	0.008671	1.01E-05	1.467269	9.70978E-05	45.2	0.282757	0.283019	9.3	0.8
AG1403_11.dat	80	0.283019	0.283016	1.48E-05	0.001355	8.44E-05	0.063832	2.67E-03	0.008674	1.04E-05	1.467223	0.000120948	44	0.282757	0.283015	9.1	1.0
Median ± 2SD																**9.4**	**0.6**

Session dd/mm/yy	2SD TEMORA	176Hf/177Hf TEMORA
s081214	0.000026	0.282675
s020315	0.000018	0.282657
s040215	0.000012	0.282657
s080515	0.000046	0.282683
s050215	0.000038	0.282672
s07-081015	0.000018	0.282662

Over 10 months

TEMORA n=98

	176Hf/177Hf (t)	eps Hf (t)
Mean	0.282670	
2SD	0.000036	1.3

PLESOVICE n=89

Mean	0.282479	
2SD	0.000027	1.0

AG1406 (s080515) n=10

AG1406_1.dat	120	0.283010	0.283007	1.15E-05	0.001342	2.48E-05	0.061993	1.44E-03	0.008659	1.14E-05	1.467273	0.00011504	43	0.282758	0.283006	8.8	0.8
AG1406_2.dat	120	0.283005	0.283002	1.14E-05	0.001271	6.76E-05	0.059201	2.28E-03	0.008664	1.08E-05	1.467271	0.00010063	43.5	0.282758	0.283001	8.6	0.8
AG1406_3.dat	120	0.282998	0.282994	1.31E-05	0.001352	4.81E-05	0.060517	1.01E-03	0.008659	1.19E-05	1.467303	9.94382E-05	44.1	0.282757	0.282993	8.3	0.9
AG1406_4.dat	120	0.283009	0.283005	1.33E-05	0.001187	3.11E-05	0.050593	1.13E-03	0.008666	1.10E-05	1.467284	0.000110931	45.1	0.282757	0.283004	8.8	0.9
AG1406_5.dat	120	0.283022	0.283019	1.37E-05	0.003034	1.35E-04	0.139088	2.80E-03	0.008672	1.73E-05	1.467281	0.000110727	44.2	0.282757	0.283016	9.2	1.0
AG1406_6.dat	120	0.283034	0.283031	1.31E-05	0.001346	7.32E-05	0.060033	1.38E-03	0.008671	9.06E-06	1.467273	0.000120415	43.1	0.282758	0.283030	9.6	0.9
AG1406_7.dat	70	0.283001	0.282998	1.41E-05	0.001385	9.17E-05	0.064106	1.33E-03	0.008652	1.43E-05	1.467285	0.000128231	43.4	0.282758	0.282997	8.5	1.0
AG1406_8.dat	120	0.283019	0.283016	1.26E-05	0.001536	4.70E-05	0.060323	1.07E-03	0.008659	1.20E-05	1.467267	0.000105959	43.2	0.282758	0.283015	9.1	0.9
AG1406_9.dat	120	0.283012	0.283009	1.22E-05	0.001351	6.19E-05	0.061242	1.29E-03	0.008675	1.28E-05	1.467308	9.64164E-05	45.7	0.282756	0.283008	8.9	0.9
AG1406_10.dat	120	0.283037	0.283033	1.22E-05	0.001387	1.53E-05	0.059123	7.65E-04	0.008669	1.05E-05	1.467273	0.00011216	45.2	0.282757	0.283032	9.7	0.9
Median ± 2SD																**8.8**	**0.9**

AG1402 (s040215) n=10

AG1402_10.dat	90	0.282980	0.283001	1.58E-05	0.000846	1.36E-05	0.036209	4.74E-04	0.009682	1.13E-05	1.467247	0.000138207	43.7	0.282758	0.283001	8.6	1.1
AG1402_09.dat	120	0.282972	0.282994	1.43E-05	0.001057	6.04E-05	0.042792	1.13E-03	0.008690	1.40E-05	1.467331	0.000122408	44.1	0.282757	0.282993	8.3	1.0
AG1402_08.dat	120	0.282962	0.282984	1.28E-05	0.001798	1.49E-04	0.073767	2.82E-03	0.008656	1.34E-05	1.467295	0.00011935	41.9	0.282759	0.282982	7.9	0.9
AG1402_07.dat	120	0.282976	0.282997	1.30E-05	0.000938	2.08E-05	0.039453	6.61E-04	0.008669	1.04E-05	1.467303	0.000101999	44.1	0.282757	0.282996	8.5	0.9
AG1402_06.dat	120	0.282988	0.283009	1.34E-05	0.001226	2.57E-05	0.050655	5.21E-04	0.008675	1.19E-05	1.467292	0.000125556	44.7	0.282757	0.283008	8.9	0.9
AG1402_05.dat	120	0.282979	0.283001	1.32E-05	0.002104	2.42E-04	0.089494	5.25E-03	0.008673	1.31E-05	1.467299	0.000110587	44.3	0.282757	0.282999	8.6	0.9
AG1402_04.dat	120	0.282976	0.282997	1.46E-05	0.000974	1.73E-05	0.040007	3.03E-04	0.008659	1.38E-05	1.467307	0.000121234	44.3	0.282757	0.282996	8.5	1.0
AG1402_03.dat	80	0.282977	0.282998	1.49E-05	0.001179	5.50E-05	0.053625	1.36E-03	0.008671	1.56E-05	1.467276	0.000147716	43.2	0.282758	0.282997	8.5	1.1
AG1402_02.dat	120	0.282981	0.283002	1.19E-05	0.000951	1.86E-05	0.038703	3.18E-04	0.008663	1.03E-05	1.467310	0.000117573	44.4	0.282757	0.283002	8.6	0.8
AG1402_01.dat	120	0.282984	0.283005	1.13E-05	0.000984	4.50E-05	0.039133	8.39E-04	0.008680	8.72E-06	1.467272	9.83355E-05	43.7	0.282758	0.283005	8.7	0.8
Median ± 2SD																**8.5**	**0.5**

HQ1402 (s080515) n=9

HQ1402_1.dat	120	0.283063	0.283060	1.22E-05	0.000948	4.01E-05	0.040428	1.05E-03	0.008649	1.01E-05	1.467248	9.27827E-05	43.5	0.282758	0.283059	10.7	0.9
HQ1402_2.dat	120	0.283086	0.283083	1.20E-05	0.000973	2.41E-05	0.042335	4.56E-04	0.008677	9.41E-06	1.467260	0.00010366	42.4	0.282758	0.283082	11.4	0.8
HQ1402_3.dat	80	0.283112	0.283108	1.70E-05	0.002616	2.44E-04	0.120061	5.24E-03	0.008711	1.78E-05	1.467324	0.000134517	42.8	0.282758	0.283106	12.3	1.2
HQ1402_4.dat	120	0.283083	0.283080	1.27E-05	0.001494	7.84E-06	0.065621	5.78E-04	0.008670	1.16E-05	1.467256	0.000102697	43.5	0.282758	0.283079	11.3	0.9
HQ1402_5.dat	100	0.283091	0.283088	1.46E-05	0.001709	5.17E-05	0.077012	1.91E-03	0.008688	1.16E-05	1.467261	0.000120335	44.1	0.282757	0.283087	11.6	1.0
HQ1402_8.dat	30	0.283050	0.283047	2.02E-05	0.001299	1.61E-04	0.055903	5.22E-03	0.008693	2.00E-05	1.467385	0.000262948	42.5	0.282758	0.283046	10.2	1.4
HQ1402_9.dat	60	0.283079	0.283076	1.68E-05	0.000860	3.06E-05	0.044407	1.36E-03	0.008659	1.13E-05	1.467191	0.000149366	43.2	0.282758	0.283075	11.2	1.2
HQ1402_10.dat	120	0.283081	0.283078	1.17E-05	0.001187	2.74E-05	0.053019	7.18E-04	0.008660	9.86E-06	1.467241	9.70321E-05	43	0.282758	0.283077	11.3	0.8
HQ1402_11.dat	80	0.283084	0.283081	1.56E-05	0.000767	3.59E-05	0.033401	5.80E-04	0.008664	1.23E-05	1.467241	0.000125227	41.6	0.282759	0.283080	11.4	1.1
Median ± 2SD																**11.3**	**1.2**

HQ1403 (s080515) n=11

HQ1403_1.dat	120	0.283050	0.283047	1.40E-05	0.000743	4.08E-05	0.033480	1.30E-03	0.008676	9.01E-06	1.467228	0.000113482	44.7	0.282757	0.283046	10.2	1.0
HQ1403_2.dat	120	0.283051	0.283048	1.18E-05	0.000556	1.32E-05	0.022285	4.36E-04	0.008673	8.68E-06	1.467251	8.8105E-05	43.7	0.282758	0.283047	10.2	0.8
HQ1403_3.dat	120	0.283074	0.283071	1.04E-05	0.000967	4.00E-05	0.037780	7.64E-04	0.008676	9.96E-06	1.467258	9.76264E-05	43.2	0.282758	0.283070	11.0	0.7
HQ1403_4.dat	70	0.283035	0.283032	1.49E-05	0.001147	6.66E-05	0.049779	2.57E-03	0.008679	1.33E-05	1.467295	0.00012855	42.4	0.282758	0.283031	9.6	1.1
HQ1403_5.dat	120	0.283061	0.283057	1.16E-05	0.001027	5.96E-05	0.040240	1.11E-03	0.008673	9.35E-06	1.467230	9.50214E-05	42.9	0.282758	0.283056	10.6	0.8
HQ1403_6.dat	90	0.283057	0.283053	1.60E-05	0.000860	3.16E-05	0.034898	7.10E-04	0.008663	1.00E-05	1.467239	0.000126764	43.5	0.282758	0.283053	10.4	1.1
HQ1403_7.dat	100	0.283036	0.283033	1.29E-05	0.000775	3.57E-05	0.029640	5.93E-04	0.008655	1.05E-05	1.467236	0.000101486	42.7	0.282758	0.283032	9.7	0.9
HQ1403_9.dat	100	0.283087	0.283083	1.30E-05	0.001134	3.28E-05	0.047810	5.81E-04	0.008674	1.09E-05	1.467230	0.000118214	43.7	0.282758	0.283082	11.5	0.9
HQ1403_10.dat	100	0.283072	0.283068	1.40E-05	0.001084	7.59E-05	0.044115	1.65E-03	0.008676	1.05E-05	1.467162	0.000103052	42.9	0.282758	0.283067	10.9	1.0
HQ1403_11.dat	70	0.283036	0.283033	1.41E-05	0.000780	3.18E-05	0.030807	1.06E-03	0.008664	1.06E-05	1.467228	0.000134107	42.5	0.282758	0.283032	9.7	1.0
HQ1403_12.dat	60	0.283059	0.283056	1.83E-05	0.001063	4.09E-05	0.047855	1.69E-03	0.008671	1.34E-05	1.467231	0.000165323	40.8	0.282759	0.283055	10.5	1.3
Median ± 2SD																**10.4**	**1.2**

AG1308A1 (s040215) n=12

AG1308A1_10.da	120	0.282956	0.282977	1.24E-05	0.001086	1.92E-05	0.051618	3.08E-04	0.008678	1.54E-05	1.467365	0.00011323	38	0.282761	0.282976	7.6	0.9
AG1308A1_09bis	120	0.282930	0.282951	1.58E-05	0.001665	4.26E-05	0.079308	2.03E-03	0.008650	1.76E-05	1.467331	0.000141319	37.1	0.282762	0.282950	6.7	1.1
AG1308A1_09	120	0.282818	0.282839	1.83E-05	0.001627	4.80E-05	0.078975	2.48E-03	0.008627	2.41E-05	1.467558	0.00015718	37.1	0.282762	0.282838	2.7	1.3
AG1308A1_08.da	120	0.283002	0.283024	2.15E-05	0.001298	3.54E-05	0.059887	1.07E-03	0.008731	2.29E-05	1.467295	0.000131132	38	0.282761	0.283023	9.3	1.5
AG1308A1_07.da	120	0.282987	0.283008	1.25E-05	0.000960	2.64E-06	0.045471	2.21E-04	0.008678	1.18E-05	1.467277	0.000106163	39.7	0.282760	0.283007	8.7	0.9
AG1308A1_06.da	80	0.282994	0.283015	2.34E-05	0.001243	3.26E-06	0.059373	2.15E-04	0.008697	2.99E-05	1.467347	0.000120501	36.8	0.282762	0.283014	8.9	1.7
AG1308A1_05.da	120	0.282978	0.282999	1.45E-05	0.000612	3.68E-06	0.030874	1.94E-04	0.008656	1.02E-05	1.467286	0.000110916	39.3	0.282760	0.282999	8.4	1.0
AG1308A1_04.da	120	0.282980	0.283001	1.83E-05	0.000744	1.30E-05	0.035329	3.19E-04	0.008673	1.68E-05	1.467290	0.000139015	36.9	0.282762	0.283000	8.4	1.3
AG1308A1_03.da	120	0.283018	0.283039	2.11E-05	0.000625	1.57E-06	0.030884	2.50E-04	0.008709	1.60E-05	1.467290	0.000118905	38.2	0.282761	0.283038	9.8	1.5
AG1308A1_02_ri	120	0.282956	0.282977	1.98E-05	0.002330	4.13E-06	0.115043	8.76E-04	0.008675	2.56E-05	1.467333	0.000136609	37.3	0.282762	0.282976	7.6	1.4
AG1308A1_02.da	120	0.282974	0.282995	2.06E-05	0.002947	1.24E-05	0.151099	1.42E-03	0.008670	2.45E-05	1.467305	0.000125243	37.3	0.282762	0.282993	8.2	1.5
AG1308A1_01.da	120	0.283018	0.283039	1.86E-05	0.000937	3.22E-06	0.045250	4.55E-04	0.008735	2.24E-05	1.467316	0.000126882	38.4	0.282761	0.283039	9.8	1.3
Median ± 2SD																**8.4**	**3.8**

AG1308A (s080515) n=10

AG1308A_1.dat	110	0.282977	0.282973	1.88E-05	0.001245	6.03E-05	0.055552	1.54E-03	0.008659	1.71E-05	1.467313	9.51535E-05	36.6	0.282762	0.282972	7.4	1.3
AG1308A_2.dat	110	0.282984	0.282981	1.77E-05	0.004264	3.75E-05	0.198092	1.46E-03	0.008657	2.62E-05	1.467279	9.52687E-05	37	0.282762	0.282978	7.6	1.3
AG1308A_3.dat	110	0.282995	0.282992	1.66E-05	0.001475	3.88E-05	0.064136	6.81E-04	0.008672	1.83E-05	1.467291	9.42396E-05	37.7	0.282761	0.282991	8.1	1.2
AG1308A_4.dat	110	0.282998	0.282995	1.90E-05	0.000684	1.71E-05	0.029171	2.72E-04	0.008660	1.48E-05	1.467306	0.000100463	36.8	0.282762	0.282994	8.2	1.3
AG1308A_5.dat	70	0.283028	0.283025	2.10E-05	0.001019	1.03E-05	0.046824	4.86E-04	0.008699	2.07E-05	1.467286	0.000111847	37.7	0.282761	0.283024	9.3	1.5
AG1308A_6.dat	80	0.282982	0.282979	2.02E-05	0.002005	1.21E-05	0.092870	6.49E-04	0.008668	2.08E-05	1.467296	0.000122456	37.4	0.282761	0.282977	7.6	1.4
AG1308A_7.dat	110	0.283011	0.283008	1.57E-05	0.002375	7.06E-06	0.100085	2.75E-04	0.008664	1.88E-05	1.467304	0.000104156	36.6	0.282762	0.283006	8.6	1.1
AG1308A_8.dat	110	0.283013	0.283010	1.75E-05	0.001374	3.26E-05	0.060755	6.35E-04	0.008692	1.74E-05	1.467254	9.63324E-05	36.7	0.282762	0.283009	8.7	1.2
AG1308A_9.dat	110	0.283034	0.283030	1.76E-05	0.001875	9.25E-05	0.082363	1.92E-03	0.008686	2.12E-05	1.467278	0.000102098	36.9	0.282762	0.283029	9.4	1.2
AG1308A_10.dat	110	0.283045	0.283042	1.95E-05	0.002509	1.84E-04	0.110198	3.82E-03	0.008700	2.08E-05	1.467287	9.63494E-05	36.4	0.282762	0.283040	9.8	1.4
Median ± 2SD																**8.4**	**1.7**

VK1404 (s050215) n=10

VK1404_01.dat	120	0.283031	0.283034	1.25E-05	0.000516	3.34E-06	0.021464	9.63E-05	0.008672	9.55E-06	1.467289	6.7117E-05	37.3	0.282762	0.283034	9.6	0.9
VK1404_02.dat	120	0.283011	0.283015	1.32E-05	0.001637	4.20E-05	0.069495	8.09E-04	0.008670	1.48E-05	1.467318	7.50035E-05	38	0.282761	0.283014	8.9	0.9
VK1404_03.dat	120	0.283024	0.283028	1.36E-05	0.000508	1.22E-05	0.021766	3.63E-04	0.008683	1.09E-05	1.467343	0.00011366	37.2	0.282762	0.283028	9.4	1.0
VK1404_04.dat	120	0.283009	0.283013	1.45E-05	0.000713	1.28E-05	0.032404	3.12E-04	0.008652	1.41E-05	1.467365	0.000124885	37.1	0.282762	0.283012	8.9	1.0
VK1404_05.dat	70	0.282990	0.282994	1.54E-05	0.001119	5.02E-05	0.050618	1.11E-03	0.008644	1.98E-05	1.467358	0.000116333	35.7	0.282763	0.282993	8.2	1.1
VK1404_06.dat	120	0.282989	0.282993	1.37E-05	0.000342	6.27E-06	0.014964	1.50E-04	0.008673	1.28E-05	1.467325	0.000112664	35.4	0.282763	0.282992	8.1	1.0
VK1404_07.dat	80	0.283008	0.283012	1.67E-05	0.000696	2.36E-05	0.029341	5.48E-04	0.008656	1.32E-05	1.467348	0.000139029	36.8	0.282762	0.283012	8.8	1.2
VK1404_08.dat	80	0.283013	0.283017	1.76E-05	0.000385	1.62E-05	0.016653	3.40E-04	0.008664	1.07E-05	1.467331	0.000125655	36.8	0.282762	0.283017	9.0	1.2
VK1404_09.dat	120	0.282997	0.283000	1.37E-05	0.000651	1.29E-05	0.031204	3.14E-04	0.008661	1.21E-05	1.467314	0.000108853	37.6	0.282761	0.283000	8.4	1.0
VK1404_10.dat	75	0.283025	0.283028	1.41E-05	0.000531	3.68E-06	0.023233	7.98E-05	0.008680	1.39E-05	1.467317	0.000138173	38.3	0.282761	0.283028	9.4	1.0
Median ± 2SD																**8.9**	**1.0**

VK1405 (s050215) n=10

VK1405_01.dat	60	0.283030	0.283034	2.62E-05	0.000742	2.58E-05	0.031617	8.03E-04	0.008703	1.83E-05	1.467347	0.000222803	34.1	0.282764	0.283033	9.5	1.8
VK1405_02.dat	120	0.283014	0.283017	1.46E-05	0.001017	5.85E-05	0.040581	1.31E-03	0.008671	1.18E-05	1.467326	0.000127317	34.7	0.282763	0.283017	9.0	1.0
VK1405_03.dat	100	0.283000	0.283003	1.51E-05	0.001592	2.97E-05	0.065062	7.17E-04	0.008660	1.55E-05	1.467342	0.000126333	36.8	0.282762	0.283002	8.5	1.1
VK1405_04.dat	40	0.282995	0.282998	1.93E-05	0.001328	2.48E-05	0.055425	5.89E-04	0.008687	2.57E-05	1.467295	0.000177551	35.5	0.282763	0.282998	8.3	1.4
VK1405_05.dat	120	0.282991	0.282995	1.51E-05	0.000812	9.64E-06	0.033629	1.43E-04	0.008670	1.40E-05	1.467326	0.000124857	35.3	0.282763	0.282994	8.2	1.1
VK1405_06.dat	120	0.283019	0.283023	1.58E-05	0.000940	1.91E-05	0.040832	4.80E-04	0.008694	1.50E-05	1.467334	0.000135373	35.8	0.282762	0.283022	9.2	1.1
VK1405_07.dat	120	0.283006	0.283010	1.74E-05	0.000594	8.81E-06	0.023284	2.34E-04	0.008674	1.12E-05	1.467317	0.000131845	34.2	0.282764	0.283010	8.7	1.2
VK1405_08.dat	80	0.282989	0.282993	1.80E-05	0.002104	1.13E-04	0.086123	2.46E-03	0.008661	1.91E-05	1.467280	0.000146272	37.3	0.282762	0.282991	8.1	1.3
VK1405_09bis.d	50	0.282991	0.282995	2.85E-05	0.000796	5.28E-05	0.035052	1.15E-03	0.008678	1.89E-05	1.467285	0.000163024	35.1	0.282763	0.282994	8.2	2.0
VK1405_10.dat	100	0.283012	0.283015	1.42E-05	0.000867	1.24E-05	0.034446	2.40E-04	0.008663	1.11E-05	1.467316	0.000132911	35.3	0.282763	0.283015	8.9	1.0
Median ± 2SD																**8.6**	**1.0**

MR1403 (s050215) n=10

MR1403_01.dat	100	0.283012	0.283016	1.84E-05	0.000954	1.06E-05	0.039360	2.51E-04	0.008663	1.78E-05	1.467341	0.000115735	34.2	0.282764	0.283015	8.9	1.3
MR1403_02.dat	120	0.282999	0.283002	1.89E-05	0.000813	7.75E-06	0.032203	1.15E-04	0.008656	1.75E-05	1.467295	0.000126854	35.5	0.282763	0.283002	8.5	1.3
MR1403_03.dat	115	0.283038	0.283042	1.65E-05	0.000650	2.36E-06	0.025774	1.93E-05	0.008672	1.55E-05	1.467311	0.000124465	35	0.282763	0.283042	9.9	1.2
MR1403_04.dat	115	0.283017	0.283021	1.89E-05	0.001675	6.14E-05	0.067886	1.37E-03	0.008689	2.82E-05	1.467288	0.000111003	35.7	0.282763	0.283020	9.1	1.3
MR1403_05.dat	115	0.283034	0.283038	2.37E-05	0.000983	3.66E-05	0.040822	9.45E-04	0.008691	2.56E-05	1.467348	0.000119481	35	0.282763	0.283037	9.7	1.7
MR1403_06.dat	115	0.283020	0.283023	1.98E-05	0.001719	1.15E-04	0.071029	2.62E-03	0.008707	2.35E-05	1.467313	0.0001505	35.1	0.282763	0.283022	9.2	1.4
MR1403_07.dat	115	0.283017	0.283021	1.73E-05	0.000678	1.38E-05	0.027510	2.84E-04	0.008666	1.63E-05	1.467303	9.19488E-05	36.1	0.282762	0.283020	9.1	1.2
MR1403_08.dat	65	0.283078	0.283082	3.22E-05	0.000972	2.91E-05	0.038390	2.55E-04	0.008730	2.82E-05	1.467506	0.000225004	36.3	0.282762	0.283081	11.3	2.3
MR1403_09.dat	115	0.283039	0.283042	1.67E-05	0.001043	6.68E-05	0.040492	1.23E-03	0.008660	1.79E-05	1.467347	7.97384E-05	35.8	0.282762	0.283042	9.9	1.2
MR1403_10.dat	120	0.283013	0.283017	1.83E-05	0.001175	1.34E-06	0.049094	2.28E-04	0.008662	2.45E-05	1.467310	0.000126686	34.4	0.282763	0.283016	8.9	1.3
Median ± 2SD																**9.1**	**1.6**

LI1303A1 (s081214) n=13

LI1303a1_25_1.	110	0.283010	0.283020	1.37E-05	0.000329	3.58E-06	0.011358	1.12E-04	0.008649	1.18E-05	1.467290	0.000102	34.6	0.282763	0.283020	9.1	1.0
LI1303a1_20.da	120	0.282996	0.283005	1.42E-05	0.000471	5.78E-06	0.018634	8.90E-05	0.008647	1.18E-05	1.467248	0.000116	34.3	0.282763	0.283005	8.5	1.0
LI1303a1_13.da	100	0.282988	0.282997	1.45E-05	0.001519	7.51E-05	0.056714	1.24E-03	0.008616	1.78E-05	1.467270	0.000128	34.2	0.282764	0.282996	8.2	1.0
LI1303a1_24.da	110	0.283034	0.283040	1.56E-05	0.001886	1.38E-04	0.083721	2.46E-03	0.008675	1.24E-05	1.467233	0.000117	34.2	0.282764	0.283042	9.9	0.9
LI1303a1_11.da	80	0.283011	0.283021	1.44E-05	0.000743	2.77E-05	0.024469	4.21E-04	0.008644	1.19E-05	1.467285	0.000122	33.8	0.282764	0.283020	9.1	1.0
LI1303a1_23.da	120	0.283002	0.283011	1.45E-05	0.002694	1.63E-05	0.092634	4.81E-04	0.008651	1.64E-05	1.467260	0.000103	33.8	0.282764	0.283010	8.7	1.0
LI1303a1_19.da	120	0.283013	0.283022	1.13E-05	0.000654	1.65E-05	0.020855	2.90E-04	0.008649	1.02E-05	1.467275	0.000100	33.7	0.282764	0.283022	9.1	0.8
LI1303a1_21.da	120	0.283009	0.283018	1.37E-05	0.002411	5.22E-05	0.082889	9.67E-04	0.008658	1.51E-05	1.467265	0.000109	33.4	0.282764	0.283016	8.9	1.0
LI1303a1_22.da	90	0.283021	0.283030	1.67E-05	0.000833	5.89E-05	0.035735	1.24E-03	0.008667	1.81E-05	1.467295	0.000133	33.2	0.282764	0.283029	9.4	1.2
LI1303a1_03.da	120	0.283003	0.283012	1.33E-05	0.001061	8.18E-06	0.037445	2.82E-04	0.008636	1.25E-05	1.467234	0.000091	33.1	0.282764	0.283012	8.8	0.9
LI1303a1_16.da	95	0.282959	0.282968	2.19E-05	0.000925	3.18E-05	0.050632	9.80E-04	0.008589	2.89E-05	1.467230	0.000203	33.1	0.282764	0.282968	7.2	1.6
LI1303a1_14.da	85	0.282970	0.282980	2.53E-05	0.000593	9.19E-06	0.032929	1.81E-04	0.008610	3.05E-05	1.467286	0.000263	33.0	0.282764	0.282979	7.6	1.8
LI1303a1_15.da	85	0.283004	0.283013	1.52E-05	0.001641	9.14E-05	0.055710	1.68E-03	0.008648	1.54E-05	1.467317	0.000125	32.9	0.282764	0.283012	8.8	1.1
Median ± 2SD																**8.8**	**1.4**

LI1303 (s081214) n=13																
LI1303_35.dat	120	0.283001	0.283010	1.69E-05	0.005064	5.04E-04	0.178688	9.18E-03	0.008670	2.38E-05	1.467230	0.000104	35.5	0.282763	0.283006	8.6	1.2
LI1303_23.dat	40	0.283028	0.283038	2.40E-05	0.004513	6.60E-04	0.155935	1.19E-02	0.008698	4.26E-05	1.467239	0.000172	35.1	0.282763	0.283035	9.6	1.7
LI1303_24.dat	120	0.283031	0.283040	2.46E-05	0.008542	2.72E-04	0.305513	4.41E-03	0.008711	3.60E-05	1.467264	0.000102	34.8	0.282763	0.283035	9.6	1.7
LI1303_25.dat	115	0.282988	0.282997	2.32E-05	0.006708	3.25E-04	0.252212	7.52E-03	0.008660	3.73E-05	1.467256	0.000096	34.7	0.282763	0.282993	8.1	1.6
LI1303_32.dat	45	0.283002	0.283011	2.03E-05	0.002533	2.61E-04	0.091593	5.10E-03	0.008648	3.31E-05	1.467160	0.000243	34.7	0.282763	0.283009	8.7	1.4
LI1303_10.dat	100	0.283047	0.283056	2.23E-05	0.003170	1.28E-04	0.115242	2.60E-03	0.008704	2.36E-05	1.467295	0.000112	34.5	0.282763	0.283054	10.3	1.6
LI1303_04.dat	80	0.283005	0.283014	1.51E-05	0.001788	1.94E-04	0.073825	4.73E-03	0.008675	1.89E-05	1.467234	0.000121	34.4	0.282763	0.283013	8.8	1.1
LI1303_11.dat	80	0.283008	0.283017	2.18E-05	0.002320	3.44E-04	0.082534	7.01E-03	0.008663	3.04E-05	1.467280	0.000130	34.4	0.282763	0.283016	8.9	1.5
LI1303_33.dat	110	0.283010	0.283019	2.63E-05	0.007232	7.06E-05	0.277616	2.25E-03	0.008681	3.49E-05	1.467213	0.000113	34.3	0.282763	0.283014	8.9	1.9
LI1303_12.dat	120	0.283006	0.283015	2.17E-05	0.006518	5.07E-05	0.222869	1.37E-03	0.008684	2.50E-05	1.467221	0.000101	34.2	0.282764	0.283011	8.8	1.5
LI1303_01.dat	70	0.283001	0.283010	1.28E-05	0.001366	2.34E-05	0.054430	3.03E-04	0.008652	1.82E-05	1.467233	0.000158	34.0	0.282764	0.283009	8.7	0.9
LI1303_22.dat	60	0.282979	0.282988	2.43E-05	0.002791	3.35E-04	0.096277	6.41E-03	0.008635	2.94E-05	1.467330	0.000232	33.5	0.282764	0.282986	7.9	1.7
LI1303_21.dat	110	0.283007	0.283016	1.62E-05	0.004598	3.62E-04	0.158238	6.61E-03	0.008678	2.21E-05	1.467239	0.000101	33.1	0.282764	0.283013	8.8	1.1
Median ± 2SD																**8.8**	**1.3**
KJ1207[d] (s07-081015) n=13																	
KJ1207_01	120	0.283019	0.283035	9.04E-06	0.000492	3.24E-05	0.021321	5.31E-04	0.008658	4.71E-06	1.467291	8.16202E-05	33.43	0.282764	0.283035	9.6	0.6
KJ1207_02	120	0.283013	0.283028	6.80E-06	0.000315	9.05E-06	0.017143	2.53E-04	0.008657	3.55E-06	1.467242	8.98236E-05	33.43	0.282764	0.283028	9.3	0.5
KJ1207_03	90	0.283017	0.283033	9.97E-06	0.001723	3.67E-05	0.072216	1.28E-03	0.008663	6.26E-06	1.467256	9.93257E-05	33.43	0.282764	0.283032	9.5	0.7
KJ1207_04	45	0.283020	0.283036	1.01E-05	0.001560	9.88E-05	0.063412	1.13E-03	0.008659	8.24E-06	1.467440	0.000125891	33.43	0.282764	0.283035	9.6	0.7
KJ1207_05	20	0.283006	0.283022	1.70E-05	0.000931	3.32E-05	0.034840	6.56E-04	0.008652	1.50E-05	1.467582	0.000156689	33.43	0.282764	0.283022	9.1	1.2
KJ1207_06	50	0.283024	0.283040	1.09E-05	0.001766	4.89E-05	0.071936	1.36E-03	0.008673	7.99E-06	1.467417	0.000151409	33.43	0.282764	0.283039	9.7	0.8
KJ1207_07	50	0.283012	0.283028	1.41E-05	0.000838	5.62E-05	0.030668	7.15E-04	0.008661	8.78E-06	1.467430	0.000146813	33.43	0.282764	0.283028	9.3	1.0
KJ1207_08	100	0.283018	0.283034	7.84E-06	0.000977	3.31E-05	0.038085	6.64E-04	0.008654	4.53E-06	1.467253	0.000107957	33.43	0.282764	0.283033	9.5	0.6
KJ1207_09	60	0.283019	0.283034	9.76E-06	0.000345	1.17E-05	0.015311	3.16E-04	0.008665	3.83E-06	1.467185	0.000163119	33.43	0.282764	0.283034	9.6	0.7
KJ1207_10	100	0.283018	0.283033	9.06E-06	0.000655	1.25E-05	0.026389	1.43E-04	0.008660	4.50E-06	1.467130	0.000169203	33.43	0.282764	0.283033	9.5	0.6
KJ1207_11	120	0.283019	0.283035	6.56E-06	0.000821	4.60E-06	0.031024	1.45E-04	0.008663	3.63E-06	1.466922	0.000235521	33.43	0.282764	0.283035	9.6	0.5
KJ1207_12	120	0.283018	0.283033	6.67E-06	0.000914	5.71E-06	0.036126	1.12E-04	0.008661	4.04E-06	1.467178	0.00010704	33.43	0.282764	0.283033	9.5	0.5
KJ1207_13	120	0.283023	0.283038	6.60E-06	0.000368	9.03E-06	0.016497	2.03E-04	0.008659	3.42E-06	1.467080	0.000133001	33.43	0.282764	0.283038	9.7	0.5
Median ± 2SD																**9.5**	**0.3**
KJ1316[d] (s07-081015) n=12																	
KJ1316_01	110	0.283011	0.283026	6.75E-06	0.000740	1.18E-05	0.035653	3.73E-04	0.008653	4.69E-06	1.467231	8.12608E-05	33.7	0.282764	0.283026	9.3	0.5
KJ1316_02	110	0.283017	0.283032	6.94E-06	0.001078	4.56E-06	0.051934	1.75E-04	0.008660	5.38E-06	1.467234	8.14257E-05	33.7	0.282764	0.283032	9.5	0.5
KJ1316_03	120	0.283014	0.283030	7.09E-06	0.000707	5.82E-06	0.033040	2.00E-04	0.008655	4.09E-06	1.467244	7.95533E-05	33.7	0.282764	0.283029	9.4	0.5
KJ1316_04	120	0.283014	0.283030	6.50E-06	0.000639	9.38E-06	0.031089	3.44E-04	0.008659	4.64E-06	1.467256	8.68652E-05	33.7	0.282764	0.283030	9.4	0.5
KJ1316_05	120	0.283012	0.283028	5.92E-06	0.001472	2.84E-05	0.070196	6.01E-04	0.008654	5.68E-06	1.467234	5.62958E-05	33.7	0.282764	0.283027	9.3	0.4
KJ1316_06	80	0.283016	0.283032	7.48E-06	0.000690	1.61E-05	0.033116	2.38E-04	0.008661	5.77E-06	1.467259	9.2429E-05	33.7	0.282764	0.283031	9.5	0.5
KJ1316_07	120	0.283010	0.283026	6.98E-06	0.000694	1.36E-05	0.032878	3.63E-04	0.008655	4.38E-06	1.467229	9.63044E-05	33.7	0.282764	0.283025	9.2	0.5
KJ1316_08	120	0.283017	0.283033	7.04E-06	0.000811	1.22E-05	0.037328	2.66E-04	0.008661	4.53E-06	1.467227	8.203E-05	33.7	0.282764	0.283032	9.5	0.5
KJ1316_09	120	0.282999	0.283014	6.23E-06	0.000730	5.79E-06	0.036417	3.01E-04	0.008655	4.36E-06	1.467206	7.71525E-05	33.7	0.282764	0.283014	8.8	0.4
KJ1316_10	120	0.283020	0.283036	7.12E-06	0.001163	4.28E-05	0.054378	8.60E-04	0.008657	5.67E-06	1.467242	8.17515E-05	33.7	0.282764	0.283035	9.6	0.5
KJ1316_11	120	0.283009	0.283025	6.21E-06	0.000647	6.91E-06	0.029988	2.45E-04	0.008651	3.75E-06	1.467228	8.55009E-05	33.7	0.282764	0.283024	9.2	0.4
KJ1316_12	70	0.283012	0.283028	7.80E-06	0.000978	2.98E-05	0.045049	6.94E-04	0.008660	5.00E-06	1.467266	0.0001107	33.7	0.282764	0.283027	9.3	0.6
Median ± 2SD																**9.4**	**0.4**
KJ1006A (s050215) n=10																	
KJ1006A_01.dat	120	0.283034	0.283038	9.31E-06	0.000339	6.12E-06	0.013866	9.12E-05	0.008666	6.79E-06	1.467292	0.000068	31.6	0.282765	0.283037	9.6	0.7
KJ1006A_02.dat	120	0.283019	0.283023	1.28E-05	0.000472	1.31E-05	0.019278	1.47E-04	0.008666	9.05E-06	1.467339	0.000111985	31.9	0.282765	0.283023	9.1	0.9
KJ1006A_03.dat	120	0.283045	0.283048	1.30E-05	0.001496	1.18E-04	0.055433	2.09E-03	0.008692	1.19E-05	1.467274	9.62927E-05	31.5	0.282765	0.283048	10.0	0.9
KJ1006A_04.dat	120	0.283027	0.283031	9.80E-06	0.000540	6.68E-06	0.022515	1.02E-04	0.008661	7.38E-06	1.467330	8.00117E-05	31.9	0.282765	0.283031	9.4	0.7
KJ1006A_05.dat	120	0.283029	0.283032	9.55E-06	0.000596	3.63E-05	0.023579	7.91E-04	0.008672	8.37E-06	1.467313	9.49803E-05	31.1	0.282765	0.283032	9.4	0.7
KJ1006A_06.dat	120	0.283026	0.283030	1.24E-05	0.000559	2.81E-05	0.023825	6.21E-04	0.008672	8.44E-06	1.467330	0.000111727	32.5	0.282765	0.283029	9.4	0.9
KJ1006A_07.dat	120	0.283025	0.283029	1.24E-05	0.000498	1.26E-05	0.021769	1.40E-04	0.008676	7.75E-06	1.467312	0.000111263	32.6	0.282765	0.283029	9.3	0.9
KJ1006A_08.dat	120	0.283031	0.283035	1.06E-05	0.000367	7.00E-06	0.015646	2.25E-04	0.008665	7.44E-06	1.467305	0.000109	32.2	0.282765	0.283035	9.5	0.8
KJ1006A_09.dat	120	0.283012	0.283016	1.22E-05	0.001071	1.37E-05	0.045553	1.82E-04	0.008668	9.98E-06	1.467321	9.94419E-05	32.1	0.282765	0.283015	8.9	0.9
KJ1006A_10.dat	120	0.283010	0.283014	1.16E-05	0.000982	6.26E-06	0.039697	6.63E-05	0.008660	9.85E-06	1.467321	0.000105601	31.7	0.282765	0.283013	8.8	0.8
Median ± 2SD																**9.4**	**0.7**
KJ1308 (s081214) n=16																	
KJ1308_22.dat	90	0.282993	0.283002	1.41E-05	0.001814	1.04E-04	0.067962	2.16E-03	0.008636	1.44E-05	1.467320	0.000123	32.3	0.282765	0.283001	8.4	1.0
KJ1308_05.dat	80	0.283000	0.283009	1.29E-05	0.000687	3.73E-05	0.024336	7.09E-04	0.008641	1.14E-05	1.467223	0.000092	31.3	0.282765	0.283009	8.6	0.9
KJ1308_28.dat	120	0.283012	0.283021	1.41E-05	0.000445	1.85E-05	0.016220	2.79E-04	0.008634	1.13E-05	1.467214	0.000107	31.3	0.282765	0.283021	9.0	1.0
KJ1308_29.dat	120	0.282997	0.283006	1.06E-05	0.000998	2.69E-05	0.033836	4.82E-04	0.008642	1.26E-05	1.467245	0.000089	31.3	0.282765	0.283005	8.5	0.7
KJ1308_08.dat	60	0.283020	0.283029	1.75E-05	0.002331	1.23E-04	0.081137	2.21E-03	0.008643	1.68E-05	1.467314	0.000156	31.1	0.282765	0.283028	9.3	1.2
KJ1308_16.dat	120	0.282962	0.282971	1.92E-05	0.000847	2.75E-05	0.038221	6.90E-04	0.008619	2.06E-05	1.467229	0.000174	31.1	0.282765	0.282970	7.2	1.4
KJ1308_21.dat	80	0.283030	0.283039	1.21E-05	0.000760	2.03E-05	0.027190	3.22E-04	0.008661	9.86E-06	1.467225	0.000143	31.1	0.282765	0.283039	9.7	0.9
KJ1308_20.dat	55	0.283031	0.283040	1.59E-05	0.000473	1.18E-05	0.015255	1.75E-04	0.008660	9.72E-06	1.467360	0.000172	31.0	0.282766	0.283040	9.7	1.1
KJ1308_38.dat	50	0.283003	0.283012	1.61E-05	0.000804	2.53E-05	0.031670	4.19E-04	0.008650	2.02E-05	1.467227	0.000156	31.0	0.282766	0.283011	8.7	1.1
KJ1308_37.dat	120	0.282997	0.283007	1.34E-05	0.000586	2.42E-05	0.025403	9.88E-04	0.008632	1.08E-05	1.467238	0.000091	30.9	0.282766	0.283006	8.5	0.9
KJ1308_14.dat	70	0.282949	0.282959	1.36E-05	0.001185	1.15E-04	0.039891	2.15E-03	0.008606	1.61E-05	1.467475	0.000173	30.8	0.282766	0.282958	6.8	1.0
KJ1308_23.dat	80	0.282987	0.282996	1.38E-05	0.001231	4.23E-05	0.044055	1.13E-03	0.008643	1.55E-05	1.467262	0.000140	30.8	0.282766	0.282996	8.1	1.0
KJ1308_35.dat	100	0.282990	0.282999	1.71E-05	0.000515	1.20E-05	0.022781	6.50E-04	0.008637	1.45E-05	1.467216	0.000136	30.7	0.282766	0.282999	8.2	1.2
KJ1308_01.dat	120	0.283006	0.283015	1.21E-05	0.000535	1.31E-05	0.019536	3.75E-04	0.008648	9.23E-06	1.467271	0.000131	30.6	0.282766	0.283015	8.8	0.9
KJ1308_10.dat	120	0.283035	0.283044	1.04E-05	0.000553	1.17E-05	0.018309	1.78E-04	0.008649	1.01E-05	1.467231	0.000095	30.1	0.282766	0.283044	9.8	0.7
KJ1308_13.dat	65	0.283007	0.283017	1.53E-05	0.001032	1.60E-05	0.037846	1.82E-04	0.008637	1.94E-05	1.467228	0.000136	30.1	0.282766	0.283016	8.8	1.1
Median ± 2SD																**8.7**	**1.6**
KJ1508 (s07-081015) n=15																	
KJ1508_01	120	0.283023	0.283039	1.02E-05	0.000948	2.76E-05	0.042395	4.84E-04	0.008665	8.02E-06	1.467305	9.57014E-05	28.3	0.282767	0.283038	9.6	0.7
KJ1508_02	120	0.283010	0.283026	9.03E-06	0.001731	3.85E-05	0.074265	7.22E-04	0.008658	8.20E-06	1.467231	8.21221E-05	28.6	0.282767	0.283025	9.1	0.6
KJ1508_03	120	0.283015	0.283031	6.69E-06	0.001402	5.36E-05	0.061989	1.53E-03	0.008655	5.86E-06	1.467266	7.56639E-05	29	0.282767	0.283030	9.3	0.5
KJ1508_04	120	0.283021	0.283037	9.41E-06	0.000596	2.07E-05	0.025482	6.56E-04	0.008658	5.22E-06	1.467233	8.91542E-05	29.4	0.282767	0.283036	9.5	0.7
KJ1508_05	120	0.283022	0.283038	7.92E-06	0.000981	2.69E-05	0.042397	8.21E-04	0.008663	6.69E-06	1.467254	7.59805E-05	27.8	0.282768	0.283038	9.6	0.6
KJ1508_06	120	0.283028	0.283044	8.52E-06	0.001019	5.45E-05	0.044000	9.28E-04	0.008670	6.58E-06	1.467233	7.59211E-05	27.7	0.282768	0.283043	9.8	0.6
KJ1508_07	120	0.283028	0.283043	8.05E-06	0.000820	2.77E-05	0.036165	9.71E-04	0.008666	5.88E-06	1.467238	8.30218E-05	29.1	0.282767	0.283043	9.8	0.6
KJ1508_08	120	0.283007	0.283023	1.16E-05	0.002487	2.87E-05	0.117715	1.47E-03	0.008663	1.04E-05	1.467221	9.00062E-05	28.7	0.282767	0.283022	9.0	0.8
KJ1508_09	45	0.283013	0.283029	1.31E-05	0.001570	4.88E-05	0.084285	2.30E-03	0.008665	1.48E-05	1.467318	0.000166438	28.3	0.282767	0.283028	9.2	0.9
KJ1508_10	120	0.283021	0.283037	8.33E-06	0.001914	5.09E-05	0.088201	4.10E-04	0.008668	8.09E-06	1.467247	7.80059E-05	28.5	0.282767	0.283036	9.5	0.6
KJ1508_11	120	0.283018	0.283034	8.21E-06	0.001039	3.71E-05	0.045495	5.93E-04	0.008655	5.80E-06	1.467203	7.61095E-05	27.8	0.282768	0.283033	9.4	0.6
KJ1508_12	120	0.283028	0.283044	8.96E-06	0.000903	2.43E-05	0.040592	3.81E-04	0.008663	6.03E-06	1.467261	7.65334E-05	28.9	0.282767	0.283044	9.8	0.6
KJ1508_13	120	0.283023	0.283039	8.50E-06	0.000617	2.84E-05	0.027944	9.97E-04	0.008661	5.46E-06	1.467205	7.98112E-05	28.6	0.282767	0.283038	9.6	0.6
KJ1508_14	120	0.283021	0.283037	7.39E-06	0.000995	1.74E-05	0.044906	9.39E-04	0.008652	6.54E-06	1.467259	9.64413E-05	28.1	0.282767	0.283036	9.5	0.5
KJ1508_15	120	0.283021	0.283037	7.33E-06	0.000787	8.76E-06	0.034582	4.05E-04	0.008656	5.09E-06	1.467233	7.94409E-05	28.5	0.282767	0.283036	9.5	0.5
Median ± 2SD																**9.5**	**0.5**
KJ1509 (s07-081015) n=13																	
KJ1509_01	120	0.283024	0.283039	8.02E-06	0.000805	1.37E-05	0.034059	2.26E-04	0.008662	6.53E-06	1.467266	8.25204E-05	27.6	0.282768	0.283039	9.6	0.6
KJ1509_02	120	0.283030	0.283045	7.22E-06	0.000590	8.22E-06	0.026040	3.45E-04	0.008663	5.31E-06	1.467253	7.01229E-05	28.2	0.282767	0.283045	9.8	0.5
KJ1509_03	120	0.283024	0.283040	7.05E-06	0.000593	9.43E-06	0.026037	1.31E-04	0.008657	5.42E-06	1.467264	8.32198E-05	28.3	0.282767	0.283039	9.6	0.5
KJ1509_04	120	0.283005	0.283021	8.76E-06	0.000957	1.82E-05	0.041008	2.54E-04	0.008654	8.04E-06	1.467258	8.11192E-05	28.3	0.282767	0.283021	9.0	0.6
KJ1509_05	120	0.283008	0.283024	6.84E-06	0.001028	2.46E-05	0.042317	7.89E-04	0.008665	6.32E-06	1.467252	7.32792E-05	28.6	0.282767	0.283023	9.1	0.5
KJ1509_06	120	0.283017	0.283032	7.16E-06	0.000468	3.75E-06	0.019836	2.04E-04	0.008660	4.52E-06	1.467246	8.22558E-05	29.5	0.282766	0.283032	9.4	0.5
KJ1509_07	120	0.283027	0.283043	6.10E-06	0.000438	1.55E-05	0.018432	4.44E-04	0.008664	4.45E-06	1.467249	7.85404E-05	28.5	0.282767	0.283042	9.7	0.4
KJ1509_08	120	0.283031	0.283046	8.11E-06	0.000727	4.59E-06	0.032632	1.57E-04	0.008670	5.63E-06	1.467248	8.55985E-05	28.2	0.282767	0.283046	9.9	0.6
KJ1509_09	120	0.283030	0.283046	8.66E-06	0.000726	1.06E-05	0.032567	3.06E-04	0.008660	5.97E-06	1.467238	8.52261E-05	27.1	0.282768	0.283046	9.8	0.6
KJ1509_10	120	0.283011	0.283027	8.49E-06	0.000534	1.02E-05	0.023966	1.86E-04	0.008658	5.59E-06	1.467219	7.66748E-05	27.6	0.282768	0.283027	9.2	0.6
KJ1509_11	120	0.283024	0.283040	7.74E-06	0.000812	2.59E-05	0.038700	9.42E-04	0.008665	6.14E-06	1.467234	9.21481E-05	27.9	0.282767	0.283040	9.6	0.5
KJ1509_12	120	0.283022	0.283037	7.78E-06	0.000759	5.95E-06	0.034436	2.64E-04	0.008666	5.61E-06	1.467257	7.19417E-05	28.5	0.282767	0.283037	9.5	0.5
KJ1509_13	120	0.283024	0.283040	7.86E-06	0.000880	4.25E-05	0.038791	7.49E-04	0.008667	6.50E-06	1.467251	8.20865E-05	28.3	0.282767	0.283039	9.6	0.6
Median ± 2SD																**9.6**	**0.6**

KJ1302A (s081214) n=13																
KJ1302A_07a.da	120	0.282988	0.282997	1.14E-05	0.001027	1.90E-05	0.032642	3.80E-04	0.008662	1.19E-05	1.467222	0.000098	47.0	0.282755	0.282996	8.5	0.8
KJ1302A_21.dat	60	0.282991	0.283000	1.78E-05	0.000367	1.28E-05	0.012225	2.74E-04	0.008638	1.32E-05	1.467232	0.000135	31.0	0.282766	0.283000	8.3	1.3
KJ1302A_07b.da	120	0.283006	0.283015	1.40E-05	0.001308	1.58E-04	0.039702	2.50E-03	0.008651	1.20E-05	1.467208	0.000097	29.3	0.282767	0.283015	8.8	1.0
KJ1302A_15.dat	120	0.283039	0.283048	1.02E-05	0.000626	1.47E-05	0.016111	2.37E-04	0.008662	8.43E-06	1.467223	0.000086	27.2	0.282768	0.283048	9.9	0.7
KJ1302A_22.dat	100	0.283036	0.283045	1.34E-05	0.000802	3.20E-05	0.022251	3.12E-04	0.008656	1.03E-05	1.467251	0.000108	27.0	0.282768	0.283045	9.8	0.9
KJ1302A_10.dat	80	0.283009	0.283018	1.97E-05	0.000782	1.46E-05	0.026725	3.31E-04	0.008655	2.13E-05	1.467199	0.000154	27.0	0.282768	0.283018	8.8	1.4
KJ1302A_13.dat	120	0.283038	0.283047	1.18E-05	0.000914	3.19E-05	0.024755	4.81E-04	0.008668	1.14E-05	1.467239	0.000096	26.8	0.282768	0.283047	9.8	0.8
KJ1302A_05.dat	80	0.283035	0.283044	1.62E-05	0.000795	4.31E-05	0.025165	8.54E-04	0.008652	1.78E-05	1.467394	0.000150	26.8	0.282768	0.283044	9.7	1.1
KJ1302A_20.dat	70	0.283012	0.283022	2.81E-05	0.000696	2.47E-05	0.029390	5.82E-04	0.008648	3.46E-05	1.467317	0.000281	26.6	0.282768	0.283021	8.9	2.0
KJ1302A_09.dat	120	0.283027	0.283037	1.03E-05	0.000663	1.71E-05	0.020051	3.92E-04	0.008655	7.40E-06	1.467219	0.000090	26.5	0.282768	0.283036	9.5	0.7
KJ1302A_23.dat	105	0.283054	0.283063	1.30E-05	0.000956	3.70E-05	0.025559	5.65E-04	0.008661	9.86E-06	1.467314	0.000148	26.5	0.282768	0.283063	10.4	0.9
KJ1302A_18.dat	120	0.283035	0.283044	1.19E-05	0.000816	1.33E-05	0.020741	1.43E-04	0.008645	9.97E-06	1.467225	0.000091	26.4	0.282768	0.283044	9.7	0.8
KJ1302A_17.dat	85	0.283044	0.283054	2.06E-05	0.001193	1.05E-04	0.045559	2.74E-03	0.008662	2.11E-05	1.467355	0.000137	26.4	0.282768	0.283053	10.1	1.5
Median ± 2SD																**9.7**	**1.3**
KJ1303A1 (s081214) n=12																	
KJ1303A2_03.da	90	0.283021	0.283031	1.32E-05	0.001056	4.34E-05	0.035436	9.98E-04	0.008670	1.02E-05	1.467340	0.000095	26.6	0.282768	0.283030	9.3	0.9
KJ1303A2_05.da	60	0.283010	0.283019	1.97E-05	0.001426	4.72E-05	0.062021	2.24E-03	0.008662	2.48E-05	1.467389	0.000251	26.6	0.282768	0.283019	8.9	1.4
KJ1303A1_09.da	90	0.283048	0.283057	1.51E-05	0.000526	1.50E-05	0.021635	3.97E-04	0.008660	1.52E-05	1.467209	0.000122	26.1	0.282769	0.283057	10.2	1.1
KJ1303A2_04.da	50	0.283039	0.283048	2.09E-05	0.000400	7.61E-06	0.014109	1.46E-04	0.008668	2.25E-05	1.467511	0.000270	26.0	0.282769	0.283048	9.9	1.5
KJ1303A1_11.da	120	0.283046	0.283055	1.25E-05	0.000333	3.02E-06	0.011651	3.50E-05	0.008658	9.07E-06	1.467241	0.000097	25.9	0.282769	0.283055	10.1	0.9
KJ1303A1_10.da	80	0.283036	0.283046	2.41E-05	0.000465	1.09E-05	0.017467	2.70E-04	0.008662	1.93E-05	1.467314	0.000148	25.7	0.282769	0.283045	9.8	1.7
KJ1303A1_08.da	120	0.283019	0.283028	1.58E-05	0.001139	1.04E-04	0.045309	2.15E-03	0.008650	1.51E-05	1.467266	0.000104	25.6	0.282769	0.283027	9.1	1.1
KJ1303A1_03.da	120	0.283048	0.283058	1.18E-05	0.000876	2.27E-05	0.030438	2.27E-04	0.008658	9.35E-06	1.467230	0.000094	25.5	0.282769	0.283057	10.2	0.8
KJ1303A1_15.da	60	0.283039	0.283048	1.92E-05	0.000419	7.94E-06	0.015942	2.73E-04	0.008654	1.32E-05	1.467290	0.000158	25.5	0.282769	0.283048	9.9	1.4
KJ1303A1_05.da	120	0.283043	0.283052	1.39E-05	0.000469	7.57E-06	0.017257	2.46E-04	0.008657	9.34E-06	1.467241	0.000119	25.4	0.282769	0.283052	10.0	1.0
KJ1303A1_13.da	100	0.283011	0.283021	1.38E-05	0.000932	5.04E-05	0.033658	8.72E-04	0.008637	1.29E-05	1.467239	0.000123	25.3	0.282769	0.283020	8.9	1.0
KJ1303A1_07.da	60	0.283067	0.283077	1.61E-05	0.000388	9.35E-06	0.015072	1.41E-04	0.008676	1.16E-05	1.467206	0.000174	25.1	0.282769	0.283077	10.9	1.1
Median ± 2SD																**9.9**	**1.2**
MR1401 (s050215) n=10																	
MR1401_01.dat	110	0.283075	0.283078	1.99E-05	0.000704	1.78E-05	0.028046	3.10E-04	0.008685	1.50E-05	1.467509	0.000337387	24.7	0.282769	0.283078	10.9	1.4
MR1401_02.dat	110	0.283023	0.283027	1.27E-05	0.000739	7.11E-05	0.026438	1.38E-03	0.008663	1.28E-05	1.467297	9.26123E-05	31	0.282766	0.283026	9.2	0.9
MR1401_03.dat	110	0.283066	0.283070	1.40E-05	0.000580	2.63E-05	0.020800	4.82E-04	0.008676	1.14E-05	1.467320	9.48823E-05	24.6	0.282770	0.283069	10.6	1.0
MR1401_04.dat	120	0.283069	0.283073	1.22E-05	0.000369	5.34E-06	0.014321	1.01E-04	0.008668	8.53E-06	1.467283	6.55485E-05	24.8	0.282769	0.283073	10.7	0.9
MR1401_05.dat	120	0.283092	0.283095	1.64E-05	0.000430	1.42E-05	0.016383	3.31E-04	0.008677	1.50E-05	1.467324	0.000119848	24.8	0.282769	0.283095	11.5	1.2
MR1401_06.dat	120	0.283090	0.283094	1.11E-05	0.000624	2.19E-05	0.022931	4.01E-04	0.008660	8.62E-06	1.467242	6.77668E-05	23.4	0.282770	0.283093	11.4	0.8
MR1401_07.dat	120	0.283088	0.283092	1.14E-05	0.000718	9.22E-06	0.029250	2.05E-04	0.008674	1.10E-05	1.467259	7.79597E-05	25.4	0.282769	0.283092	11.4	0.8
MR1401_08.dat	120	0.283072	0.283076	1.16E-05	0.000746	1.67E-05	0.027955	2.98E-04	0.008684	9.95E-06	1.467249	6.35781E-05	30.2	0.282766	0.283075	10.9	0.8
MR1401_09.dat	80	0.283096	0.283099	1.27E-05	0.000682	3.93E-05	0.028020	8.23E-04	0.008689	1.20E-05	1.467230	7.58516E-05	24.5	0.282770	0.283099	11.6	0.9
MR1401_10.dat	90	0.283093	0.283097	1.25E-05	0.000436	2.33E-05	0.017786	5.38E-04	0.008672	9.81E-06	1.467264	6.47618E-05	24.3	0.282770	0.283097	11.6	0.9
Median ± 2SD																**11.2**	**1.5**
KJ1307 (s081214) n=13																	
KJ1307_13.dat	120	0.283067	0.283076	1.21E-05	0.000703	1.32E-05	0.022559	2.00E-04	0.008651	9.65E-06	1.467225	0.000088	31.7	0.282765	0.283076	11.0	0.9
KJ1307_17.dat	120	0.283048	0.283057	1.15E-05	0.000339	1.23E-06	0.011071	4.88E-05	0.008645	8.31E-06	1.467242	0.000087	25.3	0.282769	0.283057	10.2	0.8
KJ1307_01.dat	80	0.283066	0.283075	1.32E-05	0.000829	3.71E-05	0.033677	9.26E-04	0.008665	1.14E-05	1.467212	0.000112	24.9	0.282769	0.283075	10.8	0.9
KJ1307_10.dat	75	0.283061	0.283070	1.47E-05	0.000465	4.65E-06	0.016917	9.26E-05	0.008658	8.69E-06	1.467253	0.000129	24.8	0.282769	0.283070	10.6	1.0
KJ1307_11.dat	120	0.283038	0.283047	1.11E-05	0.000622	2.56E-05	0.022438	4.78E-04	0.008645	1.05E-05	1.467270	0.000097	24.6	0.282770	0.283047	9.8	0.8
KJ1307_08.dat	50	0.283032	0.283041	2.04E-05	0.000468	2.73E-05	0.017476	4.58E-04	0.008646	1.44E-05	1.467411	0.000167	24.5	0.282770	0.283041	9.6	1.4
KJ1307_18.dat	120	0.283055	0.283064	1.09E-05	0.000557	1.40E-05	0.018194	2.05E-04	0.008656	9.35E-06	1.467254	0.000104	24.5	0.282770	0.283064	10.4	0.8
KJ1307_07.dat	120	0.283065	0.283074	1.01E-05	0.000417	2.34E-05	0.014480	3.83E-04	0.008643	8.76E-06	1.467237	0.000100	24.4	0.282770	0.283074	10.8	0.7
KJ1307_22.dat	120	0.283056	0.283065	1.25E-05	0.000497	2.24E-06	0.016492	7.12E-05	0.008650	7.67E-06	1.467260	0.000092	24.1	0.282770	0.283065	10.4	0.9
KJ1307_04.dat	120	0.283052	0.283062	9.93E-06	0.000425	3.17E-06	0.014800	1.30E-04	0.008652	8.17E-06	1.467240	0.000093	23.9	0.282770	0.283062	10.3	0.7
KJ1307_03.dat	120	0.283051	0.283060	1.06E-05	0.000616	1.61E-05	0.022523	3.72E-04	0.008656	8.18E-06	1.467250	0.000112	23.7	0.282770	0.283060	10.3	0.7
KJ1307_14.dat	120	0.283042	0.283051	1.14E-05	0.000489	1.28E-05	0.017768	2.73E-04	0.008649	1.02E-05	1.467243	0.000092	23.7	0.282770	0.283051	9.9	0.8
KJ1307_19.dat	60	0.283057	0.283066	1.43E-05	0.000524	1.44E-05	0.017748	2.94E-04	0.008646	1.13E-05	1.467347	0.000137	23.7	0.282770	0.283066	10.5	1.0
Median ± 2SD																**10.4**	**0.8**
LI1301 (s040215) n=10																	
LI1301_10.dat	120	0.283065	0.283086	1.80E-05	0.000846	3.53E-05	0.030299	6.64E-04	0.008677	1.15E-05	1.467247	0.000124112	22.9	0.282771	0.283086	11.1	1.3
LI1301_09.dat	120	0.283063	0.283084	1.42E-05	0.001034	5.33E-05	0.038022	9.20E-04	0.008680	1.30E-05	1.467267	0.000106236	23.1	0.282770	0.283083	11.1	1.0
LI1301_08.dat	120	0.283094	0.283116	1.87E-05	0.001044	3.15E-05	0.038417	5.64E-04	0.008721	2.21E-05	1.467262	0.000122912	23.2	0.282770	0.283115	12.2	1.3
LI1301_07.dat	100	0.283062	0.283083	1.72E-05	0.001008	6.43E-05	0.036454	1.20E-03	0.008690	1.52E-05	1.467304	0.000136116	23.1	0.282770	0.283082	11.0	1.2
LI1301_06.dat	100	0.283043	0.283065	1.45E-05	0.000600	2.25E-05	0.021302	3.96E-04	0.008677	1.42E-05	1.467295	0.0001158	23.5	0.282770	0.283064	10.4	1.0
LI1301_05.dat	100	0.283065	0.283086	1.63E-05	0.001103	5.56E-05	0.041147	1.10E-03	0.008696	1.57E-05	1.467271	0.000153151	22.8	0.282771	0.283086	11.1	1.2
LI1301_04.dat	110	0.283075	0.283096	1.46E-05	0.000803	3.61E-05	0.028468	6.65E-04	0.008676	1.30E-05	1.467321	0.000128407	22.4	0.282771	0.283096	11.5	1.0
LI1301_03.dat	110	0.283081	0.283103	1.72E-05	0.000959	3.36E-05	0.035194	6.27E-04	0.008707	2.19E-05	1.467326	0.000119538	22.3	0.282771	0.283102	11.7	1.2
LI1301_02.dat	110	0.283066	0.283088	1.88E-05	0.000954	3.75E-05	0.035543	7.66E-04	0.008676	1.57E-05	1.467348	0.000166923	22.9	0.282771	0.283087	11.2	1.3
LI1301_01.dat	110	0.283070	0.283092	1.20E-05	0.001111	8.08E-05	0.042228	1.59E-03	0.008667	1.40E-05	1.467323	9.53874E-05	22.4	0.282771	0.283091	11.3	0.9
Median ± 2SD																**11.2**	**0.9**
KJ1325A (s081214) n=14																	
KJ1325A_12.dat	120	0.283071	0.283080	1.05E-05	0.001319	8.10E-05	0.042104	1.57E-03	0.008655	8.39E-06	1.467246	0.000097	22.9	0.282771	0.283080	10.9	0.7
KJ1325A_05.dat	120	0.283056	0.283066	1.15E-05	0.001151	5.99E-05	0.037001	1.03E-03	0.008656	9.87E-06	1.467256	0.000115	22.6	0.282771	0.283065	10.4	0.8
KJ1325A_09.dat	120	0.283056	0.283065	1.25E-05	0.001150	1.62E-05	0.040420	3.60E-04	0.008655	9.98E-06	1.467240	0.000107	22.5	0.282771	0.283064	10.4	0.9
KJ1325A_04.dat	120	0.283046	0.283055	1.07E-05	0.000929	2.11E-05	0.032225	2.70E-04	0.008659	1.15E-05	1.467271	0.000098	22.4	0.282771	0.283055	10.0	0.8
KJ1325A_19	90	0.283079	0.283088	1.15E-05	0.001054	7.84E-05	0.033481	1.59E-03	0.008664	1.34E-05	1.467346	0.000150	22.4	0.282771	0.283087	11.2	0.8
KJ1325A_21.dat	120	0.283065	0.283074	1.11E-05	0.000948	2.63E-05	0.027940	4.87E-04	0.008652	8.14E-06	1.467290	0.000107	22.4	0.282771	0.283074	10.7	0.8
KJ1325A_03.dat	80	0.283079	0.283089	1.50E-05	0.001482	7.50E-05	0.048756	1.27E-03	0.008676	1.24E-05	1.467285	0.000129	22.3	0.282771	0.283088	11.2	1.1
KJ1325A_01.dat	80	0.283047	0.283056	1.36E-05	0.001087	3.93E-05	0.035041	8.20E-04	0.008652	1.29E-05	1.467274	0.000128	22.1	0.282771	0.283056	10.1	1.0
KJ1325A_02.dat	80	0.283037	0.283046	1.56E-05	0.001022	2.32E-05	0.041427	8.55E-04	0.008662	1.54E-05	1.467197	0.000152	22.1	0.282771	0.283046	9.7	1.1
KJ1325A_07.dat	120	0.283075	0.283084	1.11E-05	0.000971	2.33E-05	0.034488	4.69E-04	0.008669	1.10E-05	1.467281	0.000100	22.1	0.282771	0.283084	11.1	0.8
KJ1325A_20.dat	120	0.283066	0.283075	1.04E-05	0.000708	5.19E-05	0.023270	8.53E-04	0.008665	8.97E-06	1.467279	0.000093	22.1	0.282771	0.283075	10.7	0.7
KJ1325A_15.dat	120	0.283065	0.283074	1.15E-05	0.001165	6.48E-05	0.035517	9.65E-04	0.008658	9.52E-06	1.467255	0.000121	22.0	0.282771	0.283073	10.7	0.8
KJ1325A_18.dat	100	0.283080	0.283089	1.25E-05	0.001089	4.69E-05	0.033715	7.37E-04	0.008673	1.06E-05	1.467270	0.000130	21.9	0.282771	0.283089	11.2	0.9
KJ1325A_14.dat	120	0.283048	0.283058	1.08E-05	0.001308	9.17E-05	0.040307	1.46E-03	0.008641	8.68E-06	1.467251	0.000097	21.7	0.282771	0.283057	10.1	0.8
Median ± 2SD																**10.7**	**1.0**
KJ1324A (s081214) n=16																	
KJ1324A_16.dat	100	0.283069	0.283078	1.24E-05	0.000632	1.95E-05	0.018742	3.22E-04	0.008658	1.05E-05	1.467249	0.000115	23.0	0.282771	0.283078	10.9	0.9
KJ1324A_10.dat	100	0.283058	0.283067	1.53E-05	0.000929	1.60E-05	0.027847	2.58E-04	0.008666	1.08E-05	1.467254	0.000123	22.7	0.282771	0.283067	10.5	1.1
KJ1324A_09.dat	100	0.283049	0.283058	1.19E-05	0.001091	2.49E-05	0.033073	3.98E-04	0.008649	1.10E-05	1.467282	0.000122	22.5	0.282771	0.283058	10.1	0.8
KJ1324A_14.dat	100	0.283056	0.283066	1.41E-05	0.000884	2.24E-05	0.026881	3.50E-04	0.008666	1.12E-05	1.467239	0.000113	22.4	0.282771	0.283065	10.4	1.0
KJ1324A_08.dat	100	0.283044	0.283053	1.34E-05	0.001046	4.46E-05	0.031670	7.94E-04	0.008652	1.00E-05	1.467250	0.000118	22.3	0.282771	0.283053	10.0	0.9
KJ1324A_27.dat	120	0.283072	0.283081	1.05E-05	0.000929	2.41E-05	0.026761	3.91E-04	0.008654	9.87E-06	1.467224	0.000094	22.3	0.282771	0.283081	11.0	0.7
KJ1324A_18.dat	90	0.283059	0.283068	1.58E-05	0.001286	6.84E-05	0.041005	1.15E-03	0.008656	1.38E-05	1.467254	0.000123	22.2	0.282771	0.283068	10.5	1.1
KJ1324A_17.dat	100	0.283059	0.283069	1.27E-05	0.000845	4.52E-05	0.026969	7.81E-04	0.008664	1.21E-05	1.467216	0.000132	22.1	0.282771	0.283068	10.2	1.0
KJ1324A_24.dat	120	0.283079	0.283088	1.32E-05	0.001126	4.19E-05	0.036604	7.72E-04	0.008677	1.25E-05	1.467242	0.000085	22.1	0.282771	0.283088	11.2	0.9
KJ1324A_32.dat	60	0.283088	0.283097	1.74E-05	0.001186	8.64E-05	0.035955	1.48E-03	0.008666	1.26E-05	1.467196	0.000169	22.1	0.282771	0.283097	11.5	1.2
KJ1324A_01.dat	100	0.283048	0.283057	4.22E-05	0.001229	9.26E-05	0.065670	2.02E-03	0.008668	4.20E-05	1.467134	0.000510	22.0	0.282771	0.283057	10.1	3.0
KJ1324A_23.dat	75	0.283059	0.283069	1.51E-05	0.000966	3.47E-05	0.028675	6.76E-04	0.008643	1.26E-05	1.467238	0.000145	22.0	0.282771	0.283068	10.5	1.1
KJ1324A_02.dat	100	0.283065	0.283075	2.09E-05	0.000710	4.15E-05	0.033684	9.58E-04	0.008682	2.74E-05	1.467197	0.000242	21.9	0.282771	0.283074	10.7	1.5
KJ1324A_05.dat	110	0.283045	0.283055	1.29E-05	0.000927	4.42E-05	0.029054	7.45E-04	0.008652	1.07E-05	1.467248	0.000114	21.9	0.282771	0.283054	10.0	0.9
KJ1324A_06.dat	100	0.283043	0.283053	1.36E-05	0.000972	3.51E-05	0.031680	7.36E-04	0.008652	1.32E-05	1.467290	0.000106	21.9	0.282771	0.283052	9.9	1.0
KJ1324A_28.dat	120	0.283075	0.283084	1.14E-05	0.001065	4.49E-05	0.030874	6.51E-04	0.008648	9.57E-06	1.467231	0.000095	21.9	0.282771	0.283084	11.1	0.8
Median ± 2SD																**10.5**	**1.0**
KJ1313 (s081214) n=13																	
KJ1313_07.dat	120	0.283061	0.283070	1.13E-05	0.001362	3.40E-05	0.046880	7.58E-04	0.008653	1.13E-05	1.467197	0.000098	22.0	0.282771	0.283070	10.6	0.8
KJ1313_11.dat	50	0.283009	0.283018	2.42E-05	0.001095	7.46E-05	0.054728	2.72E-03	0.008610	2.56E-05	1.467236	0.000169	21.8	0.282771	0.283018	8.7	1.7
KJ1313_31.dat	120	0.283072	0.283081	1.10E-05	0.001077	3.00E-05	0.040594	1.04E-03	0.008664	9.60E-06	1.467188	0.000081	21.7	0.282771	0.283080	10.9	0.8
KJ1313_09.dat	120	0.283094	0.283103	1.01E-05	0.001311	2.24E-05	0.046533	3.72E-04	0.008661	1.01E-05	1.467233	0.000075	21.4	0.282772	0.283103	11.7	0.7
KJ1313_13.dat	100	0.283071	0.283081	9.59E-06	0.001119	2.43E-05	0.038575	6.53E-04	0.008660	8.89E-06	1.467217	0.000103	21.4	0.282772	0.283080	10.9	0.7
KJ1313_01.dat	120	0.283065	0.283074	1.02E-05	0.000685	8.35E-06	0.026083	5.02E-04	0.008665	8.05E-06	1.467267	0.000092	21.3	0.282772	0.283074	10.7	0.7
KJ1313_04.dat	120	0.283085	0.283094	1.03E-05	0.000987	3.39E-05	0.032918	4.60E-04	0.008668	8.24E-06	1.467274	0.000093	21.3	0.282772	0.283094	11.4	0.7
KJ1313_05.dat	120	0.283060	0.283069	1.13E-05	0.001702	8.72E-05	0.061424	1.55E-03	0.008648	9.51E-06	1.467231	0.000088	21.3	0.282772	0.283068	10.5	0.8
KJ1313_33.dat	90	0.283084	0.283093	1.23E-05	0.002062	1.58E-04	0.076523	3.15E-03	0.008677	1.49E-05	1.467250	0.000110	21.2	0.282772	0.283093	11.3	0.9
KJ1313_03.dat	90	0.283048	0.283057	1.12E-05	0.001185	2.78E-05	0.041062	7.75E-04	0.008647	1.01E-05	1.467252	0.000086	21.1	0.282772	0.283057	10.1	0.8
KJ1313_34.dat	70	0.283079	0.283088	1.09E-05	0.000996	5.25E-05	0.035855	1.26E-03	0.008661	1.20E-05	1.467322	0.000162	21.0	0.282772	0.283088	11.2	0.8
KJ1313_06.dat	120	0.283073	0.283083	1.10E-05	0.001355	4.77E-05	0.044450	1.06E-03	0.008653	9.82E-06	1.467250	0.000090	20.9	0.282772	0.283082	11.0	0.8
KJ1313_16.dat	100	0.283066	0.283075	1.34E-05	0.001260	7.33E-05	0.044331	1.13E-03	0.008655	9.53E-06	1.467215	0.000092	20.9	0.282772	0.283074	10.7	0.9
Median ± 2SD																**10.9**	**1.5**

[a] Using the age obtained by LA-ICPMS in this study (Table DR2)

[b] Using CHUR values of Bouvier et al. (2008)

[c] Plesovice age from Sláma et al. (2008) and Temora-2 from Woodhead and Hergt (2005)

[d] A mean age is shown because we measured on a zircon batch used for oxygen isotopes, where LA-ICPMS has not been performed

STANDARDS

Analysis (TM: n=98; PL: n=89)	# cycles integrated	176Hf/177Hf	2se	176Lu/177Hf	2se	173Yb/177Hf	1se	178Hf/177Hf	2se	Age (Ma)[c]	176Hf/177Hf (t) CHUR*	176Hf/177Hf (t)	εHf (t)	2se	εHf offset from ref
s081214															
TEMORA-2 (n=11)															
TM_10-1.dat	120	0.282695	0.000011	0.001104	0.000008	0.039679	0.000157	1.467264	0.000083	417	0.282522	0.282687	5.8	0.8	0.0
TM_10-3.dat	120	0.282704	0.000013	0.001344	0.000005	0.047713	0.000187	1.467244	0.000083	417	0.282522	0.282693	6.1	0.9	0.2
TM_10-4.dat	120	0.282684	0.000012	0.000682	0.000007	0.021606	0.000136	1.467224	0.000095	417	0.282522	0.282679	5.5	0.9	-0.2
TM_10-5.dat	80	0.282689	0.000015	0.000646	0.000018	0.020646	0.000242	1.467281	0.000102	417	0.282522	0.282684	5.7	1.0	-0.1
TM_10-6.dat	120	0.282666	0.000013	0.001221	0.000050	0.042481	0.000973	1.467261	0.000086	417	0.282522	0.282657	4.7	0.9	-1.0
TM_10-7.dat	110	0.282685	0.000013	0.001410	0.000030	0.049623	0.000453	1.467309	0.000094	417	0.282522	0.282674	5.4	0.9	-0.4
TM_10-9.dat	120	0.282682	0.000013	0.001830	0.000029	0.062679	0.000593	1.467313	0.000115	417	0.282522	0.282667	5.1	0.9	-0.6
TM_10-11.dat	120	0.282671	0.000014	0.002196	0.000030	0.074988	0.000421	1.467246	0.000092	417	0.282522	0.282654	4.7	1.0	-1.1
TM_10-12.dat	120	0.282676	0.000014	0.000500	0.000002	0.017410	0.000152	1.467229	0.000082	417	0.282522	0.282672	5.3	1.0	-0.5
TM_10-13.dat	110	0.282671	0.000012	0.000531	0.000005	0.018070	0.000155	1.467236	0.000082	417	0.282522	0.282667	5.1	0.9	-0.6
TM_10-14.dat	90	0.282694	0.000013	0.000540	0.000007	0.018364	0.000156	1.467276	0.000081	417	0.282522	0.282690	5.9	0.9	0.1
											Mean	**0.282675**	**5.4**		**-0.4**
											2SD	**0.000026**	**0.9**		
										Normalization factor		**1.000040**			
PLESOVICE (n=12)															
PL_10-2.dat	120	0.282493	0.000012	0.000116	0.000002	0.006596	0.000043	1.467241	0.000132	337	0.282573	0.282492	-2.8	0.8	0.3
PL_10-3.dat	120	0.282485	0.000011	0.000091	0.000001	0.004919	0.000038	1.467252	0.000092	337	0.282573	0.282485	-3.1	0.8	0.1
PL_10-4.dat	120	0.282472	0.000013	0.000091	0.000000	0.004619	0.000033	1.467239	0.000087	337	0.282573	0.282471	-3.6	0.9	-0.4
PL_10-5.dat	120	0.282473	0.000011	0.000133	0.000002	0.006504	0.000026	1.467268	0.000099	337	0.282573	0.282473	-3.6	0.8	-0.3
PL_10-6.dat	120	0.282471	0.000011	0.000091	0.000000	0.004554	0.000023	1.467281	0.000100	337	0.282573	0.282471	-3.6	0.8	-0.4
PL_10-7.dat	120	0.282467	0.000012	0.000132	0.000002	0.006406	0.000025	1.467274	0.000101	337	0.282573	0.282466	-3.8	0.8	-0.5
PL_10-8.dat	120	0.282477	0.000011	0.000128	0.000002	0.006284	0.000021	1.467292	0.000087	337	0.282573	0.282477	-3.4	0.8	-0.2
PL_10-9.dat	120	0.282470	0.000012	0.000126	0.000001	0.006186	0.000016	1.467297	0.000085	337	0.282573	0.282469	-3.7	0.9	-0.4
PL_10-10.dat	120	0.282475	0.000012	0.000128	0.000001	0.006189	0.000018	1.467290	0.000094	337	0.282573	0.282475	-3.5	0.8	-0.2
PL_10-11.dat	120	0.282467	0.000010	0.000128	0.000001	0.006250	0.000018	1.467237	0.000086	337	0.282573	0.282466	-3.8	0.7	-0.5
PL_10-12.dat	120	0.282468	0.000012	0.000130	0.000001	0.006340	0.000019	1.467257	0.000088	337	0.282573	0.282468	-3.7	0.8	-0.5
PL_10-13.dat	120	0.282484	0.000010	0.000128	0.000001	0.006283	0.000022	1.467273	0.000077	337	0.282573	0.282483	-3.2	0.7	0.0
											Mean	**0.282475**	**-3.5**		**-0.2**
											2SD	**0.000016**	**0.6**		
										Normalization factor		**1.000026**			
										Average Normalization factor (TM + PL)		**1.000033**			
s020315															
TEMORA-2 (n=6)															
TM_14-06.dat	120	0.282661	0.000010	0.001286	0.000042	0.051175	0.000713	1.467281	0.000074	417	0.282522	0.282651	4.6	0.7	-1.2
TM_14-05.dat	90	0.282671	0.000011	0.000641	0.000010	0.027281	0.000298	1.467286	0.000086	417	0.282522	0.282666	5.1	0.8	-0.7
TM_14-04.dat	120	0.282671	0.000010	0.000684	0.000015	0.028029	0.000266	1.467273	0.000067	417	0.282522	0.282666	5.1	0.7	-0.7
TM_14-03.dat	120	0.282659	0.000010	0.001376	0.000013	0.056426	0.000316	1.467291	0.000075	417	0.282522	0.282648	4.4	0.7	-1.3
TM_14-02.dat	120	0.282673	0.000010	0.001028	0.000020	0.043901	0.000507	1.467275	0.000061	417	0.282522	0.282665	5.0	0.7	-0.7
TM_14-01.dat	120	0.282657	0.000011	0.001038	0.000024	0.042986	0.000634	1.467294	0.000071	417	0.282522	0.282649	4.5	0.7	-1.2
											Mean	**0.282657**	**4.8**		**-1.0**
											2SD	**0.000018**	**0.6**		
										Normalization factor		**1.000101**			
PLESOVICE (n=6)															
PL_14-06.dat	120	0.282472	0.000009	0.000127	0.000001	0.008157	0.000019	1.467284	0.000064	337	0.282573	0.282472	-3.6	0.6	-0.3
PL_14-05.dat	120	0.282472	0.000010	0.000128	0.000001	0.007959	0.000019	1.467283	0.000078	337	0.282573	0.282472	-3.6	0.7	-0.3
PL_14-04.dat	120	0.282479	0.000009	0.000128	0.000001	0.007993	0.000021	1.467294	0.000093	337	0.282573	0.282478	-3.4	0.6	-0.1
PL_14-03.dat	120	0.282468	0.000009	0.000128	0.000001	0.007981	0.000019	1.467325	0.000073	337	0.282573	0.282468	-3.7	0.7	-0.5
PL_14-02.dat	120	0.282465	0.000010	0.000129	0.000001	0.008005	0.000023	1.467294	0.000085	337	0.282573	0.282465	-3.8	0.7	-0.6
PL_14-01.dat	120	0.282478	0.000010	0.000112	0.000002	0.007527	0.000054	1.467305	0.000074	337	0.282573	0.282477	-3.4	0.7	-0.2
											Mean	**0.282472**	**-3.6**		**-0.3**
											2SD	**0.000011**	**0.4**		
										Normalization factor		**1.000036**			
										Average Normalization factor (TM + PL)		**1.000069**			
s040215															
TEMORA-2 (n=8)															
TM_6-4.dat	120	0.282677	0.000011	0.001612	0.000016	0.064218	0.000263	1.467288	0.000091	417	0.282522	0.282664	5.0	0.8	-0.7
TM_6-3.dat	100	0.282657	0.000011	0.001360	0.000032	0.050297	0.000592	1.467284	0.000085	417	0.282522	0.282647	4.4	0.8	-1.3
TM_6-2.dat	100	0.282669	0.000012	0.001453	0.000052	0.056158	0.000870	1.467304	0.000088	417	0.282522	0.282658	4.8	0.8	-0.9
TM_6-1.dat	100	0.282675	0.000011	0.001566	0.000027	0.057178	0.000592	1.467302	0.000077	417	0.282522	0.282662	5.0	0.8	-0.8
TM_5-4.dat	120	0.282666	0.000012	0.000669	0.000005	0.027633	0.000214	1.467287	0.000112	417	0.282522	0.282661	4.9	0.9	-0.8
TM_5-3.dat	120	0.282668	0.000012	0.001351	0.000020	0.058949	0.000635	1.467294	0.000083	417	0.282522	0.282657	4.8	0.9	-1.0
TM_5-2.dat	120	0.282662	0.000013	0.001084	0.000011	0.045966	0.000350	1.467321	0.000091	417	0.282522	0.282654	4.7	0.9	-1.1
TM_5-1.dat	120	0.282663	0.000015	0.001598	0.000016	0.072868	0.000438	1.467284	0.000114	417	0.282522	0.282650	4.5	1.1	-1.2
											Mean	**0.282657**	**4.8**		**-1.0**
											2SD	**0.000012**	**0.4**		
										Normalization factor		**1.000104**			
PLESOVICE (n=10)															
PL_6-5.dat	120	0.282464	0.000011	0.000163	0.000001	0.011833	0.000095	1.467292	0.000103	337	0.282573	0.282463	-3.9	0.8	-0.6
PL_6-4.dat	120	0.282464	0.000011	0.000097	0.000001	0.006162	0.000055	1.467268	0.000083	337	0.282573	0.282464	-3.9	0.8	-0.6
PL_6-3.dat	120	0.282475	0.000013	0.000092	0.000001	0.005649	0.000030	1.467303	0.000086	337	0.282573	0.282475	-3.5	0.9	-0.2
PL_6-2.dat	120	0.282478	0.000010	0.000074	0.000002	0.004248	0.000055	1.467292	0.000070	337	0.282573	0.282477	-3.4	0.7	-0.2
PL_6-1.dat	120	0.282480	0.000011	0.000076	0.000001	0.004447	0.000030	1.467267	0.000075	337	0.282573	0.282479	-3.3	0.8	-0.1
PL_5-5.dat	120	0.282470	0.000013	0.000067	0.000002	0.004327	0.000040	1.467294	0.000082	337	0.282573	0.282470	-3.6	0.9	-0.4
PL_5-4.dat	120	0.282482	0.000012	0.000070	0.000001	0.004889	0.000041	1.467295	0.000080	337	0.282573	0.282482	-3.2	0.8	0.0
PL_5-3.dat	120	0.282447	0.000012	0.000090	0.000001	0.006988	0.000081	1.467358	0.000090	337	0.282573	0.282446	-4.5	0.8	-1.2
PL_5-2.dat	120	0.282456	0.000013	0.000076	0.000000	0.004911	0.000016	1.467298	0.000069	337	0.282573	0.282456	-4.2	0.9	-0.9
PL_5-1.dat	120	0.282478	0.000014	0.000069	0.000000	0.004456	0.000021	1.467297	0.000095	337	0.282573	0.282478	-3.4	1.0	-0.1
											Mean	**0.282469**	**-3.7**		**-0.4**
											2SD	**0.000023**	**0.8**		
										Normalization factor		**1.000046**			
										Average Normalization factor (TM + PL)		**1.000075**			

s080515

TEMORA-2 (n=24)																
TM-NW_13_1.dat	90	0.282698	0.000012	0.001226	0.000022	0.065550	0.001703	1.467234	0.000127	417	0.282522	0.282688	5.9	0.9	0.1
TM-NW_13_2.dat	120	0.282713	0.000018	0.001328	0.000031	0.073036	0.001563	1.467294	0.000100	417	0.282522	0.282703	6.4	1.3	0.6
TM-NW_13_3.dat	110	0.282670	0.000017	0.001449	0.000048	0.076968	0.000589	1.467305	0.000095	417	0.282522	0.282658	4.8	1.2	-0.9
TM-NW_13_4.dat	110	0.282716	0.000018	0.001059	0.000050	0.056145	0.001525	1.467296	0.000112	417	0.282522	0.282708	6.6	1.3	0.7
TM-NW_13_5.dat	110	0.282680	0.000018	0.001375	0.000013	0.078925	0.000957	1.467296	0.000115	417	0.282522	0.282669	5.2	1.3	-0.6
TM-NW_13_6.dat	110	0.282673	0.000015	0.001369	0.000012	0.076764	0.000926	1.467307	0.000121	417	0.282522	0.282662	4.9	1.0	-0.8
TM-NW_13_7.dat	110	0.282644	0.000017	*0.001449*	0.000010	0.069119	0.000401	1.467288	0.000090	417	0.282522	0.282633	3.9	1.2	-1.8
TM-NW_13_8.dat	110	0.282674	0.000014	0.001454	0.000012	0.069566	0.000325	1.467340	0.000103	417	0.282522	0.282663	5.0	1.0	-0.8
TM-NW_13_9.dat	110	0.282704	0.000016	0.001485	0.000013	0.071653	0.000480	1.467280	0.000089	417	0.282522	0.282692	6.0	1.1	0.2
TM-NW_13_10.da	120	0.282685	0.000018	0.001470	0.000012	0.072129	0.000598	1.467278	0.000094	417	0.282522	0.282673	5.3	1.2	-0.4
TM-NW_13_11.da	120	0.282680	0.000015	0.001383	0.000039	0.065565	0.000668	1.467281	0.000086	417	0.282522	0.282669	5.2	1.1	-0.6
TM-NW_13_12.da	120	0.282707	0.000015	0.001408	0.000039	0.067239	0.000647	1.467265	0.000080	417	0.282522	0.282696	6.1	1.1	0.3
TM-NW_13_13.da	120	0.282655	0.000019	0.001622	0.000092	0.082488	0.003417	1.467254	0.000079	417	0.282522	0.282642	4.2	1.4	-1.5
TM-NW_13_14.da	120	0.282681	0.000017	0.001622	0.000099	0.079273	0.003326	1.467254	0.000083	417	0.282522	0.282669	5.2	1.2	-0.6
TM-NW_13_15.da	120	0.282704	0.000016	0.001624	0.000015	0.078641	0.001211	1.467194	0.000095	417	0.282522	0.282691	6.0	1.1	0.2
TM-NW_13_16.da	120	0.282687	0.000018	0.001400	0.000010	0.067765	0.000678	1.467281	0.000090	417	0.282522	0.282676	5.4	1.3	-0.3
TM-NW_13_17.da	120	0.282717	0.000017	0.001313	0.000009	0.064649	0.000678	1.467286	0.000094	417	0.282522	0.282707	6.5	1.2	0.7
TM-NW_13_18.da	120	0.282679	0.000018	0.001880	0.000016	0.090096	0.001507	1.467244	0.000108	417	0.282522	0.282664	5.0	1.3	-0.7
TM-NW_13_19.da	120	0.282705	0.000019	0.002452	0.000069	0.118372	0.002990	1.467251	0.000103	417	0.282522	0.282686	5.8	1.3	0.0
TM-NW_13_20.da	120	0.282709	0.000017	0.000542	0.000003	0.025273	0.000395	1.467265	0.000101	417	0.282522	0.282705	6.5	1.2	0.6
TM-NW_13_21.da	120	0.282718	0.000016	0.000627	0.000025	0.028989	0.000887	1.467266	0.000099	417	0.282522	0.282714	6.8	1.1	0.9
TM-NW_13_22.da	120	0.282713	0.000015	0.000568	0.000005	0.025435	0.000252	1.467286	0.000103	417	0.282522	0.282709	6.6	1.0	0.8
TM-NW_13_23.da	120	0.282707	0.000015	0.000525	0.000001	0.023168	0.000200	1.467285	0.000109	417	0.282522	0.282703	6.4	1.1	0.6
TM-NW_13_24.da	120	0.282721	0.000015	0.000549	0.000001	0.023970	0.000234	1.467219	0.000110	417	0.282522	0.282717	6.9	1.0	1.0
											Mean	**0.282683**	**5.7**		**-0.1**
											2SD	**0.000046**	**1.6**		
										Normalization factor		**1.000010**			
PLESOVICE (n=18)															
PL-NW_13_1.dat	110	0.282479	0.000014	0.000130	0.000004	0.008208	0.000098	1.467289	0.000116	337	0.282573	0.282478	-3.3	1.0	-0.1
PL-NW_13_2.dat	110	0.282488	0.000013	0.000074	0.000004	0.004805	0.000105	1.467333	0.000098	337	0.282573	0.282487	-3.0	0.9	0.2
PL-NW_13_3.dat	110	0.282494	0.000013	0.000068	0.000004	0.004441	0.000095	1.467318	0.000099	337	0.282573	0.282494	-2.8	0.9	0.4
PL-NW_13_4.dat	110	0.282475	0.000014	0.000070	0.000005	0.004558	0.000116	1.467304	0.000109	337	0.282573	0.282474	-3.5	1.0	-0.3
PL-NW_13_5.dat	110	0.282482	0.000013	0.000064	0.000003	0.004244	0.000077	1.467281	0.000094	337	0.282573	0.282482	-3.2	0.9	0.0
PL-NW_13_6.dat	110	0.282472	0.000015	0.000063	0.000002	0.004202	0.000054	1.467273	0.000082	337	0.282573	0.282472	-3.6	1.0	-0.3
PL-NW_13_7.dat	120	0.282476	0.000013	0.000065	0.000003	0.004375	0.000084	1.467257	0.000095	337	0.282573	0.282476	-3.4	0.9	-0.2
PL-NW_13_8.dat	120	0.282483	0.000013	0.000065	0.000003	0.004481	0.000076	1.467266	0.000093	337	0.282573	0.282483	-3.2	0.9	0.0
PL-NW_13_9.dat	120	0.282490	0.000013	0.000065	0.000003	0.004260	0.000082	1.467286	0.000119	337	0.282573	0.282489	-3.0	0.9	0.2
PL-NW_13_10.da	120	0.282479	0.000015	0.000067	0.000003	0.004430	0.000071	1.467287	0.000090	337	0.282573	0.282479	-3.3	1.0	-0.1
PL-NW_13_11.da	120	0.282489	0.000014	0.000086	0.000005	0.005489	0.000124	1.467240	0.000100	337	0.282573	0.282489	-3.0	1.0	0.2
PL-NW_13_12.da	120	0.282484	0.000014	0.000117	0.000007	0.007390	0.000167	1.467281	0.000118	337	0.282573	0.282483	-3.2	1.0	0.0
PL-NW_13_13.da	120	0.282506	0.000013	0.000128	0.000004	0.008131	0.000078	1.467253	0.000099	337	0.282573	0.282506	-2.4	0.9	0.8
PL-NW_13_14.da	120	0.282509	0.000013	0.000134	0.000002	0.008618	0.000156	1.467267	0.000094	337	0.282573	0.282508	-2.3	1.0	0.9
PL-NW_13_15.da	120	0.282499	0.000014	0.000142	0.000003	0.009013	0.000153	1.467267	0.000098	337	0.282573	0.282498	-2.7	1.0	0.5
PL-NW_13_16.da	120	0.282505	0.000012	0.000144	0.000001	0.009191	0.000074	1.467242	0.000102	337	0.282573	0.282504	-2.4	0.9	0.7
PL-NW_13_17.da	120	0.282521	0.000012	0.000130	0.000002	0.008651	0.000150	1.467231	0.000103	337	0.282573	0.282520	-1.9	0.8	1.3
PL-NW_13_18.da	120	0.282525	0.000013	0.000121	0.000005	0.007835	0.000107	1.467243	0.000102	337	0.282573	0.282524	-1.7	0.9	1.4
											Mean	**0.282491**	**-2.9**		**0.3**
										Normalization factor		**0.999966**			
										Average Normalization factor (TM + PL)		**0.999988**			

s050215

TEMORA-2 (n=19)																
TM_12-1.dat	120	0.282668	0.000014	0.001882	0.000008	0.088149	0.000499	1.467330	0.000101	417	0.282522	0.282653	4.6	1.0	-1.1
TM_12-2.dat	120	0.282669	0.000012	0.001500	0.000006	0.068077	0.000415	1.467316	0.000100	417	0.282522	0.282657	4.8	0.9	-1.0
TM_12-3.dat	110	0.282663	0.000015	0.001536	0.000006	0.068777	0.000150	1.467354	0.000106	417	0.282522	0.282651	4.6	1.0	-1.2
TM_12-4.dat	120	0.282659	0.000014	0.001601	0.000024	0.072411	0.000862	1.467320	0.000099	417	0.282522	0.282646	4.4	1.0	-1.3
TM_12-5.dat	95	0.282684	0.000016	0.002507	0.000031	0.119238	0.001033	1.467348	0.000111	417	0.282522	0.282664	5.0	1.1	-0.7
TM_12-6.dat	115	0.282692	0.000015	0.001463	0.000017	0.063440	0.000243	1.467334	0.000139	417	0.282522	0.282680	5.6	1.1	-0.2
TM_12-7.dat	120	0.282685	0.000014	0.000821	0.000014	0.030791	0.000265	1.467324	0.000081	417	0.282522	0.282679	5.5	1.0	-0.2
TM_12-8.dat	120	0.282696	0.000014	0.000879	0.000018	0.034481	0.000413	1.467298	0.000124	417	0.282522	0.282689	5.9	1.0	0.1
TM_12-9.dat	120	0.282696	0.000012	0.000664	0.000021	0.026938	0.000377	1.467295	0.000093	417	0.282522	0.282691	6.0	0.8	0.2
TM_12-10.dat	120	0.282666	0.000015	0.001332	0.000037	0.056532	0.000859	1.467323	0.000105	417	0.282522	0.282655	4.7	1.1	-1.0
TM_12-11.dat	120	0.282707	0.000019	0.001501	0.000029	0.062704	0.000545	1.467260	0.000170	417	0.282522	0.282695	6.1	1.3	0.3
TM_12-12.dat	120	0.282663	0.000012	0.001182	0.000046	0.052922	0.001185	1.467325	0.000090	417	0.282522	0.282654	4.7	0.9	-1.1
TM_12-13.dat	120	0.282657	0.000014	0.001643	0.000079	0.075052	0.002043	1.467318	0.000100	417	0.282522	0.282644	4.3	1.0	-1.4
TM_12-14.dat	120	0.282677	0.000014	0.001513	0.000015	0.068160	0.000427	1.467287	0.000086	417	0.282522	0.282665	5.0	1.0	-0.7
TM_12-15.dat	120	0.282707	0.000011	0.001203	0.000045	0.050403	0.001299	1.467243	0.000081	417	0.282522	0.282697	6.2	0.8	0.4
TM_12-16.dat	120	0.282683	0.000010	0.001002	0.000034	0.041891	0.000882	1.467320	0.000074	417	0.282522	0.282675	5.4	0.7	-0.4
TM_12-17.dat	120	0.282705	0.000013	0.001276	0.000027	0.052820	0.000746	1.467306	0.000087	417	0.282522	0.282695	6.1	0.9	0.3
TM_12-18.dat	120	0.282679	0.000012	0.000879	0.000034	0.037778	0.000862	1.467276	0.000076	417	0.282522	0.282672	5.3	0.8	-0.5
TM_12-19.dat	120	0.282708	0.000011	0.000780	0.000028	0.032910	0.000728	1.467277	0.000067	417	0.282522	0.282701	6.3	0.8	0.5
											Mean	**0.282672**	**5.3**		**-0.5**
											2SD	**0.000038**	**1.3**		
										Normalization factor		**1.000050**			
PLESOVICE (n=15)															
PL_12-1.dat	120	0.282473	0.000017	0.000070	0.000000	0.004347	0.000022	1.467334	0.000146	337	0.282573	0.282473	-3.5	1.2	-0.3
PL_12-2.dat	120	0.282485	0.000016	0.000069	0.000001	0.003956	0.000020	1.467322	0.000133	337	0.282573	0.282484	-3.1	1.1	0.1
PL_12-3.dat	120	0.282474	0.000015	0.000069	0.000000	0.004186	0.000010	1.467301	0.000130	337	0.282573	0.282474	-3.5	1.1	-0.3
PL_12-4.dat	120	0.282480	0.000015	0.000059	0.000001	0.003527	0.000013	1.467318	0.000140	337	0.282573	0.282479	-3.3	1.1	-0.1
PL_12-5.dat	120	0.282480	0.000014	0.000076	0.000000	0.004819	0.000028	1.467324	0.000132	337	0.282573	0.282479	-3.3	1.0	-0.1
PL_12-6.dat	120	0.282490	0.000014	0.000061	0.000001	0.003809	0.000046	1.467277	0.000114	337	0.282573	0.282489	-3.0	1.0	0.2
PL_12-7.dat	120	0.282496	0.000012	0.000104	0.000001	0.006359	0.000020	1.467288	0.000110	337	0.282573	0.282495	-2.8	0.8	0.4
PL_12-8.dat	120	0.282485	0.000014	0.000110	0.000000	0.006826	0.000020	1.467315	0.000140	337	0.282573	0.282484	-3.1	1.0	0.1
PL_12-9.dat	120	0.282495	0.000011	0.000107	0.000001	0.006625	0.000027	1.467298	0.000091	337	0.282573	0.282494	-2.8	0.8	0.4
PL_12-10.dat	120	0.282471	0.000013	0.000103	0.000002	0.006297	0.000015	1.467309	0.000093	337	0.282573	0.282471	-3.6	0.9	-0.4
PL_12-11.dat	120	0.282499	0.000014	0.000103	0.000000	0.006466	0.000038	1.467274	0.000121	337	0.282573	0.282498	-2.7	1.0	0.5
PL_12-12.dat	120	0.282506	0.000013	0.000087	0.000002	0.005607	0.000077	1.467317	0.000127	337	0.282573	0.282505	-2.4	0.9	0.8
PL_12-13.dat	120	0.282496	0.000013	0.000097	0.000001	0.006076	0.000023	1.467308	0.000141	337	0.282573	0.282495	-2.7	0.9	0.4
PL_12-14.dat	120	0.282496	0.000011	0.000081	0.000001	0.004961	0.000025	1.467288	0.000093	337	0.282573	0.282496	-2.7	0.8	0.5
PL_12-15.dat	120	0.282517	0.000012	0.000074	0.000001	0.004648	0.000022	1.467286	0.000116	337	0.282573	0.282517	-2.0	0.8	1.2
											Mean	**0.282489**	**-3.0**		**0.2**
											2SD	**0.000026**	**0.9**		
										Normalization factor		**0.999976**			
										Average Normalization factor (TM + PL)		**1.000013**			

s07-081015

TEMORA-2 (n=30)																
run1\TEM_2-1.d	120	0.282677	0.000009	0.001264	0.000024	0.053438	0.000374	1.467225	0.000066	417	0.282522	0.282667	5.1	0.6	-0.6
run1\TEM_2-2.d	110	0.282674	0.000009	0.001328	0.000006	0.056682	0.000218	1.467251	0.000062	417	0.282522	0.282664	5.0	0.6	-0.7
run1\TEM_2-3.d	120	0.282659	0.000008	0.001023	0.000046	0.045373	0.001074	1.467262	0.000074	417	0.282522	0.282651	4.5	0.6	-1.2
run1\TEM_2-4.d	120	0.282669	0.000009	0.000825	0.000016	0.034147	0.000305	1.467260	0.000100	417	0.282522	0.282663	5.0	0.7	-0.8
run1\TEM_2-5.d	120	0.282658	0.000008	0.000870	0.000007	0.036936	0.000041	1.467225	0.000085	417	0.282522	0.282651	4.6	0.6	-1.2
run1\TEM_2-6.d	120	0.282674	0.000009	0.001354	0.000016	0.057213	0.000470	1.467282	0.000095	417	0.282522	0.282663	5.0	0.7	-0.8
run1\TEM_2-7.d	120	0.282674	0.000010	0.001472	0.000030	0.062047	0.000813	1.467246	0.000102	417	0.282522	0.282662	4.9	0.7	-0.8
run1\TEM_2-8.d	120	0.282662	0.000009	0.000973	0.000023	0.040791	0.000543	1.467241	0.000108	417	0.282522	0.282654	4.7	0.6	-1.1
run1\TEM_2-9.d	120	0.282677	0.000009	0.001264	0.000018	0.051923	0.000340	1.467252	0.000090	417	0.282522	0.282667	5.1	0.7	-0.6
run1\TEM_2-10.	120	0.282673	0.000010	0.000747	0.000022	0.032328	0.000520	1.467245	0.000095	417	0.282522	0.282668	5.1	0.7	-0.6
run1\TEM_2-11.	120	0.282660	0.000009	0.000840	0.000005	0.035376	0.000199	1.467239	0.000088	417	0.282522	0.282654	4.6	0.6	-1.1
run1\TEM_2-12.	120	0.282668	0.000009	0.000728	0.000020	0.031715	0.000757	1.467273	0.000099	417	0.282522	0.282662	4.9	0.6	-0.8
run1\TEM_2-13.	120	0.282677	0.000009	0.000721	0.000010	0.030220	0.000355	1.467295	0.000087	417	0.282522	0.282671	5.3	0.6	-0.5
run1\TEM_2-14.	120	0.282659	0.000008	0.000892	0.000032	0.036987	0.000749	1.467297	0.000091	417	0.282522	0.282652	4.6	0.6	-1.1
run1\TEM_2-15.	120	0.282685	0.000010	0.000498	0.000010	0.021882	0.000262	1.467245	0.000117	417	0.282522	0.282681	5.6	0.7	-0.2
run2\TEM_2-1.d	120	0.282680	0.000007	0.001502	0.000011	0.073530	0.000141	1.467242	0.000097	417	0.282522	0.282668	5.2	0.5	-0.6
run2\TEM_2-2.d	100	0.282666	0.000006	0.001143	0.000037	0.049711	0.000394	1.467269	0.000063	417	0.282522	0.282657	4.8	0.5	-1.0
run2\TEM_2-3.d	120	0.282678	0.000008	0.001254	0.000028	0.060069	0.001237	1.467265	0.000069	417	0.282522	0.282668	5.2	0.6	-0.6
run2\TEM_2-4.d	120	0.282683	0.000006	0.000935	0.000010	0.041663	0.000322	1.467236	0.000094	417	0.282522	0.282676	5.4	0.4	-0.3
run2\TEM_2-5.d	80	0.282663	0.000007	0.000645	0.000024	0.027874	0.000321	1.467236	0.000113	417	0.282522	0.282658	4.8	0.5	-0.9
run2\TEM_2-6.d	120	0.282666	0.000007	0.000552	0.000009	0.024530	0.000258	1.467299	0.000095	417	0.282522	0.282661	4.9	0.5	-0.8
run2\TEM_2-7.d	120	0.282695	0.000007	0.001470	0.000009	0.072567	0.000430	1.467226	0.000078	417	0.282522	0.282683	5.7	0.5	-0.1
run2\TEM_2-8.d	80	0.282676	0.000008	0.001432	0.000021	0.072343	0.000437	1.467283	0.000107	417	0.282522	0.282664	5.0	0.6	-0.7
run2\TEM_2-9.d	120	0.282675	0.000006	0.001213	0.000037	0.052784	0.001177	1.467335	0.000089	417	0.282522	0.282666	5.1	0.4	-0.7
run2\TEM_2-10.	120	0.282658	0.000006	0.001360	0.000040	0.063015	0.000995	1.467234	0.000069	417	0.282522	0.282647	4.4	0.4	-1.3
run2\TEM_2-11.	120	0.282675	0.000006	0.001210	0.000033	0.054882	0.001092	1.467215	0.000083	417	0.282522	0.282666	5.1	0.4	-0.7
run2\TEM_2-12.	120	0.282675	0.000006	0.000945	0.000050	0.044138	0.000981	1.467228	0.000086	417	0.282522	0.282668	5.2	0.4	-0.6
run2\TEM_1-2.d	120	0.282668	0.000013	0.000882	0.000002	0.052809	0.000612	1.467225	0.000105	417	0.282522	0.282661	4.9	0.9	-0.8
run2\TEM_1-3.d	120	0.282661	0.000010	0.001368	0.000013	0.067717	0.000414	1.467253	0.000080	417	0.282522	0.282651	4.5	0.7	-1.2
run2\TEM_1-4.d	120	0.282656	0.000009	0.001108	0.000005	0.057979	0.000508	1.467251	0.000079	417	0.282522	0.282647	4.4	0.7	-1.3
											Mean	**0.282662**	**5.0**		**-0.8**
											2SD	**0.000018**	**0.6**		
										Normalization factor		**1.000083**			

PLESOVICE (n=28)

run1\PL_2-1.da	120	0.282474	0.000006	0.000112	0.000001	0.008151	0.000026	1.467235	0.000078	337	0.282573	0.282473	-3.5	0.5	-0.3
run1\PL_2-2.da	120	0.282469	0.000007	0.000062	0.000000	0.004473	0.000006	1.467255	0.000074	337	0.282573	0.282468	-3.7	0.5	-0.5
run1\PL_2-3.da	120	0.282480	0.000007	0.000062	0.000000	0.004484	0.000017	1.467259	0.000077	337	0.282573	0.282480	-3.3	0.5	-0.1
run1\PL_2-4.da	120	0.282464	0.000007	0.000072	0.000001	0.005121	0.000050	1.467209	0.000074	337	0.282573	0.282463	-3.9	0.5	-0.6
run1\PL_2-5.da	120	0.282472	0.000007	0.000096	0.000000	0.006961	0.000039	1.467229	0.000089	337	0.282573	0.282472	-3.6	0.5	-0.3
run1\PL_2-6.da	120	0.282487	0.000007	0.000090	0.000001	0.006455	0.000049	1.467254	0.000081	337	0.282573	0.282486	-3.1	0.5	0.1
run1\PL_2-7.da	120	0.282486	0.000006	0.000083	0.000001	0.005903	0.000057	1.467246	0.000069	337	0.282573	0.282486	-3.1	0.5	0.1
run1\PL_2-8.da	120	0.282485	0.000008	0.000081	0.000003	0.005827	0.000120	1.467218	0.000077	337	0.282573	0.282485	-3.1	0.6	0.1
run1\PL_2-9.da	120	0.282478	0.000008	0.000103	0.000000	0.007416	0.000024	1.467233	0.000066	337	0.282573	0.282477	-3.4	0.5	-0.2
run1\PL_2-10.d	120	0.282478	0.000007	0.000103	0.000000	0.007321	0.000024	1.467234	0.000076	337	0.282573	0.282478	-3.4	0.5	-0.1
run1\PL_2-11.d	120	0.282478	0.000007	0.000105	0.000000	0.007641	0.000022	1.467241	0.000082	337	0.282573	0.282478	-3.4	0.5	-0.1
run1\PL_2-12.d	120	0.282478	0.000007	0.000105	0.000000	0.007703	0.000014	1.467253	0.000075	337	0.282573	0.282477	-3.4	0.5	-0.2
run1\PL_2-13.d	120	0.282469	0.000007	0.000111	0.000002	0.007784	0.000047	1.467245	0.000087	337	0.282573	0.282468	-3.7	0.5	-0.5
run1\PL_2-14.d	120	0.282480	0.000007	0.000116	0.000002	0.008378	0.000080	1.467265	0.000078	337	0.282573	0.282479	-3.3	0.5	-0.1
run1\PL_2-15.d	120	0.282485	0.000007	0.000100	0.000002	0.006892	0.000058	1.467243	0.000079	337	0.282573	0.282485	-3.1	0.5	0.1
run2\PL_2-1_da	120	0.282472	0.000006	0.000117	0.000001	0.009016	0.000030	1.467225	0.000106	337	0.282573	0.282471	-3.6	0.4	-0.4
run2\PL_2-2.da	120	0.282473	0.000008	0.000114	0.000000	0.008864	0.000032	1.467167	0.000256	337	0.282573	0.282473	-3.5	0.6	-0.3
run2\PL_2-3.da	120	0.282472	0.000007	0.000101	0.000000	0.007772	0.000072	1.467215	0.000178	337	0.282573	0.282471	-3.6	0.5	-0.4
run2\PL_2-4.da	120	0.282476	0.000005	0.000126	0.000000	0.008610	0.000020	1.467226	0.000080	337	0.282573	0.282475	-3.5	0.4	-0.2
run2\PL_2-5.da	120	0.282469	0.000006	0.000126	0.000000	0.008917	0.000042	1.467218	0.000144	337	0.282573	0.282468	-3.7	0.4	-0.5
run2\PL_2-6.da	120	0.282469	0.000005	0.000130	0.000000	0.008824	0.000038	1.466837	0.000289	337	0.282573	0.282468	-3.7	0.4	-0.5
run2\PL_2-7.da	120	0.282475	0.000004	0.000148	0.000001	0.010291	0.000041	1.467230	0.000069	337	0.282573	0.282474	-3.5	0.3	-0.3
run2\PL_2-8.da	120	0.282470	0.000007	0.000130	0.000000	0.008729	0.000032	1.465661	0.000732	337	0.282573	0.282469	-3.7	0.5	-0.4
run2\PL_1-1.da	120	0.282468	0.000008	0.000068	0.000002	0.004627	0.000080	1.467236	0.000068	337	0.282573	0.282468	-3.7	0.6	-0.5
run2\PL_1-2.da	120	0.282475	0.000007	0.000068	0.000002	0.004540	0.000075	1.467219	0.000077	337	0.282573	0.282475	-3.5	0.5	-0.2
run2\PL_1-3.da	120	0.282466	0.000008	0.000070	0.000002	0.004803	0.000068	1.467246	0.000082	337	0.282573	0.282465	-3.8	0.5	-0.6
run2\PL_1-4.da	120	0.282475	0.000007	0.000062	0.000002	0.004260	0.000052	1.467250	0.000073	337	0.282573	0.282475	-3.5	0.5	-0.2
run2\PL_1-5.da	75	0.282471	0.000008	0.000058	0.000002	0.004035	0.000052	1.467245	0.000086	337	0.282573	0.282470	-3.6	0.6	-0.4
											Mean	**0.282474**	**-3.5**		**-0.3**
											2SD	**0.000012**	**0.4**		
										Normalization factor		**1.000028**			
								Average Normalization factor (TM + PL)				**1.000056**			

Table DR5: Results of in situ SIMS oxygen isotope analyses.

Analysis (n=280)	Spot location single grain	$^{18}O/^{16}O$	1σ (%) Inter-session	$\delta^{18}O$ (SMOW)	2σ (‰) Inter-session
AG1304A (n=20)					
AG1304A_1/1	Core	0.00201580	0.0099	5.28	0.20
AG1304A_11/1	Core	0.00201578	0.0095	5.28	0.19
AG1304A_11/2	Rim	0.00201589	0.0094	5.33	0.19
AG1304A_12/1	Core	0.00201546	0.0111	5.12	0.22
AG1304A_12/2	Rim	0.00201546	0.0094	5.12	0.19
AG1304A_13/1	Core	0.00201557	0.0076	5.17	0.15
AG1304A_13/2	Rim	0.00201548	0.0107	5.13	0.21
AG1304A_18/1	Core	0.00201566	0.0118	5.21	0.24
AG1304A_18/2	Rim	0.00201586	0.0114	5.32	0.23
AG1304A_25/1	Core	0.00201583	0.0099	5.30	0.20
AG1304A_25/2	Rim	0.00201533	0.0106	5.05	0.21
AG1304A_30/1	Core	0.00201556	0.0108	5.16	0.22
AG1304A_4/1	Core	0.00201511	0.0084	4.94	0.17
AG1304A_4/2	Intermediate	0.00201552	0.0085	5.15	0.17
AG1304A_4/3	Rim	0.00201579	0.0077	5.28	0.15
AG1304A_17/1	Core	0.00201571	0.0081	5.24	0.16
AG1304A_17/2	Rim	0.00201558	0.0108	5.18	0.22
AG1304A_32/1	Core	0.00201576	0.0097	5.26	0.19
AG1304A_32/2	Rim	0.00201573	0.0080	5.25	0.16
AG1304A_5/1	Core	0.00201560	0.0079	5.19	0.16
Median ± 2SD				**5.20**	**0.19**
AG1401 (n=20)					
AG1401_1/1	Core	0.00201376	0.0122	4.27	0.24
AG1401_1/2	Rim	0.00201358	0.0079	4.18	0.16
AG1401_11/1	Core	0.00201396	0.0118	4.37	0.24
AG1401_11/2	Intermediate	0.00201368	0.0089	4.23	0.18
AG1401_11/3	Rim	0.00201444	0.0098	4.61	0.20
AG1401_16/1	Core	0.00201361	0.0114	4.20	0.23
AG1401_17/1	Core	0.00201559	0.0076	5.18	0.15
AG1401_17/2	Intermediate	0.00201550	0.0113	5.13	0.23
AG1401_17/3	Rim	0.00201509	0.0082	4.93	0.16
AG1401_3/1	Core	0.00201384	0.0096	4.31	0.19
AG1401_3/2	Rim	0.00201499	0.0101	4.88	0.20

AG1401_7/1	Core	0.00201491	0.0098	4.84	0.20
AG1401_10/1	Core	0.00201394	0.0104	4.36	0.21
AG1401_13/1	Core	0.00201406	0.0081	4.42	0.16
AG1401_13/2	Rim	0.00201452	0.0084	4.65	0.17
AG1401_18/1	Core	0.00201374	0.0083	4.26	0.17
AG1401_22/1	Core	0.00201373	0.0090	4.25	0.18
AG1401_22/2	Rim	0.00201472	0.0112	4.75	0.22
AG1401_6/1	Core	0.00201547	0.0102	5.12	0.20
AG1401_6/2	Rim	0.00201494	0.0083	4.86	0.17
Median ± 2SD				**4.51**	**0.69**
AG1402 (n=20)					
AG1402_1/1	Core	0.00201614	0.0077	5.46	0.15
AG1402_1/2	Rim	0.00201561	0.0113	5.19	0.23
AG1402_18/1	Core	0.00201634	0.0098	5.56	0.20
AG1402_18/2	Rim	0.00201600	0.0095	5.39	0.19
AG1402_3/1	Core	0.00201598	0.0104	5.38	0.21
AG1402_3/2	Rim	0.00201583	0.0101	5.30	0.20
AG1402_6/1	Core	0.00201576	0.0096	5.27	0.19
AG1402_6/2	Rim	0.00201586	0.0107	5.32	0.21
AG1402_9/1	Core	0.00201609	0.0078	5.43	0.16
AG1402_9/2	Intermediate	0.00201578	0.0101	5.28	0.20
AG1402_9/3	Rim	0.00201589	0.0101	5.33	0.20
AG1402_10/1	Core	0.00201593	0.0089	5.35	0.18
AG1402_14/1	Core	0.00201587	0.0085	5.32	0.17
AG1402_16/1	Core	0.00201587	0.0075	5.32	0.15
AG1402_19/1	Core	0.00201580	0.0102	5.29	0.20
AG1402_19/2	Intermediate	0.00201597	0.0079	5.37	0.16
AG1402_19/3	Rim	0.00201572	0.0088	5.24	0.18
AG1402_22/1	Core	0.00201584	0.0099	5.30	0.20
AG1402_8/1	Core	0.00201585	0.0087	5.31	0.17
AG1402_8/2	Rim	0.00201592	0.0096	5.35	0.19
Median ± 2SD				**5.32**	**0.16**
HQ1403 (n=20)					
HQ1403_1/1	Core	0.00201615	0.0086	5.46	0.17
HQ1403_1/2	Rim	0.00201553	0.0117	5.15	0.23
HQ1403_11/1	Core	0.00201611	0.0106	5.44	0.21
HQ1403_11/2	Rim	0.00201605	0.0106	5.41	0.21
HQ1403_12/1	Core	0.00201643	0.0108	5.60	0.22
HQ1403_17/1	Core	0.00201606	0.0133	5.42	0.27
HQ1403_17/2	Rim	0.00201604	0.0076	5.41	0.15
HQ1403_2/1	Core	0.00201600	0.0106	5.39	0.21
HQ1403_2/2	Rim	0.00201575	0.0113	5.26	0.23
HQ1403_22/1	Core	0.00201574	0.0112	5.25	0.22
HQ1403_3/1	Core	0.00201595	0.0112	5.36	0.22
HQ1403_4/1	Core	0.00201614	0.0104	5.46	0.21
HQ1403_7/1	Core	0.00201632	0.0099	5.55	0.20
HQ1403_15/1	Core	0.00201698	0.0098	5.87	0.20
HQ1403_15/2	Rim	0.00201581	0.0093	5.29	0.19
HQ1403_16/1	Core	0.00201616	0.0082	5.47	0.16
HQ1403_16/2	Rim	0.00201631	0.0098	5.54	0.20
HQ1403_18/1	Core	0.00201601	0.0075	5.39	0.15
HQ1403_20/1	Core	0.00201609	0.0119	5.43	0.24
HQ1403_22/2	Rim	0.00201595	0.0089	5.36	0.18
Median ± 2SD				**5.42**	**0.30**

AG1308A (n=20)					
AG1308A_10/1	Core	0.00201590	0.0097	5.34	0.19
AG1308A_10/2	Rim	0.00201598	0.0103	5.38	0.21
AG1308A_17/1	Core	0.00201600	0.0077	5.39	0.15
AG1308A_17/2	Rim	0.00201626	0.0088	5.51	0.18
AG1308A_18/1	Core	0.00201613	0.0110	5.45	0.22
AG1308A_18/2	Rim	0.00201629	0.0086	5.53	0.17
AG1308A_2/1	Core	0.00201574	0.0086	5.26	0.17
AG1308A_2/2	Rim	0.00201582	0.0095	5.29	0.19
AG1308A_20/1	Core	0.00201581	0.0103	5.29	0.21
AG1308A_20/2	Rim	0.00201631	0.0096	5.54	0.19
AG1308A_3/1	Core	0.00201588	0.0111	5.33	0.22
AG1308A_3/2	Rim	0.00201589	0.0094	5.33	0.19
AG1308A_4/1	Core	0.00201597	0.0087	5.37	0.17
AG1308A_9/1	Core	0.00201558	0.0115	5.18	0.23
AG1308A_9/2	Rim	0.00201579	0.0089	5.28	0.18
AG1308A_5/1	Core	0.00201592	0.0090	5.35	0.18
AG1308A_6/1	Core	0.00201629	0.0073	5.53	0.15
AG1308A_6/2	Rim	0.00201630	0.0110	5.54	0.22
AG1308A_7/1	Core	0.00201653	0.0107	5.65	0.21
AG1308A_7/2	Rim	0.00201633	0.0095	5.55	0.19
Median ± 2SD				**5.37**	**0.25**
VK1405 (n=20)					
VK1405_10/1	Core	0.00201584	0.0085	5.31	0.17
VK1405_11/1	Core	0.00201592	0.0088	5.35	0.18
VK1405_11/2	Rim	0.00201581	0.0120	5.29	0.24
VK1405_16/1	Core	0.00201535	0.0095	5.06	0.19
VK1405_4/1	Core	0.00201566	0.0093	5.21	0.19
VK1405_4/2	Rim	0.00201564	0.0091	5.20	0.18
VK1405_5/1	Core	0.00201598	0.0084	5.38	0.17
VK1405_5/2	Intermediate	0.00201560	0.0101	5.19	0.20
VK1405_5/3	Rim	0.00201527	0.0136	5.02	0.27
VK1405_8/1	Core	0.00201569	0.0090	5.23	0.18
VK1405_9/1	Core	0.00201589	0.0108	5.33	0.22
VK1405_9/2	Rim	0.00201577	0.0099	5.27	0.20
VK1405_1/1	Core	0.00201571	0.0099	5.24	0.20
VK1405_23/1	Core	0.00201571	0.0095	5.24	0.19
VK1405_23/2	Rim	0.00201636	0.0114	5.57	0.23
VK1405_14/1	Core	0.00201562	0.0093	5.20	0.19
VK1405_15/1	Core	0.00201603	0.0081	5.40	0.16
VK1405_20/1	Core	0.00201574	0.0128	5.26	0.26
VK1405_13/1	Core	0.00201596	0.0128	5.37	0.26
VK1405_27/1	Core	0.00201592	0.0096	5.35	0.19
Median ± 2SD				**5.26**	**0.24**
MR1403 (n=20)					
MR1403_1/1	Core	0.00201637	0.0090	5.57	0.18
MR1403_1/2	Rim	0.00201610	0.0082	5.44	0.16
MR1403_10/1	Core	0.00201655	0.0092	5.66	0.18
MR1403_11/1	Core	0.00201628	0.0090	5.53	0.18
MR1403_11/2	Rim	0.00201632	0.0092	5.54	0.18
MR1403_12/1	Core	0.00201655	0.0114	5.66	0.23
MR1403_12/2	Rim	0.00201671	0.0090	5.74	0.18
MR1403_13/1	Core	0.00201640	0.0092	5.59	0.18
MR1403_13/2	Rim	0.00201623	0.0084	5.50	0.17
MR1403_19/1	Core	0.00201611	0.0090	5.44	0.18
MR1403_2/1	Core	0.00201622	0.0090	5.50	0.18
MR1403_2/2	Rim	0.00201610	0.0103	5.44	0.21
MR1403_3/1	Core	0.00201635	0.0084	5.56	0.17
MR1403_21/1	Core	0.00201647	0.0100	5.62	0.20
MR1403_21/2	Rim	0.00201639	0.0085	5.58	0.17
MR1403_6/1	Core	0.00201641	0.0094	5.59	0.19
MR1403_6/2	Rim	0.00201645	0.0077	5.61	0.15
MR1403_7/1	Core	0.00201613	0.0093	5.45	0.19
MR1403_8/1	Core	0.00201664	0.0088	5.71	0.18
MR1403_9/1	Core	0.00201661	0.0076	5.69	0.15
Median ± 2SD				**5.58**	**0.18**

LI1303A1 (n=20)					
LI1303A1_2/1	Core	0.00201650	0.0079	5.63	0.16
LI1303A1_2/2	Intermediate	0.00201634	0.0109	5.56	0.22
LI1303A1_2/3	Rim	0.00201648	0.0088	5.62	0.18
LI1303A1_3/1	Core	0.00201639	0.0094	5.58	0.19
LI1303A1_3/2	Rim	0.00201634	0.0084	5.55	0.17
LI1303A1_5/1	Core	0.00201657	0.0119	5.67	0.24
LI1303A1_5/2	Rim	0.00201640	0.0086	5.58	0.17
LI1303A1_6/1	Core	0.00201655	0.0107	5.66	0.21
LI1303A1_6/2	Rim	0.00201652	0.0099	5.64	0.20
LI1303A1_7/1	Core	0.00201668	0.0091	5.73	0.18
LI1303A1_7/2	Rim	0.00201668	0.0088	5.73	0.18
LI1303A1_8/1	Core	0.00201639	0.0118	5.58	0.24
LI1303A1_12/1	Core	0.00201658	0.0104	5.67	0.21
LI1303A1_12/2	Rim	0.00201647	0.0090	5.62	0.18
LI1303A1_15/1	Core	0.00201633	0.0073	5.55	0.15
LI1303A1_16/1	Core	0.00201671	0.0090	5.74	0.18
LI1303A1_17/1	Core	0.00201639	0.0108	5.58	0.22
LI1303A1_18/1	Core	0.00201655	0.0073	5.66	0.15
LI1303A1_19/1	Core	0.00201680	0.0081	5.79	0.16
LI1303A1_19/2	Rim	0.00201657	0.0114	5.67	0.23
Median ± 2SD				**5.64**	**0.14**
KJ1207 (n=20)					
KJ1207_1/1	Core	0.00201657	0.0113	5.67	0.23
KJ1207_1/2	Intermediate	0.00201647	0.0089	5.62	0.18
KJ1207_1/3	Rim	0.00201631	0.0078	5.54	0.16
KJ1207_10/1	Core	0.00201597	0.0120	5.37	0.24
KJ1207_10/2	Rim	0.00201574	0.0103	5.26	0.21
KJ1207_2/1	Core	0.00201597	0.0100	5.37	0.20
KJ1207_2/2	Rim	0.00201638	0.0086	5.58	0.17
KJ1207_3/1	Core	0.00201630	0.0107	5.53	0.21
KJ1207_3/2	Rim	0.00201629	0.0077	5.53	0.15
KJ1207_5/1	Core	0.00201609	0.0090	5.43	0.18
KJ1207_5/2	Rim	0.00201580	0.0088	5.28	0.18
KJ1207_7/1	Core	0.00201637	0.0080	5.57	0.16
KJ1207_12/1	Core	0.00201589	0.0100	5.33	0.20
KJ1207_14/1	Core	0.00201624	0.0085	5.50	0.17
KJ1207_16/1	Core	0.00201635	0.0089	5.56	0.18
KJ1207_17/1	Core	0.00201605	0.0097	5.41	0.19
KJ1207_17/2	Rim	0.00201561	0.0082	5.19	0.16
KJ1207_4/1	Core	0.00201619	0.0073	5.48	0.15
KJ1207_9/1	Core	0.00201654	0.0091	5.66	0.18
KJ1207_9/2	Rim	0.00201627	0.0097	5.52	0.19
Median ± 2SD				**5.51**	**0.27**

KJ1002 (n=21)					
KJ1002_1/1	Core	0.00201635	0.0095	5.56	0.19
KJ1002_1/2	Rim	0.00201594	0.0092	5.35	0.18
KJ1002_11/1	Core	0.00201569	0.0087	5.23	0.17
KJ1002_11/2	Rim	0.00201557	0.0089	5.17	0.18
KJ1002_16/1	Core	0.00201572	0.0098	5.24	0.20
KJ1002_16/2	Intermediate	0.00201615	0.0086	5.46	0.17
KJ1002_16/3	Rim	0.00201607	0.0100	5.42	0.20
KJ1002_2/1	Core	0.00201639	0.0092	5.58	0.18
KJ1002_2/2	Rim	0.00201616	0.0078	5.47	0.16
KJ1002_3/1	Core	0.00201663	0.0101	5.70	0.20
KJ1002_3/2	Rim	0.00201632	0.0093	5.55	0.19
KJ1002_6/1	Core	0.00201576	0.0098	5.27	0.20
KJ1002_6/2	Intermediate	0.00201573	0.0130	5.25	0.26
KJ1002_6/3	Rim	0.00201604	0.0093	5.41	0.19
KJ1002_9/1	Core	0.00201650	0.0086	5.64	0.17
KJ1002_9/2	Rim	0.00201625	0.0095	5.51	0.19
KJ1002_18/1	Core	0.00201653	0.0083	5.65	0.17
KJ1002_18/2	Rim	0.00201612	0.0094	5.45	0.19
KJ1002_24/1	Core	0.00201649	0.0092	5.63	0.18
KJ1002_24/2	Intermediate	0.00201617	0.0094	5.47	0.19
KJ1002_24/3	Rim	0.00201631	0.0093	5.54	0.19
Median ± 2SD				**5.47**	**0.31**
KJ1316 (n=19)					
KJ1316_1/1	Core	0.00201653	0.0078	5.65	0.16
KJ1316_13/1	Core	0.00201642	0.0093	5.59	0.19
KJ1316_14/1	Core	0.00201654	0.0121	5.66	0.24
KJ1316_14/2	Rim	0.00201644	0.0085	5.61	0.17
KJ1316_16/1	Core	0.00201666	0.0081	5.71	0.16
KJ1316_2/1	Core	0.00201602	0.0113	5.40	0.23
KJ1316_2/2	Rim	0.00201635	0.0108	5.56	0.22
KJ1316_4/1	Core	0.00201676	0.0102	5.76	0.20
KJ1316_4/2	Rim	0.00201647	0.0087	5.62	0.17
KJ1316_5/1	Core	0.00201638	0.0092	5.58	0.18
KJ1316_9/1	Core	0.00201696	0.0095	5.86	0.19
KJ1316_9/2	Rim	0.00201672	0.0084	5.75	0.17
KJ1316_18/1	Core	0.00201689	0.0082	5.83	0.16
KJ1316_18/2	Rim	0.00201648	0.0095	5.62	0.19
KJ1316_20/1	Core	0.00201673	0.0086	5.75	0.17
KJ1316_21/1	Core	0.00201659	0.0086	5.68	0.17
KJ1316_23/1	Core	0.00201634	0.0098	5.56	0.20
KJ1316_6/1	Core	0.00201640	0.0090	5.58	0.18
KJ1316_7/1	Core	0.00201643	0.0089	5.60	0.18
Median ± 2SD				**5.62**	**0.22**

KJ1302A (n=20)					
KJ1302A_13/1	Core	0.00201648	0.0125	5.63	0.25
KJ1302A_13/2	Rim	0.00201663	0.0097	5.70	0.19
KJ1302A_2/1	Core	0.00201640	0.0107	5.58	0.21
KJ1302A_2/2	Rim	0.00201651	0.0091	5.64	0.18
KJ1302A_3/1	Core	0.00201631	0.0075	5.54	0.15
KJ1302A_3/2	Rim	0.00201607	0.0089	5.42	0.18
KJ1302A_4/1	Core	0.00201635	0.0085	5.56	0.17
KJ1302A_4/2	Rim	0.00201618	0.0116	5.48	0.23
KJ1302A_5/1	Core	0.00201640	0.0111	5.58	0.22
KJ1302A_5/2	Rim	0.00201628	0.0089	5.52	0.18
KJ1302A_6/1	Core	0.00201623	0.0087	5.50	0.17
KJ1302A_7/1	Core	0.00201637	0.0102	5.57	0.20
KJ1302A_14/1	Core	0.00201630	0.0087	5.53	0.17
KJ1302A_16/1	Core	0.00201643	0.0097	5.60	0.19
KJ1302A_17/1	Core	0.00201636	0.0106	5.57	0.21
KJ1302A_19/1	Core	0.00201583	0.0087	5.30	0.17
KJ1302A_19/2	Rim	0.00201582	0.0086	5.29	0.17
KJ1302A_8/1	Core	0.00201627	0.0101	5.52	0.20
KJ1302A_9/1	Core	0.00201620	0.0092	5.49	0.18
KJ1302A_9/2	Rim	0.00201620	0.0099	5.49	0.20
Median ± 2SD				**5.54**	**0.20**
KJ1324A (n=20)					
KJ1324A_1/1	Core	0.00201712	0.0097	5.94	0.19
KJ1324A_1/2	Rim	0.00201689	0.0075	5.83	0.15
KJ1324A_10/1	Core	0.00201709	0.0122	5.93	0.24
KJ1324A_10/2	Rim	0.00201701	0.0105	5.89	0.21
KJ1324A_17/1	Core	0.00201686	0.0092	5.82	0.18
KJ1324A_17/2	Intermediate	0.00201713	0.0095	5.95	0.19
KJ1324A_17/3	Rim	0.00201689	0.0101	5.83	0.20
KJ1324A_4/1	Core	0.00201729	0.0084	6.03	0.17
KJ1324A_4/2	Rim	0.00201692	0.0095	5.84	0.19
KJ1324A_5/1	Core	0.00201741	0.0089	6.09	0.18
KJ1324A_5/2	Rim	0.00201708	0.0076	5.92	0.15
KJ1324A_8/1	Core	0.00201694	0.0115	5.86	0.23
KJ1324A_8/2	Rim	0.00201692	0.0093	5.84	0.19
KJ1324A_9/1	Core	0.00201692	0.0086	5.84	0.17
KJ1324A_16/1	Core	0.00201719	0.0110	5.98	0.22
KJ1324A_16/2	Rim	0.00201714	0.0086	5.95	0.17
KJ1324A_18/1	Core	0.00201708	0.0082	5.92	0.16
KJ1324A_18/2	Rim	0.00201698	0.0085	5.88	0.17
KJ1324A_22/1	Core	0.00201719	0.0103	5.98	0.21
KJ1324A_22/2	Rim	0.00201727	0.0098	6.02	0.20
Median ± 2SD				**5.92**	**0.15**

LI1301 (n=20)					
LI1301_11/1	Core	0.00201661	0.0082	5.69	0.16
LI1301_2/1	Core	0.00201725	0.0106	6.01	0.21
LI1301_2/2	Intermediate	0.00201732	0.0097	6.04	0.19
LI1301_2/3	Rim	0.00201684	0.0075	5.81	0.15
LI1301_3/1	Core	0.00201682	0.0086	5.79	0.17
LI1301_3/2	Rim	0.00201706	0.0100	5.91	0.20
LI1301_4/1	Core	0.00201735	0.0095	6.06	0.19
LI1301_4/2	Rim	0.00201744	0.0094	6.10	0.19
LI1301_5/1	Core	0.00201719	0.0090	5.98	0.18
LI1301_5/2	Rim	0.00201684	0.0085	5.81	0.17
LI1301_8/1	Core	0.00201708	0.0099	5.93	0.20
LI1301_15/1	Core	0.00201732	0.0117	6.04	0.23
LI1301_16/1	Core	0.00201716	0.0088	5.96	0.18
LI1301_16/2	Intermediate	0.00201708	0.0102	5.93	0.20
LI1301_16/3	Rim	0.00201697	0.0076	5.87	0.15
LI1301_17/1	Core	0.00201740	0.0094	6.08	0.19
LI1301_21/1	Core	0.00201712	0.0092	5.94	0.18
LI1301_21/2	Rim	0.00201721	0.0104	5.99	0.21
LI1301_6/1	Core	0.00201722	0.0090	6.00	0.18
LI1301_6/2	Rim	0.00201728	0.0095	6.03	0.19
Median ± 2SD				**5.97**	**0.22**

Standard

S0081_UAMT		0.00201497		4.87	

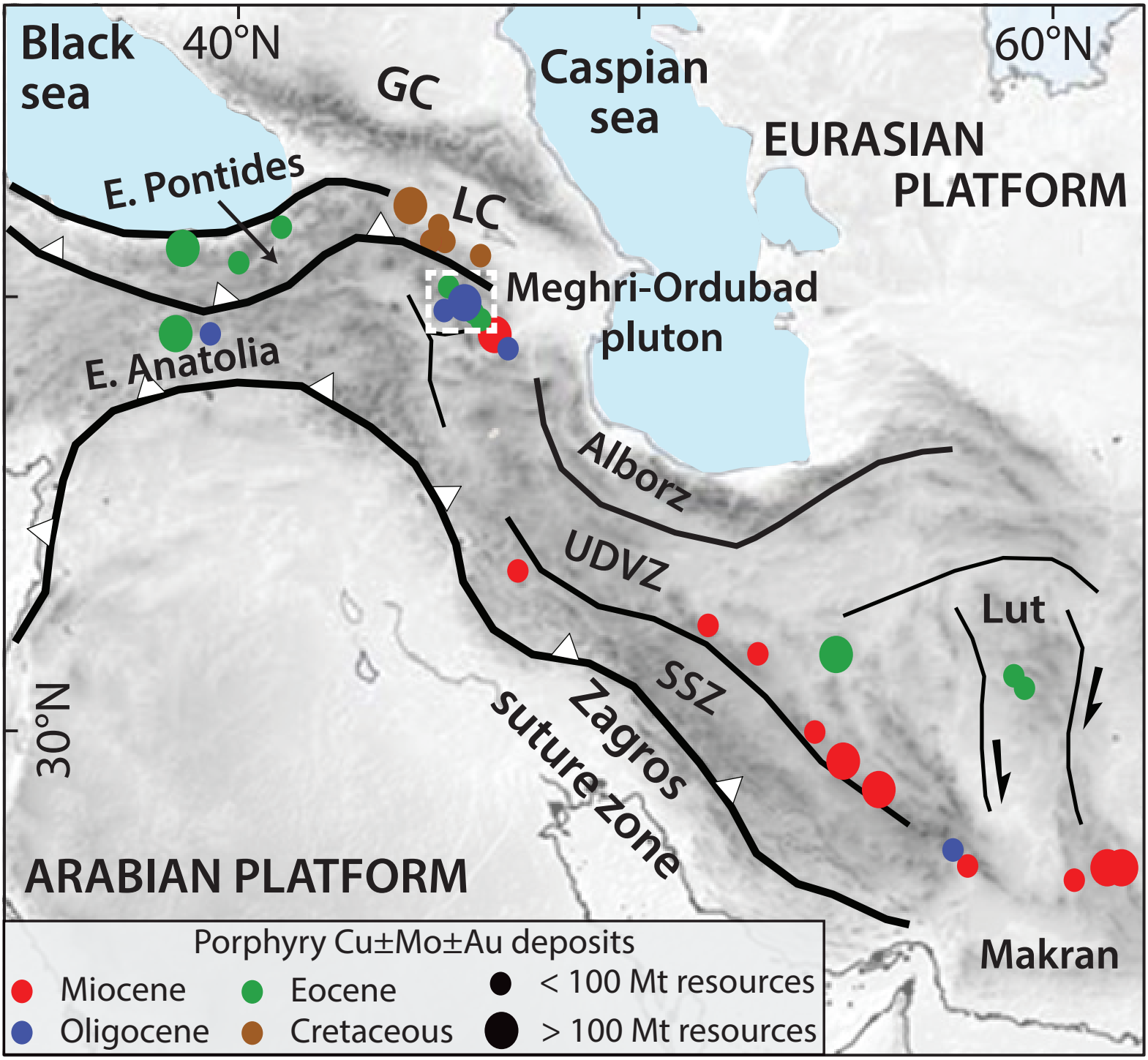

Figure DR1: Distribution of porphyry Cu±Mo±Au deposits grouped by ages and sizes along the Afro-Arabian collision zone located in the central Tethyan metallogenic belt. Locations and ages of porphyry deposits are derived principally from Singer et al. (2008), with updated information from Aghazadeh et al. (2015) and Richards (2015). Suture zones and structures are derived from Mouthereau et al. (2012) and the topographic relief background map from ETOPO1 (1'×1' resolution) Global Relief data (http://www.ngdc.noaa.gov). Abbreviations are Greater Caucasus (GC), Lesser Caucasus (LC), Sanandaj-Sirjan Zone (SSZ) and Urumieh-Dokhtar Volcanic Zone (UDVZ).

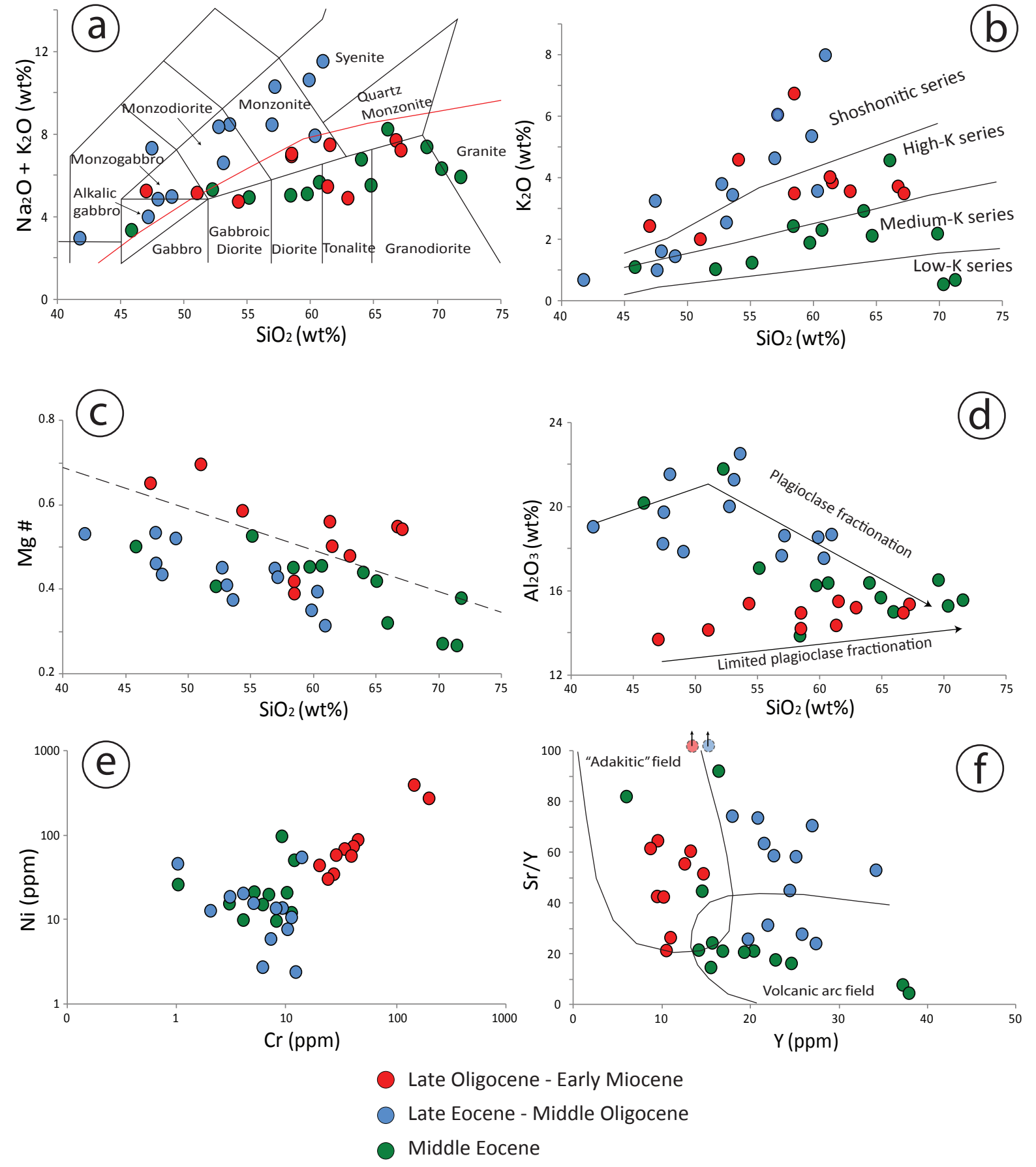

Figure DR2: a) Total Alkali Silica (TAS) diagram (Le Maître et al.,1989). b) K_2O vs. SiO_2 Harker diagram (Pecerillo and Taylor, 1976). c) Mg# vs. SiO_2 Harker diagram. d) Al_2O_3 vs. SiO_2 Harker diagram. e) Ni vs. Cr. f) Sr/Y vs. Y.

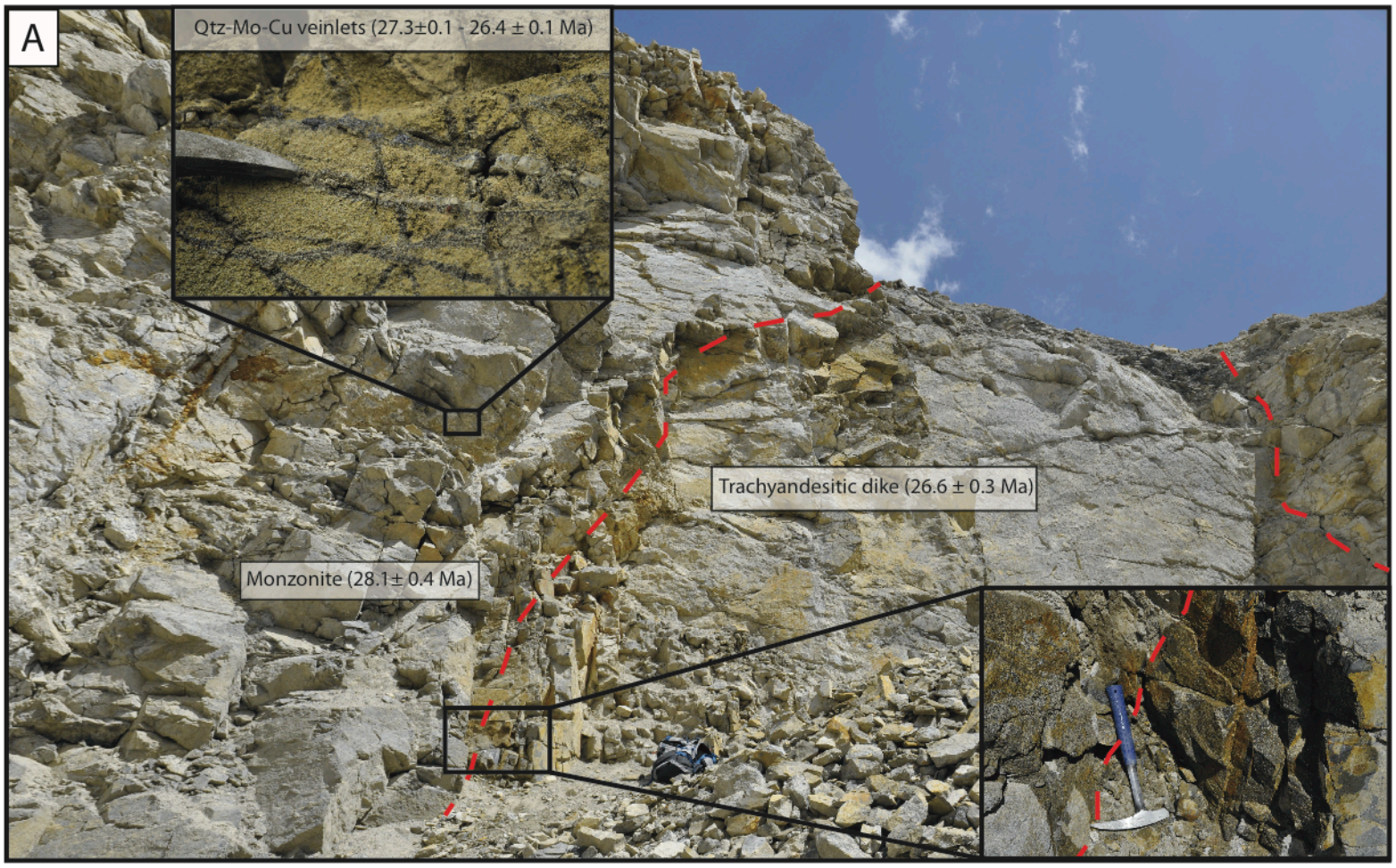

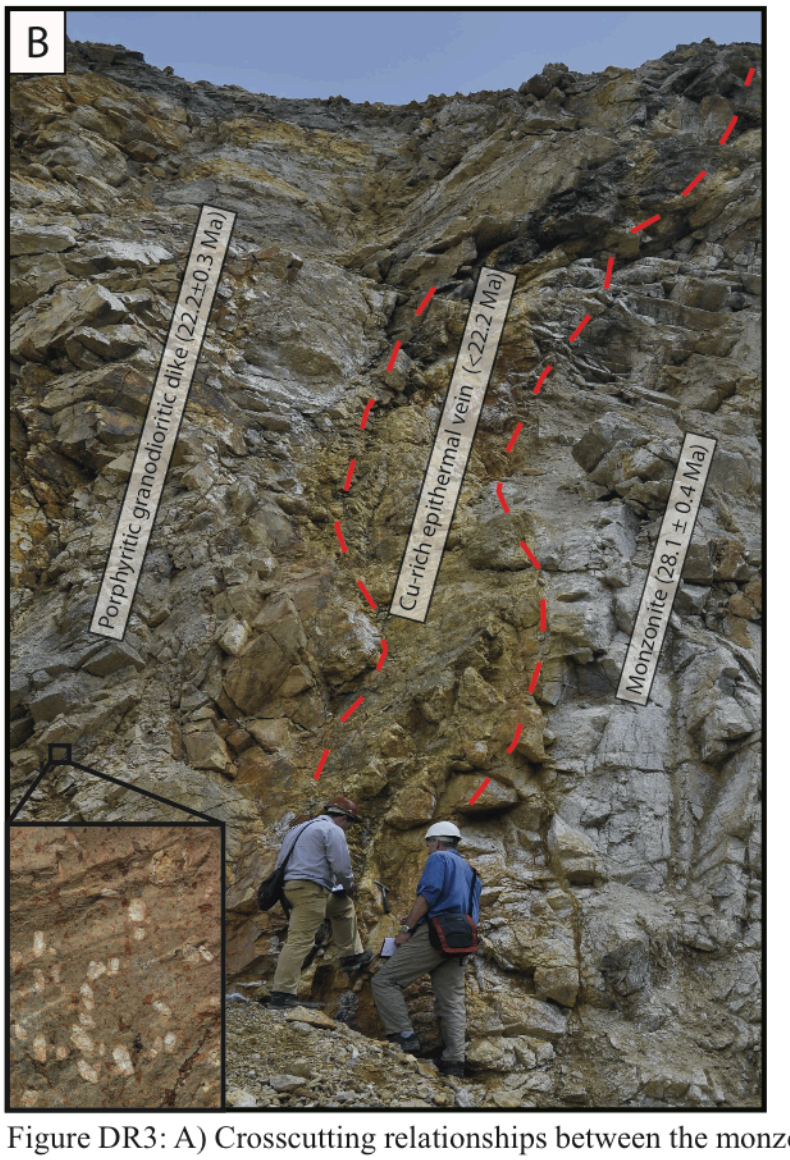

Figure DR3: A) Crosscutting relationships between the monzonite-bearing mineralization and the trachyandesitic dike. B) Crosscutting relationships showing a Cu-rich epithermal vein crosscutting the altered monzonite (propylitic, potassic) and creating an important hydrothermal alteration (kaolinitisation, silicification) of the porphyritic granodioritic dike.

REFERENCES

Aghazadeh, M., Hou, Z., Badrzadeh, Z., and Zhou, L., 2015, Temporal–spatial distribution and tectonic setting of porphyry copper deposits in Iran: Constraints from zircon U–Pb and molybdenite Re–Os geochronology: Ore Geology Reviews, v. 70, p. 385-406, doi:10.1016/j.oregeorev.2015.03.003.

Le Maitre, R. W. B., Dudek, P., Keller, A., Lameyre, J., Le Bas, J., Sabine, M.J., Schmid, P.A., Sorensen, R., Streckeisen, H., Woolley, A. and Zanettin, A.R., 1989, A classification of igneous rocks and glossary of terms: Recommendations of the International Union of Geological Sciences, Subcommission on the Systematics of Igneous Rocks: Blackwell Scientific Publications, Oxford, 193 p.

Mouthereau, F., Lacombe, O. and Vergés, J., 2012, Building the Zagros collisional orogen: timing, strain distribution and the dynamics of Arabia/Eurasia plate convergence: Tectonophysics, v. 532, p. 27-60, doi:10.1016/j.tecto.2012.01.022.

Pecerillo, A., and Taylor, S.R., 1976, Geochemistry of Eocene calc-alkaline volcanic rocks from the Kastamanou area, northern Turkey: Contributions to Mineralogy and Petrology, v. 58, p. 63–81, doi: 10.1007/BF00384745.

Richards, J.P., 2015, Tectonic, magmatic, and metallogenic evolution of the Tethyan orogen: from subduction to collision: Ore Geology Review, v. 70, p. 323-345, doi: 10.1016/j.oregeorev.2014.11.009.

Singer, D. A., Berger, V. I., Moring, B. C., 2008, Porphyry copper deposits of the world: database and grade and tonnage models: U.S. Geological Survey Open-File Report 2008-1155, 45 p. (http://pubs.usgs.gov/of/2008/1155/).